The University Of Sheffield.

Katnip, a novel microtubule and autophagy regulator

Georgina Paris Starling

Supervisor: Dr Jason King

A thesis submitted in partial fulfillment of the requirements for the degree of Doctor of Philosophy

Department of Biomedical Science

University of Sheffield

December 2020

Abstract

Katnip is an uncharacterised yet evolutionary conserved protein which contains 3 repeats of a unique protein domain called DUF4457. Recent work has identified that loss of katnip function in humans, results in Joubert's syndrome, a rare ciliopathy. The loss of katnip in these patients, as well as animal models, caused cilia dysfunction due to the loss of microtubule organisation in the axoneme.

Katnip was also identified in a genetic screen for new autophagy regulators in the social amoeba *Dictyostelium discoideum*. These unicellular organisms have no cilia, and therefore suggests a non-cilia role for katnip which affects autophagy.

This thesis found that the loss of katnip in *Dictyostelium discoideum* results in an autophagy defect due to slower autophagosome formation and degradation. A degradation defect was also identified in phagocytosis and macropinocytosis, both of which rely on lysosomal trafficking for vesicle degradation along with autophagy. Based on these results, katnip mutants were hypothesised to have a general lysosomal trafficking defect.

In order to identify the root cause of this trafficking defect, GFP-katnip was overexpessed in both *Dictyostelium discoideum* cells and multiple mammalian cell lines. GFP-katnip was observed at the centrosome of all these cells with a high cytoplasmic background. Unusually, GFP-katnip was seen to localise to microtubules in highly expressing mammalian cells and upon oxidative damage in *Dictyostelium discoideum* . Therefore, I hypothesis that in addition to binding the centrosome, katnip is able to bind to microtubules, but only under certain conditions. Oxidative damage is used to induce microtubule damage, and therefore, GFP-katnip may be able to bind to points of microtubule damage.

Katnip mutants cells also had a sensitivity to GFP-tubulin expression, which caused an elongation of mitosis, specifically anaphase, and increased tangling of microtubules. I hypothesis that GFP-tubulin may induce more microtubule

damage events in these cells and therefore, katnip may function to tolerate microtubule damage.

This thesis confirms a new non-cilia role for katnip, due to the identification of its binding and affecting interphase microtubules. This thesis present katnip as a potential candidate for a microtubule damage protein which can bind to sites of microtubule damage and is necessary for tolerating damage. This loss of microtubule maintenance and accumulation of damage may cause the organisation defect observed in GFP-tubulin expressing cells as well as axoneme microtubules in Joubert's patients. The loss of microtubules organisation results in the general lysosomal trafficking defects, which may also be present in mammalian cells. Therefore, katnip mutant patients may be more susceptible to diseases affected by loss of autophagy including cancers and neurodegenerative diseases.

An expert is a person who has made all the mistakes which can be made, in a narrow field.

Niels Bohr (Via Ellen Allwood after a particularly long, yet unsuccessful day of protein purification)

They don't think it be like it is, but it do.

Major league baseball player, Oscar Gamble

Acknowledgments

27th August 2020, Broomhill, Sheffield

First and foremost, I would like to thank my supervisor Jason King who has been a source of endless expertise and constant enthusiasm over the course of my PhD. In addition to teaching me, and generally putting up with me going on about how great microtubules are, Jason has guided the project to where it is now, and has always made me feel positive and energised to carry on, even when I was convinced everything was going horribly wrong.

This also extends to the other members of the King lab, both previous and current. Thanks to Cat and Ben for teaching me how the lab works and being so welcoming when I first joined. And to Chris and James, who still provide the King lab with its friendly environment which I am always thankful for.

I would also like to thank all the people who have been interested in the project and offered me advice, solutions and support. This applies especially to my advisors, Liz Symthe and Kai Erdmann, who always managed to find time to engage with the project and offer their guidance. And to Ellen Allwood, who helped me so much with the protein purification.

I would like to thank Maria, for many a lunch, 3pm snack break and dinner for ranting, celebrating and everything in between. To the members of fat friday, who always provided cake and excellent company, and to all the other members of D-floor for chats/procrastination/letting me 'borrow' things. And to Patrick, Judit, Kate, Laura, Mohamed, Angie and Hoger; I feel incredibly lucky to be

working in such a friendly environment which is all down to the lovely people who work in the Florey building.

Outside of the university, I would like to thanks Leigh-Anne and Tori for their fantastic friendship and support, you guys never fail to make me feel better even on my darkest days. I would also like to thank Stuart (Maria's fiance), Mac (Leigh-Anne's husband) and Ed (Tori's partner) for generally putting up with me lazing around their houses, eating their food and going on about science. My thanks also to my all brilliant school friends, Emily, Sarah and Helen. I feel incredible lucky to have met people who support me, understand me and I get on so well with, so early in life.

And obviously, I would like to thank all my family. Who have all provided me with a education which cannot be taught in classrooms or learnt from books. But, a special thanks to my Auntie and Uncle, Nadine and Tom (and Charlie, Oliver and Lola), who have been an unyielding and constant source of support and love throughout my entire time as a student. And to Grandad and James, who have taught me to never stop questioning and learning. And, of course, to Mum and Dad, no thanks could ever be enough for the love or support that you have provided me, and I am the person I am today because of you.

Contents

List of Figures

List of Tables

Abbreviation	Meaning
α-ATAT1	alpha-tubulin N-acetylatransferase 1
AAA	ATPase associated with diverse cellular activities
Arg/Lys or R/L	Arginine/Lysine
ALS	Amyotrophic lateral sclerosis
ATP	Adenosine triphosphate
BSA	Bovine serum albumin
cAMP	Cyclic adenosine monophosphate
Da	Daltons
dH2O	Deionised water
DMEM	Dulbecco's modified eagle medium
DMSO	Dimethyl sulfoxide
DNA	Deoxyribonucleic acid
DTT	Dithiothreitol
DUF	Domain of unknown function
EDTA	Ethylenediaminetetraacetic acid
EGTA	ethylene glycol-bis(β-aminoethyl ether)-N,N,N,N-tetraacetic acid
EM	electron microscopy
FBS	Foetal bovine serum
FITC	Fluorescein isothiocyanate
GCP	γ-tubulin complex component protein
GDP	Guanine diphosphate
GEF	Guanine exchange factor
GFP	Green fluorescence protein
GST	Glutathione s-transferase
GTP	Guanine triphosphate
HEPES	(4-(2-hydroethyl)-1-piperazineethanesulfonic acid
Htt	Huntington
IFT	Intraflagella transport
IPTG	Isopropyl β-D-1-thiogalactopyranoside
JSRD	Jouberts syndrome and related disorders

kDa	Kilodalton
KO	Knockout
L	Litre
LC3	Microtubule binding proteins 1A/1B light chain 3B
MAP	Microtubule associated protein
min	Minute
mL	Millilitre
mM	Millimolar
MRI	Magnetic resonance imaging
MTOC	Microtubule organising centre
mTOR	Mechanisitic target of rapamycin
NFT	Neurofillbriliary tangles
nM	Nanomolar
NMDAR	N-methyl-D-aspartate receptor
oC	Celsuis
PAS	Phagophore assembly site
PBS	Phosphate buffered saline
PCM	Pericentriolar matrix
PCR	Polymerase chain reaction
PE	Phosphatidylethanoamine
PFA	Paraformaldehyde
PI	Phospholipid phosphatidylinositol
PI3K	Phosphoinositide 3-kinase
PI3P	Phosphatidylinositol 3-phosphate
PIPES	Piperazine-N, N'-bis
PTM	Post translational modification
REMI	Restriction enzyme mediated integration
ROS	Reactive oxygen species
SAS-6	Spindle assembly abnormal protein 6
SD	Standard deviation

SDS	Sodium dodecyl sulphate
SDS-PAGE	Sodium dodecyl sulphate-polyacrylamide gel electrophoresis
SEM	Standard error of the mean
SOB	Super optimal broth
SOD1	Superoxide dimutase 1
TAE	Tris-acetate-EDTA
TCA	Tricarboxylate acid
TOG	Tumour overexpressed gene
TPA	Total proteolytic activity
TRITC	Tetramethylrhodamine
TuRC	Tubulin ring complex
μg	Microgram
μL	Microlitre
μM	Micromolar
Vps34	Vacuolar protein sorting 34
WT	Wild type

Chapter 1

Introduction

1.1 Autophagy

1.1.1 Types of autophagy

Autophagy is the innocuous process whereby damaged or unwanted intracellular material is degraded by cells. Resulting components are recycled back to *de novo* pathways. It is important for the removal of material, some of which can be harmful and pathogenic to the cell. Autophagy is also necessary for surviving starvation, whereby cells rely on the autophagy to generate nutrients.

There are 3 major types of autophagy; macroautophagy, microautophagy, and chaperone mediated autophagy (figure 1.1).

In macroautophagy, intracellular cargo is encapsulated in a double membraned vesicle called an autophagosome. Complete autophagosomes are then transported to lysosomes for their degradation. Many of the genes involved in macroautophagy have been identified, of which 41 have been identified in yeast (Klionsky et al., 2003; Mizushima, 2007) and 128 in humans (due to increased redundancy of these proteins in mammalian cells, figure 1.3).

Microautophagy does not rely on the creation of a vesicle and instead directly engulfs proteins through membrane invagination into the lysosome via

autophagic tubes regulated by Atg332p (Li et al., 2012). Microautophagy is also important for surviving starvation, but as its name suggests, works on a much smaller scale.

Chaperone mediated autophagy traffics proteins directly through the lysosomal membrane for degradation in an Hsc70 regulated process (Agarraberes et al., 1997). It is highly selective and can transport as little as a single protein at a time.

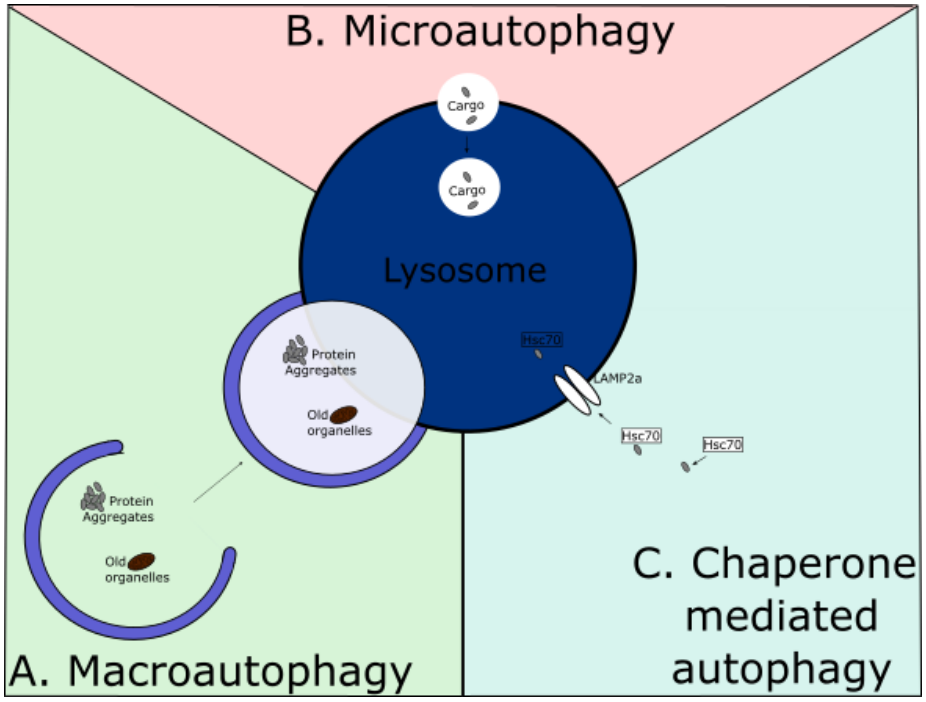

Figure 1.1: **The 3 types of autophagy**

A. In macroautophagy, a double membraned vesicles is formed around cargo, including protein aggregates and organelles. These vesicles, called autophagosomes, are then trafficked and fuse with lysosomes to degrade components. B. The lysosomal lumen invaginates to receive cargo in microautophagy. C. In chaperone mediated autophagy, single proteins are tagged with hsc70 and transported across the lysosomal membrane by LAMP2.

Macroautophagy is the best characterised form of autophagy, and is the focus of this work, and will be subsequently referred to as autophagy.

1.1.2 Functions of autophagy

Nutrient sensing and surviving starvation

Autophagy occurs endogenously at low basal levels but can be induced at higher levels under multiple cellular stresses, including DNA damage, growth factor withdrawal, starvation, hypoxia, and structural remodelling during development (Mizushima, 2007; Mathew et al., 2007).

Inducing autophagy during starvation increases the amount of autophagosomes created and degraded. This increase in cargo degradation releases more amino acids and *de novo* components back into the cell, creating an intracellular source of nutrients in the absence of extracellular ones. For example, degraded autophagy cargo has been observed to integrate into the tricarboxylate acid (TCA) cycle to increase levels of ATP (adenosine triphosphate) production (Lum et al., 2005).

When extracellular nutrients are present, they bind to receptor tyrosine kinases on the plasma membrane surface. This activates mTOR (mechanistic target of rapamycin) via PI3k (Phosphoinositide 3-kinase)/Akt signalling (Lum et al., 2005). Active mTOR suppresses autophagy by hyperphosphorylating Atg13, preventing it from binding ULK1 (Atg1 in *Dictyostelium discoideum*), a protein necessary for the activation of the autophagy signalling cascade. Upon starvation, mTOR is deactivated and Atg13 can bind to ULK1/Atg1 allowing the recruitment of downstream Atg proteins (section 1.1.3).

ULK1/Atg1 is essential for autophagosome initialisation and therefore, ULK1/Atg1 mutants are unable to undergo autophagy. An inability to survive starvation has been shown in a wide variety of species when mutants lack ULK1/Atg1 (or equivalent orthologues) (Maiuri et al., 2007; Bassham et al., 2006).

Proteostasis and organelle removal

Proteostasis is a natural regulated removal of old and/or faulty proteins via the cell clearing systems which include ubiquitin dependant proteosome degradation and autophagy. These differ as the proteosomal degradation targets individual proteins for degradation via ubiquitination and then individually unfolds and feeds proteins through a narrow channel in the proteosome to facilitate disassembly. This process is slower but highly specific, whereas autophagy can degrade large bulky cargo, and is therefore employed to degrade large protein aggregates. Aggregates cannot be removed by the proteosome system due to its inability to unfold the proteins to thread through the proteosome pore (Levine and Kroemer, 2008).

Due to this, autophagy is the only process able to remove protein aggregates as well as other large cargo, including organelles. Autophagy mediates the removal of organelles such as mitochondria (mitophagy), peroxisomes (pexophagy), lysosomes, chloroplasts, and portions of the nuclei (Anding and Baehrecke, 2017). This regulates the quality and number of organelles in the cell and is protective due to the removal of faulty or leaking organelles (e.g. depolarised mitochondria).

Inappropriate protein aggregation and misfolding is a hallmark of several neurodegenerative diseases, including Huntington's disease (dependant on the increased expansion of polyglutamine tract in the Huntington protein), Alzheimer's (due to the increased aggregation of mutant Tau protein), spongiform encephalopathies (due to mutant prion folding protein), α-synucleins in the development of familial Parkinson's disease, and mutant SOD1 (superoxide dismutase 1) accumulation in amyotrophic lateral sclerosis (ALS). These proteins can become misfolded and result in improper protein aggregates due to several causes include genetic mutations and deregulated signalling pathways. Autophagy is required for the removal of these toxic protein aggregates, and therefore loss of functional autophagy is heavily associated with the development and progression of neurodegenerative diseases.

Aggregates can cause further reduction in autophagy by recruiting and retaining autophagy related proteins. This sequesters them from autophagy pathways and further reduces the clearance of aggregates (Shi et al., 2010; Zhang et al., 2007).

Apoptosis

As described in more detail in section 1.1.4, autophagy has an established role in regulating apoptosis. Increased numbers of autophagosomes are seen in cells directly before apoptosis, but whether this functions to prevent apoptosis, or is a prerequisite to certain types of apoptosis is still unknown (Maiuri et al., 2007).

Apoptosis is indirectly suppressed under higher levels of autophagy induction as when Bcl2 is freed from binding with Beclin-1/Atg6 upon autophagy induction, is acts to inhibit Bax and Bak proteins which promote apoptosis (Marquez and Xu, 2012).

Autophagy and cancer

Autophagy has role in both protecting and contributing to cancer progression.

Nutrient deprivation is common in solid tumours with poor vascularisation. Constitutive upregulation of autophagy is therefore found in multiple cancers due to tumourgenic mutations which cause the overexpression of Atg proteins to increase nutrient availability and aid survival (Paglin et al., 2001).

In contrast to its role in aiding tumour survival, autophagy also has a protective affect against cancer development under certain conditions.

The switch between protective and tumourgenic effects of autophagy appears to be dependent on autophagy gene, tissue, tumour severity, and mutations.

Xenophagy

Xenophagy is the removal of intracellular pathogens by autophagy and therefore forms part of the immune defenses. Xenophagy has been reported to

clear many bacterial pathogens including *Mycobacterium tuberculosis* (Gutierrez et al., 2004).

All of these functions of autophagy make it very important for cell homeostasis and disease prevention. Despite the identification of these important roles, not all the machinery involved in autophagosome formation and regulation is known. The primary aim of this project initially was to identify other autophagy related proteins to further our understanding of this pathway.

1.1.3 Mechanism of autophagy

Initiation and nucleation

Autophagy is a highly regulated process which occurs at a low basal level under normal conditions. When required, the rate of autophagy can be rapidly upregulated to increase its degradative capacity. The events that induce autophagy fall into 2 main categories; maintaining intracellular homeostasis (removal of protein aggregates, intracellular pathogens, organelle turnover) and extracellular cues (starvation)(section 1.1.2). In addition to the low basal levels of autophagy, selective autophagy can also occur, whereby autophagosomes form around specific intracellular cargo. Cargo is specified by multiple ubiquitination tags (similar to the ubiquitin-proteosome system) which are recognised by receptor proteins including SQSTMI, OPTN, NBR1 and p62 (the last two of whihc binds to ubiquitinated proteins), which interact with LC3 (Atg8 in *Dictyostelium discoideum*) on autophagosome membranes to link ubiquitinated substrates to autophagy machinery (Farré and Subramani, 2016).

Upon autophagy induction, components of the autophagy initiation complex will begin to accumulate at specialised subdomains of the endoplasmic reticulum known as the omegasome (Axe et al., 2008). Although the initiation machinery is broadly conserved across species, yeast and other fungi have a divergent structure, instead of an omegasome, called the PAS (phagophore assembly site), which is separate from the ER and all other organelles (King, 2012).

The first step in autophagy formation is ULK1/Atg1 binding to Atg13. This pair then binds to FIP200 along with Atg101 and Atg13 to form the ULK1/Atg1 initiation complex. This complex phosphorylates and activates downstream autophagy proteins ready for membrane nucleation including Beclin 1 and PI3K/VPS34 complex.

Phagophore expansion

Upon ULK1/Atg1 initiation complex recruitment to the site of autophagosome formation, the scaffold autophagy proteins Atg11 and Atg17 recruit proteins in order to drive membrane expansion. The autophagosome forms its double membrane by folding over a single, continuous membrane, called the isolation membrane, which then fuses into two membranes upon autophagosome completion.

Membrane for the forming autophagosome is sequestered from the ER membrane adjacent to the omegasome (Novikoff et al., 1971; Tooze and Yoshimori, 2010), but can also come from other membraned organelles such as the mitochondria, endosomes and the plasma membrane (Matsunaga et al., 2010; Mari et al., 2010).

Expansion requires recruitment of the class III phosphoinositide 3-kinase Vps34 (vacuolar protein sorting 34), which is recruited and regulated by a complex formed of Beclin 1 (Atg6 in yeast) and Vps15 (Kang et al., 2011).

This reaction, its addition to the phosphorylation of the phospholipid phosphatidylinositol (PI) in the membrane to phosphatidylinositol 3-phosphate (PI3P), drives membrane expansion (Nascimbeni et al., 2017).

LC3/Atg8 is a 'ubiquitin like' protein due to its conserved ubiquitin like structural fold (Sugawara et al., 2004). Localised diffuse in the cytoplasmic during normal conditions, LC3/Atg8 is conjugated to the lipid phosphatidylethanolamine (PE) on the autophagosome inner and outer membrane. Firstly, its final C-terminal residue is cleaved by Atg4, exposing this site for lipid binding. After this step, it goes through multiple other lipidation steps requiring the ubiquitin-

like enzymes E1 like (Atg7 in yeast) and E2 like (Atg3 in yeast) catalysed by the interaction of Atg12 to Atg5. The final result is the conjugation of LC3/Atg8 to the PE and its incorporation into the autophagosomal membrane (Kirisako et al., 2000). LC3/Atg8 in its lipidated form contributes to membrane expansion of autophagosome through regulating membrane curvature and size.

Autophagosome closure is still not completely characterised but is known to be dependent on ESCRT proteins and Rab5 (Zhou et al., 2017, 2019).

Fusion and degradation

Upon formation of a complete autophagosome, they are loaded onto microtubules to be trafficked to lysosomes, the acidic organelles which facilitate cargo degradation. They are trafficked towards the perinuclear region (retrograde trafficking) where many lysosomes reside.

Once in contact with lysosomes, the outer membrane of the autophagosomes is tethered via proteins including LC3, Atg5 and stx17 on the autophagosomal membrane and Rab7, EPG5 and TECPR1 on the lysosomal surface.

The membranes then undergo fusion (which requires VAMP7,8 and STX17) with the lysosomal membrane to release the inner membraned vesicle into the lysosomes (Nakamura and Yoshimori, 2017). This fused vesicle is called the autolysosome. Cargo is degraded by the catabolic enzymes within the lysosome, such as the acid hydrolases and proteases e.g cathepsin D (Levine and Kroemer, 2008).

The LC3/Atg8 embedded in the outer membrane of the autophagosome is cleaved off by Atg4 and recycled, whereas LC3/Atg8 proteins embedded in the inner membrane are degraded along with the cargo.

Following cargo degradation, their constituent components such as amino acids are released from the lysosome via vacuolar permeases and amino acid transporters (facilitated by Atg22) to be reused in the *de novo* synthesis of proteins.

Autophagy is classed as a lysosomal pathway, meaning the terminal des-

tination of vesicles created are lysosomes. Other lysosomal pathways include macropinocytosis and phagocytosis. Although initiation and formation of these vesicles differ between pathways to suit their different functions, they share much of the same machinery for their degradation, including microtubule trafficking and lysosomal fusion.

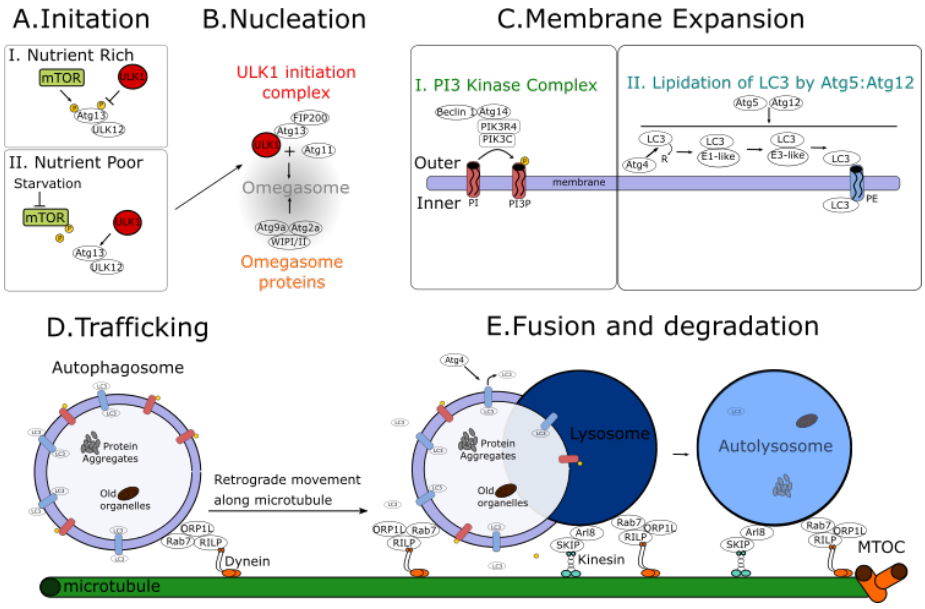

Figure 1.2: **The major steps of autophagy**

The major steps of autophagy as described in section 1.1.3. A. Initiation includes the complexing of ULK1/Atg1 to Atg13 once its hyperphosphorylation by mTOR has been inhibited by starvation. B. Nucleation requires the complexing of ULK1/Atg1 initiation complex and omegasome proteins which accumulate adjacent to the ER to form the omegasome. C. The formation of PI3P as well as the lipidation of LC3/Atg8 to PE on the auotphagosome membrane drives membrane expansion. D. Upon closure, autophagosomes are loaded on to microtubules via adaptor proteins and dynein before being trafficked towards the perinuclear region to contact and fuse with lysosomes for degradation. E. Resulting degraded material is used for nutrients in the cells.

	Dicty/Yeast Name	Mammalian Name	Autophagy Stage	Function
Atg1 protein kinase complex	Atg1	ULK1/2	Initation	Serine/threonine kinase which initaites autophagy upon Atg13 binding
	Atg17	FIP200	Initation	Scaffold protein, subunit of Atg1 complex
	Atg13	Atg13	Initation	sub unit of Atg1 complex, phosphorylated by TOR to prevent binding
	Atg29		Initation	Sub unit of Atg1 complex
PAS complex	Atg9	Atg9A, TTG9B	Membrane nucleation	necessary for PAS accumulation and autophagosome formation
	Atg2	Atg2a, Atg2b	Membrane nucleation	necessary for autophagosome formation
	Atg18	WIPI1, WIP2	Membrane nucleation	PIP3 binding complex necessary for recruitment
PI3 Kinase complex	Atg6/Vsp30	Beclin1	Membrane nucleation and expansion	necessary for autophagosome membrane expansion
	Atg14	Atg14/Atg14L/BARKOR	Membrane nucleation and expansion	involved in membrane expansion complex, may not be essential
	Vps15	PIK3R4	Membrane nucleation and expansion	serine/threonine-protein kinase essential to recruit Atg8/LC3
	Vps34	PIK3C	Membrane nucleation and expansion	phosphatidylinositol 3-kinase essential to recruit Atg8 and Atg12-Atg5 conjugate
	PI (phosphatidylinositol)	PI (phosphatidylinositol)	Membrane nucleation and expansion	lipid on autophagosomal membrane
	PI3P (phosphatidylinositol 3-phospha	PI3P (phosphatidylinositol 3-phosphate)	Membrane nucleation and expansion	lipid on autophagosomal membrane necessary for recruitment of downstream Atg proteins
Atg8Conjugation system	Atg8a	LC3-I, GABARAP, GATE-16	Membrane expansion	Ubiquitin like protein
	Atg8b	LC3-II	Membrane expansion	Lipidation Atg8 proteins, attached to PE on the autophagosomal membrane
	PE (phosphatidyethanolamine)	PE (phosphatidyethanolamine)	Membrane expansion	Lipid embedded in autophagosomal membrane which Atg8 is attached to
	Atg3	Atg3	Membrane expansion	E2- like enzyme bound to Atg8 as a prerequisite to it's lipidation
	Atg4	Atg4a, Atg4b, Atg4c, Atg4d	Membrane expansion	cysteine protease necessary for the cleavage or arginine from Atg8a and cleavage from PE of Atg8b
	Atg7	Atg7	Membrane expansion	E1- like enzymes, binds Atg8 as a prerequisite to it's lipidation
	Atg10	Atg10	Membrane expansion	E2- like enzyme bound to Atg8 as a prerequiste to it's lipidation as well as binding Atg12, and Atg7
	Atg16	Atg16L1, Atg16L2	Membrane expansion	Binds Atg5 as part of the Atg12-Atg5 complex
	Atg12	Atg12	Membrane expansion	Ubiquitin like protein
	Atg5	Atg5	Membrane expansion	Binds to Atg12 to facilitate the lipidation of Atg8 to PE

Figure 1.3: **List of autophagy proteins**

List of the major autophagy proteins involved in macroautophagy and their nomenclature in *Dictyostelium discoideum* /yeast species (first column) and mammalian (second column) proteosomes. Proteins separated by commas indicates there are multiple proteins which share the same function whereas separation by a front slash (/) indicates different names for the same proteins. Blanks in the human names means that homologues have not been identified or may not exist. More comprehensive lists including all identified autophagy proteins (as of 2016) can be found in Wen and Klionsky (2016).

Autophagy is a complex process, and although much of the basic machinery for autophagosome formation is known, our knowledge of all the factors required for functional autophagy is incomplete, including additional factors which may indirectly affect the autophagic pathways and be important for disease. Many of the autophagy genes have been well documented in yeast, but the process of autophagy is different between yeast and mammalian cells. Multiple autophagy genes which are essential for autophagy in mammalian cells are not present in yeast e.g. the omegosome protein Atg101 which is not found in yeast (King, 2012). This suggests that yeast autophagy studies, which much of our knowledge surrounding autophagy is based on, may not have covered all of the essential autophagy genes and many may still be uncharacterised (Tian et al., 2010). Due to the redundancy in the mammalian genome, it can be difficult identify and elucidate the exact role and impact of specific proteins. *Dictyostelium discoideum* represents a good compromise between yeast and mammalian cells, as they have complex autophagy pathways, similar to mammalian cells, but have limited redundancy between proteins.

1.1.4 *Dictyostelium discoideum* as a model to study autophagy

Dictyostelium discoideum is a soil dwelling social amoeba that lives as individual cells, feeding on environmental bacteria but also possesses multicellular life cycle stages. Having first being identified in 1939 (Thom and Raper, 1939), it has been investigated to better understand its complex lifestyle, but is used now as a biomedical model of chemotaxis, phagocytosis, macropinocytosis, autophagy,

and microtubule motors (section 1.3.5). Autophagy in *Dictyostelium discoideum* closely represents mammalian autophagy as they form omegasomes adjacent to the ER, which differs from the PAS formed in yeast. Several genes which are known to be important for mammalian autophagy, but are lost in yeast, have been found in *Dictyostelium discoideum* e.g. VMP1, a Beclin 1 adaptor which functions in autophagosome/ER membrane contact (Wang et al., 2020), and EI24, which is necessary for basal autophagy induction (Devkota et al., 2016; King, 2012).

Dictyostelium discoideum life cycle

Dictyostelium discoideum has a complex life cycle with unicellular and multicellular stages (figure 1.4). As single cells, cells chemotax towards bacterially secreted folate acid and engulf them for nutrients. During this stage, cells feed by macropinocytosis and phagocytosis, both of which rely on lysosomal digestion as autophagy does (Vines and King, 2019). These processes are highly conserved between *Dictyostelium discoideum* and mammalian cells, especially immune cells as both *Dictyostelium discoideum* and immune cells are classed as professional phagocytes.

Over time, single cells will eat the local nutrients until there are not enough to support single cells survival. Under these starvation conditions, cells will begin secreting cAMP (cyclic adenosine monophosphate) and aggregate in a 'slug' of up to 100,000 cells. This slug then travels towards light (phototaxis) and heat (thermotaxis) to the surface, where a fruiting body is formed. During these aggregation stages, genes involved in phagocytosis are downregulated and cells undergo phagocytic suppression. A small number of cells (approximately 1%) will undergo phagocytic upregulation and are responsible for the removal of toxic waste and environmental pathogens whilst the slug travels. These are known as sentinel cells and their function is similar to that of mammalian immune cells (Katoh et al., 2007).

When forming a fruiting body, some cells will take on the role of forming a

stalk whilst others will become part of the spore containing head. Around 20% of cells in the stalk are signalled to undergo vacuolar cell death, forming large cell corpses with a hard exterior, which provide structural support to elongate the stalk (Otto et al., 2003). The stalk will keep growing until it is no longer strong enough to support the weight of the fruiting body and collapses causing the spore to fall into an new environment with abundant nutrients (Strassmann et al., 2000). Here the spore will germinate and release many new *Dictyostelium discoideum* cells which will behave as unicellular organisms until starvation is once again reached.

This process and structure is evolutionary conserved and found in many species across a wide variety of phylum including other amoeba such as Corpomyxa and as far away as bacterium Myxococcus (Du et al., 2015), signifying its usefulness in reaching new nutrient rich areas.

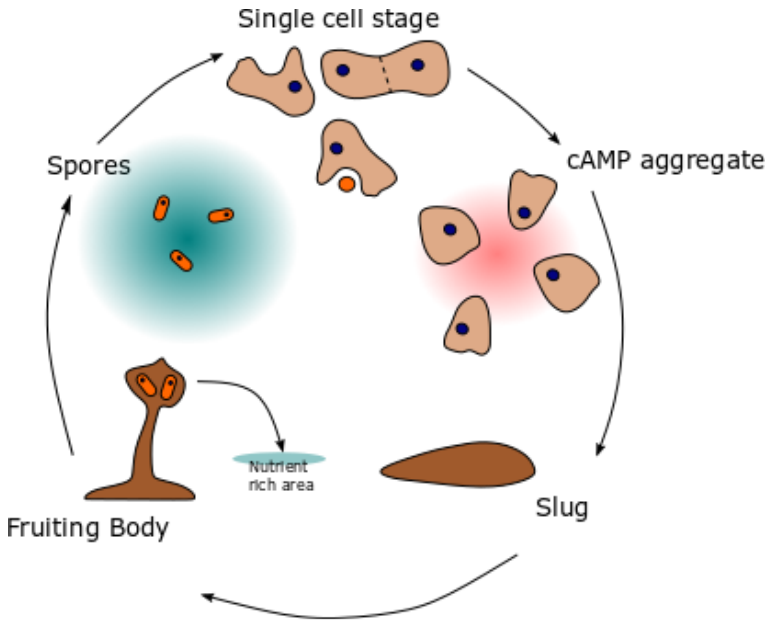

Figure 1.4: **The major stages of *Dictyostelium discoideum* life cycle**

The life cycle of *Dictyostelium discoideum* . At the single cell stage, cells feed on liquid nutrients and phagocytosed bacteria until the local environment becomes depleted of nutri-

ents. Upon starvation, cells clump together dependent on cAMP secretion and chemotaxis. They form a tight aggregate which forms into a slug, the first multi cellular stage. This slug moves towards the soil surface where it forms a fruiting body with long stalk and spore head. The stalk collapses, and the fruiting body lands in a new adjacent area which is (hopefully) nutrient rich. These spores then hatch and mature into single amoebae once more and the cycle repeats itself.

Advantages of *Dictyostelium discoideum* as a model

Dictyostelium discoideum genetics

The entire *Dictyostelium discoideum* genome has been sequenced and includes 6 chromosomes which encode around 12,500 proteins (Eichinger et al., 2005). It contains many gene homologues found in the mammalian genome which have been lost from yeast, including several important genes for autophagy (Torija et al., 2006; Tian et al., 2010; Calvo-Garrido and Escalante, 2010). It also shares a similar complex intracellular architecture to mammalian cells, including features such as a radial microtubule array (Roos et al., 1984; R. Graf, C. Daunderer, 2000; Klopfenstein et al., 2002) and a flexible plasma membrane (Mesquita et al., 2017) which are not found in yeast cells.

Even though *Dictyostelium discoideum* has around double the number of genes of yeast, it has relatively little genetic redundancy and is haploid, making it a good candidate for knocking out genes of interest (Eichinger et al., 2005). *Dictyostelium discoideum* knockout and knockin strains have been generated for many decades using homologous recombination, but due to recent developments using CRISPR, multiple knockout strains can be easily and quickly generated. *Dictyostelium discoideum* is especially suited to CRISPR due to its ease of culturing, speed of duplication, and high efficiency (72.9-100%) of knockouts (Sekine et al., 2018). The reduced redundancy of the *Dictyostelium discoideum* proteome, whilst still maintaining complex machinery, means knockout defects

produce phenotypes similar to mammalian cell defects without the variability (Schapira, 2006; Ae et al., 2009).

Use as a model of intracellular trafficking

The main advantages of *Dictyostelium discoideum* as a model of intracellular trafficking is their consistent phagocytosis and macropinocytosis. Even though both macrophages and neutrophils are also professional phagocytes, they still require initiation for phagocytosis, whereas *Dictyostelium discoideum* requires no induction in tissues culture conditions and has been shown to perform phagocytosis at a higher rate than both these cells (Rupper and Cardelli, 2001). *Dictyostelium discoideum* cells rely on macropinocytosis (in liquid media) and phagocytosis (on bacterial lawns) for their food sources. This allows for easy mutant screening as defects in these two pathways can be easily quantified by growth.

In addition to identified regulatory proteins, *Dictyostelium discoideum* has been used to elucidate the complex and multi staged process of macropinocytosis maturation (Buckley and King, 2017; Vines and King, 2019).

Autophagy conservation in *Dictyostelium discoideum*

Autophagy is necessary for surviving starvation in *Dictyostelium discoideum* , demonstrating the conserved role for autophagy with mammalian cells (Otto et al., 2003; King et al., 2011). *Dictyostelium discoideum* genome contains homologues of many of the mammalian autophagy genes which are not present in yeast, including proteins required in the formation of an omegasome (yeast form a phagophore assembly site (PAS). Therefore, even though previously yeast has been used as a model of autophagy, *Dictyostelium discoideum* is arguably a better model due to its greater conservation at the genetic and mechanistic level. Confusingly, even though *Dictyostelium discoideum* autophagy resembles mammalian autophagy, all of its autophagy genes have yeast nomenclature.

Autophagy in *Dictyostelium discoideum* development

In addition to its classical recycling role, autophagy is also has a role in development in *Dictyostelium discoideum* (Otto et al., 2003). Autophagy is required for surviving starvation, and as most of the *Dictyostelium discoideum* multicellular developmental stages occur under starvation, autophagy has an important role during development. *Dictyostelium discoideum* strains with known autophagy mutations produced fruiting bodies which are shorter and thicker than their wild type counterparts, suggesting that autophagy is required for the remodelling of cells during the fruiting body stage (Otto et al., 2003). The fruiting body is made of dead vacuolated cells which have been surrounded with cellulose to create 'brick' like structures to form the structural basis of the stalk. This vacuolar cell death has been shown to be dependent on autophagy and requires two types of cell signalling; starvation and subsequent cAMP chemotaxis, and then the secretion of polyketide DIF-1. DIF-1 and autophagy together initiate vacuolar cell death, whereas DIF-1 signalling alone results in necrotic cell death (Luciani et al., 2011; Kosta et al., 2004).

In severe autophagy mutants, such as *Atg1*$^{-}$ cells, no fruiting body can be formed due to cells being unable to survive starvation (Otto et al., 2003). In other mutants with milder autophagy defects, cells can survive but are unable to make enough vacuolated dead cells to form a normal fruiting body (Otto et al., 2003, 2004). This demonstrates the combined importance of autophagy in both development and nutrient recycling pathways.

Many essential and regulatory autophagy proteins have been identified and studied in *Dictyostelium discoideum* (Mesquita et al., 2017), although previous work has been focused on identifying essential autophagy proteins which produce very severe phenotypes. There are likely many uncharacterised and/or unknown autophagy regulators which have a non-essential but important role in regulating autophagy.

1.1.5 Using *Dictyostelium discoideum* to identify new autophagy regulators

Identification of katnip

Prior to this project, the laboratory of Richard Kessin (Columbia University, USA now retired) performed a REMI (restriction enzyme mediated integration) genetic screen in *Dictyostelium discoideum* in order to identify new regulators of autophagy. The principle of the screen was based on the change of cell density upon starvation caused by autophagic degradation of the cytosol. After 24 hours' starvation, the increased density of wild type cells can be separated from autophagy mutants, whose density remains unchanged, by centrifugation on a Percoll gradient. This was performed with a pooled library of mutants by the Kessin lab, isolating several mutant lines. These were then further assessed for the autophagy-related phenotypes of disrupted development and inability to survive starvation. However, after identifying the disrupted loci, no further analysis or validation was performed.

One gene identified by this screen was highly conserved with the mammalian gene KIAA0556, which at the time of the screen was completely uncharacterised, although in 2015 was identified as the causative mutation of a subset of Joubert's syndrome cases and renamed katnip (shorten from katanin interacting protein).

The molecular function of katnip was uncharacterised at this time, and no function in autophagy had been investigated. Therefore, the function of Katnip was the main aim of this project.

1.2 Katnip

1.2.1 Features of katnip

Katnip is 7,548bp in the *Dictyostelium discoideum* genome (DD_G0275861) and encodes a 283,196 Dalton (Da) protein. In the human genome, where it is also known as KIAA0556 and JBTS26 due to its role in Joubert's syndrome, it is a 230,253bp gene found at chr16:27,550,119-27,780,371 and encodes a 193,92 Da protein.

Katnip is highly conserved, and the majority of the conserved amino acid sequence fall into its 3 repeats of a domain of unknown function, DUF4457 (figure 1.5). As well as having high conservation between species in this region, there is high sequence similarity between the 3 repeats within the genes themselves.

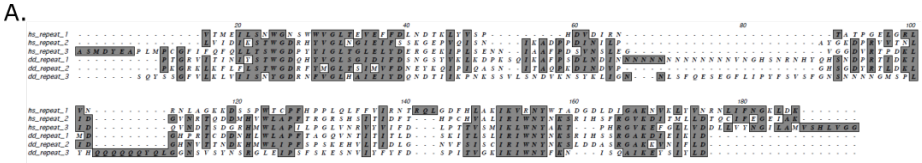

Figure 1.5: **Sequence conservation between human and *Dictyostelium discoideum* DUF4457**

A. The sequence similarity between DUF4457 domains between the 3 repeats of human katnip and *Dictyostelium discoideum* katnip. Residues in dark boxes are conserved, dashes represent unaligned sequence which is too big to correspond.

Katnip has clear orthologues in every branch of the eukaryotic tree with the notable exception of the fungi (including yeast species) and *Drosophila melanogaster* branch, although it is present in other insects. Absence in the main species used for genetic screening may account for the lack of research performed on it.

Although highly conserved across evolution (figure 1.6), DUF4457 is not found in any other proteins, making it unique to katnip. Furthermore, katnip

orthologues show no similarity to any other proteins, meaning that its sequence cannot be used to hypothese on its function.

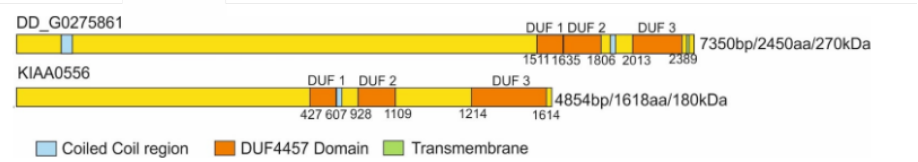

Figure 1.6: **Schematic of katnip mammalian and *Dictyostelium discoideum* genes**

A. Schematic of katnip in *Dictyostelium discoideum* (DD_G0275861) and mammalian (KIAA0556) genomes annotated with protein domains and locations. Small numbers at the base of gene schematics represent the amino acid start and end number of each DUF4457 domain.

1.2.2 Katnip's role in disease

Although initially identified during the KIAA gene screen in 1997 (Kikuno et al., 2004; Ohara et al., 1997), it was not until 2015 that the gene was discovered to be mutated in a multiplex consanguineous family which suffered from Joubert's syndrome (Sanders et al., 2015).

Katnip has been implicated in multiple diseases affecting the brain. Including the identification of heterozygous mutation (either c.2373del or c.4551+1GA) in patients suffering from hypothalamic hamartoma, a tumour growth on the hypothalamus associated with hormonal problems (Fujita et al., 2019). In 2018, a screen was performed in order to identify genes which were deferentially methylated between Alzheimer's patients brain samples with no and very high levels of neurofibrillary tangles (NFTs). NFTs are the result of misfolded Tau protein aggregating into toxic bodies in the brain tissues. Tau is natively a microtubule stabilising protein which dissociates from microtubules following misfolding.

Katnip was one of only 2 proteins identified to be differentially methylated and was significantly less methylated in samples with high tangles grading (grades III - IV) compared to no tangles (grade MA) (Andres-Benito et al.,

2018). This also resulted in the reduced expression of both katnip and katanin in brains samples with high NFTs when compared to control samples. Interestingly katanin was also found to be expressed less in tissues with less katnip expression.

Tau has been previously reported to protect microtubules from katanin dependant severing (Qiang, 2006); it may be that loss of Tau from microtubules signals a downregulation of katanin, and potentially katnip, in order to protect microtubules from severing.

Katnip and Joubert's syndrome

Joubert's syndrome is a group of disorders which present similar symptoms as the results of cilia dysfunction. Cilia are small, microtubule-based projections from the cell surface which are important for cell signalling and fluid flow (section 1.3.4).

The gold standard of diagnosis is presence of molar tooth abnormality in the mid-brain, which is found in patients which have dysfunctional cilia during development (Romani et al., 2013). It is visible with MRI (magnetic resonance imaging) and formed due to the deepened interpeduncular fossa because of underdevelopment of the cerebellar vermis and an abnormal brain stem. These brain development defects are thought to be the result of reduced spinal fluid movement, due to defects in fluid flow caused by reduced cilia beating function and/or number (depending on mutation). These anatomical brain defects result in behavioural symptoms, and in the most severe cases, a complete loss of motor and language skills. A variety of other neurological symptoms are also found, including trouble in moving eyes side to side (oculomotor apraxia), abnormal breathing (apnea), reduced co-ordination (ataxia) (Romani et al., 2013).

In addition to these, there are a range of disorders which have a higher frequency in Joubert's sufferers but are not directly caused by the brain deformations nor found in every patient. These are called 'Joubert's syndrome and related disorders' (JSRD) and include retinal dystrophy, endocrine disorders,

and a higher propensity to develop liver and kidney disease (possibility due to endocrine imbalance).

Katnip has so far been implicated as the causative gene mutation in 7 confirmed cases of Joubert's syndrome from 4 different families (Sanders et al., 2015; Roosing et al., 2016; Cauley et al., 2019; Niceta et al., 2020), although it is likely that there are more Joubert's patients who carry katnip mutations but have not been genetically tested. All the identified families carry different homozygous mutations, recorded at c.2674C T (Sanders et al., 2015), c.4220del (Roosing et al., 2016) and c.3756dupC (Niceta et al., 2020)(mutation reported in Cauley et al., 2019 could not be accessed). The c.2674CT mutations reported in Sanders et al. (2015) was confirmed to lead to a complete loss of the protein, whereas the other mutations where not assessed.

Patients carrying Joubert's-causing mutations in katnip exhibited classical molar tooth abnormalities, JSRD and other symptoms including global developmental delay, hypotonia, uncontrolled eye movements, and moderate endocrine defects which required hormonal supplements (including growth hormones).

Similar phenotypes were also observed in animal models lacking katnip orthologues. Similar brain defects were replicated in mice carrying a homozygous mutation in the orthologue of katnip, and had reduced cilia beat frequency and ventricular fluid movement (Sanders et al., 2015). Zebrafish carrying a mutation of the orthologue of katnip exhibited defects associated with classical Joubert's gene mutations (Lee et al., 2012) including curly tails, smaller head and abdominal edema (Roosing et al., 2016) (brain morphology was not investigated in these mutants).

To investigate cilia structure upon katnip disruption, 2 *C. elegans* strains were created carrying two mutants both resulting in shortened mRNA of katnip (208aa and 132aa compared to native 568aa). Both strains exhibited severe loss of microtubule organisation in the cilia; a reduced A-tubule number (40% reduction) and 'ectopic doublets'; doublets which were localised outside the usual circular microtubule organisation of motile cilia (section 1.3.4, figure 1.10).

Katnip mutations have also been linked to concomitant mutations (mean-

ing there is an above average occurrence of mutations in both genes) in other ciliopathy-related genes including kif7, a kinesin like protein important for the transport of neuronal receptor NMDAR (N-methyl-D-aspartate receptor)(Niceta et al., 2020) and ADGRV1, a G-coupled protein receptor which is thought to be important for intracellular protein transport at the plasma membrane (Roosing et al., 2016).

1.2.3 Katnip's protein interactors

Tandem affinity mass spectrometry was used to identify the protein interactors of katnip, and identified multiple tubulin subunits and other MAPs (microtubule associated proteins) suggesting that katnip can interact with microtubules. All of the katanin subunits were also identified, as well as multiple IFT (intraflagellar transport) proteins found in cilia (Sanders et al., 2015).

Katnip and microtubules

All the data from animal models provides further evidence of a conserved role of katnip in cilia regulation and animal models exhibit symptoms similar to those found in Joubert's patients. Data from *C. elegans* further implicates a role for katnip in regulating microtubule organisation in cilia.

Cilia on patient derived fibroblasts were found to be less numerous and longer when compared to fibroblasts harvested from familial controls. Tagged katnip constructs (both GFP and TAP tagged) were observed to localise to the basal body of the cilia in hTERT-RPE1 cell lines and lightly decorate the length of the cilia (overlapping with acetylated tubulin staining) with an enrichment at the tip (Sanders et al., 2015).

Cells expressing high amounts GFP-katnip had a greater resistance to Nodocazole, a microtubule depolymerisation agent which depolymerises unstable microtubules. Upon very high expression of GFP-katnip, enrichenment on cilia microtubules was observed, which was hypothesised by the authors to increase microtubule acetylation levels and therefore stability, resulting in the greater

resistance to Nocodazole, although this was only hypothesised and not tested.

GFP-katnip also pelleted with microtubules in a pull-down assay, suggesting it binds to microtubules and Sanders et al. (2015) also comments that the tagged construct appeared to localise to 'filamentous structures' in the cytoplasm, but did not expand on this any further.

This is evidence that katnip's role may not be just limited to the cilia and might affect interphase microtubules as well. *Dictyostelium discoideum* have the katnip gene but no cilia. Therefore, there must be a more general, non cilia specific role for katnip. This may be as a microtubule regulator which affects all microtubules and, in turn, affects autophagy, as identified by the REMI screen.

1.3 Microtubules

In addition to its role in cilia microtubule regulation, data suggest that katnip may bind to interphase microtubules, although how it might is completely unknown. Microtubules are formed from α and β-tubulin subunits which associate into heterodimers before self-assembling into a microtubule in the presence of guanine triphosphate (GTP). Complete microtubules have a biopolymer structure which undergo dynamic instability whereby they cycle through periods of stochastic shortening and lengthening dependant on the concentration of available tubulin ((Mitchison and Kirschner, 1984), figure 1.7). Microtubules are regulated through the alteration of tubulin structure and binding of proteins to affect this dynamic instability. This leads to a complex and adaptable regulation which allows microtubules to have their wide and varied set of functions.

1.3.1 Microtubule structure and dynamics

Microtubule nucleation

α and β-tubulin

Tubulin subunits are encoded by 18 different tubulin isoforms (8 α and 8 β) in the human genome and are deferentially upregulated in different tissues dependent on microtubule function. All tubulins are globular proteins of around 450 amino acids in length and 50kDa each. α and β-tubulin endogenously complex in the cell to form tubulin heterodimers which exist freely in the cytoplasm until polymerisation. Tubulin proteins fold to form guanine nucleotide pockets (Nogales et al., 1999) on their N-terminus, which can bind GTP. In α -tubulin, this is a non-exchangeable reaction, whereby GTP is hidden within an 'N-site' and cannot be reached by GTP exchange factors (GEFs) for hydrolysis. However, in β-tubulin, the protein folds differently (due to differences in amino acid code) causing the GTP to be exposed, following which it is known as the E-site (Downing and Nogales, 1998). Once bound to GTP, both tubulins take

on a straight conformation which facilitates their integration into microtubules. However, as the GTP in β-tubulin is exposed, it can be hydrolyzed into GDP (guanine diphosphate) via GEF activity, causing it to undergo a conformational change into a curved conformation. In this conformation, β-tubulin more readily dissociates from microtubules.

γ-tubulin

γ-tubulin is a subtype of tubulin responsible for acting as a seed for microtubule polymerisation (Oakley and Oakley, 1989). γ- tubulin complexes with other proteins into a γ-tubulin ring complex (γ-TuRC), which is localised at microtubule organising centres (MTOC) along with δ and ϵ-tubulin which play a role in centriole structure.

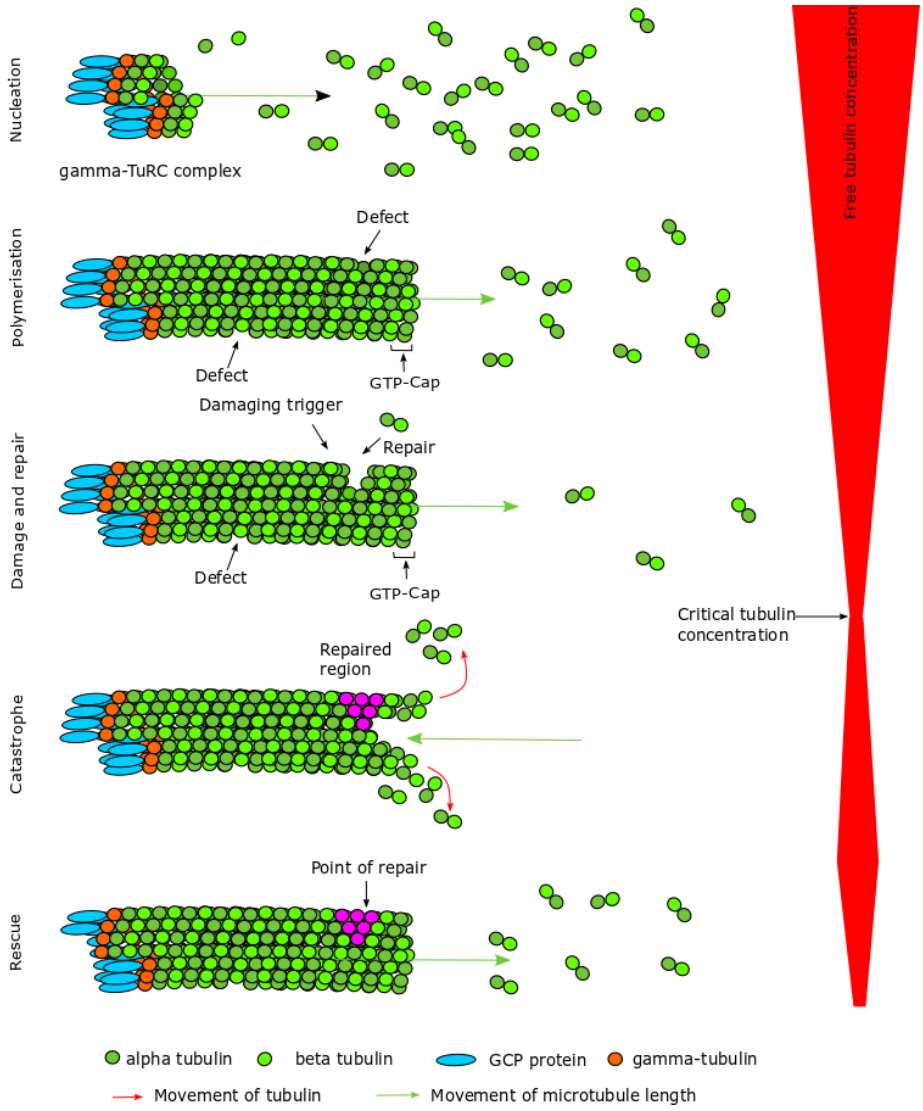

Figure 1.7: **Dynamic instability of microtubules**

Microtubules are nucleated by γ-TuRC complex formed of 13 GCP (γ-tubulin complex component protein) proteins and γ-tubulin subunits. From this base, α and β-tubulin dimers polymerise into microtubules.

Microtubule organising centres (MTOCs)

Microtubule organising centres are any site where microtubule formation begins.

Normally associated with γ-tubulin dependent microtubule polymerisation from the nuclear tethered centrosome, they are also found in the basal body for cilia microtubule growth and at the edge of polymerised epithelial cells.

Incubation of α and β-tubulin with GTP is enough to induce microtubule formation *in vitro*, but within the cell, this is a highly regulated process catalysed from γ-tubulin seeds. γ-tubulin complexes with GCP (γ-tubulin complex proteins) to make the γ-TuRC complex providing the structural basis of the ring shape of microtubule (Oakley et al., 2015). From this template, heterodimers of α and β-tubulin (α first) bind to the γ-tubulin and polymerise away from the ring.

Therefore, the γ-TuRC complex is responsible for the number of protofilaments the resulting microtubule has, although the protofilament number can shift during polymerisation, constituting a form of microtubule damage ((Chretien et al., 1992), section 1.3.3).

During interphase, microtubules polymerise from γ-TuRC seeds and spread out across cytoplasm. α and β-tubulin subunits polymerise end to end into protofilaments, with the minus end (ending with a α -tubulin) at the seed and the plus end (ending with a β-tubulin) polarising them.

The γ-TuRC complex remains attached to the microtubules, and prevents both the polymerisation and depolymerization from its plus end (Kollman et al., 2011).

Centrioles

Centrioles are specialised microtubule structures which make up part of the MTOC, responsible for nucleating microtubules. They are formed upon the complexing of spindle assembly abnormal protein 6 (SAS-6) which assemble at 40^oC angles forming a ring providing the centrosome with its distinct cartwheel shape (Kitagawa et al., 2011; Van Breugel et al., 2011). From this, γ-TuRC seeds form 9 short microtubules which are arranged into straight triplets and extend from the assembled SAS-6 ring to form a hollow cylinder. The microtubules in centrioles are heavily post translationally modified, including high levels of

acetylation, detyrosination, polyglycylation, and polyglutamylation (Magiera and Janke, 2014) and grow more slowly than their dynamic cytoplasmic counterparts (Gönczy and Hatzopoulos, 2019).

Centrosomes

A centrosome is formed of two orthogonal centrioles which recruit a dense protein cloud around them called the pericentriolar matrix (PCM) (Woodruff et al., 2014).

During mitosis, these two centrioles separate to nucleate the kinetochore, interpolar and astral microtubules at polar ends of the spindle. Post mitosis, centrioles will duplicate, the original centriole (the mother) acting as a template for the duplicated one (the daughter). The daughter centriole will then be tethered orthogonally to the outer nuclear envelope acting as a MTOC in the resultant daughter cell.

Centrosomally associated proteins have a variety of functions including regulating microtubule polymerisation, organisation, and mitosis. Katnip was observed to localise to the centrosome in hTERT-RPE1 cells (Sanders et al. (2015)).

Microtubule polymerisation

The polymerisation of tubulin into microtubules is facilitated by the incorporation of GTP into α and β-tubulin subunits. This structurally alters the tubulin monomers to straight conformations allowing incorporation into microtubules. GTP binding alters the position of the structural M-loop in tubulin, allowing it to come into contact with the GTP binding domain of the adjacent tubulin and bind (Amos and Schlieper, 2005). Upon incorporation into the microtubule lattice, the unstructured C-terminal end of the tubulin, the 'tubulin tail', sticks up away from the main body, allowing for binding of enzymes which post-translationally modify tubulin to further regulate protein binding and microtubule stability (section 1.3.2).

Tubulin protofilaments, made up of single chains of end-to-end α and β-tubulin subunits, are laterally connected through homodimer interactions (e.g. α-tubulin to α-tubulin interactions) (Downing and Nogales, 1998). Regular mammalian microtubules are formed of 13 protofilaments, as this number leads to the smallest amount of twisting, allowing microtubule motors to walk along straight protofilaments for long distances (Hirokawa, 1998; Vale, 2003). Protofilament number is set by the centrioles in mammalian cells (section 1.3.1), but varies between species (Chaaban and Brouhard, 2017). Specialised microtubule structures are constructed via different tubulin isoforms (Amos and Schlieper, 2005) and polymerisation conditions (Mitchison and Kirschner, 1984).

In order to stabilise microtubules during polymerisation, a GTP bound tubulin cap is added to the growing end of the microtubule. A single GTP-tubulin monomer is enough to stabilise an entire protofilament (Caplow and Shanks, 1996) and increases the stability of the microtubule whilst growing as it prevents the hydrolysis of GTP-tubulin from the minus end. Loss of this cap is a pre-requisite to catastrophe.

Microtubule polymerisation is dependent on the tubulin concentration in the local area. If the critical concentration is reached or exceeded, tubulin monomers will be incorporated into the growing microtubule, but below this, microtubules switch to depolymerisation. This leads to tubulin monomers being released back into the local area, increasing the concentration again.

Upon microtubule polymerisation, the plus end always ends with a β-tubulin subunit where minus ends always end with an α -tubulin. This means that the plus end is much more dynamic than the minus end, as they can polymerise and depolymerise more quickly due to the exposed E-site in β-tubulin, although some microtubule polymerisation can still occur at the minus end (Tran et al., 1997).

Microtubule depolymerization and catastrophe

All GTP bound to β-tubulin will eventually be hydrolysed given time. GTP hydrolysis of the E-site of β-tubulin is slow (0.054 min per reaction), but the final distal minus end β-tubulin subunit is eventually hydrolysed causing depolymerisation of the microtubule and giving microtubules their dynamic instability (David-Pfeuty et al., 1979; Mitchison and Kirschner, 1984).

This happens at the end of the microtubules, as the forces of neighbouring tubulin in the microtubule shaft prevent curved tubulin monomers escaping. Depolymerization travels down the microtubule, towards the minus end, as the minus end peels away.

The switch between microtubule polymerisation and depolymerization is known as microtubule catastrophe and behaves stochastically (Desai and Mitchison, 1997).

Polymerised microtubules' energetic state means neighbouring tubulin subunits have very little energy connecting them. Therefore, polymerised microtubules are always very close to their depolymerisation conditions. Because of this, microtubules require little energy to catalyse depolymerisation, and are able to respond to cellular cues very quickly (Triclin et al., 2018). Their sensitivity and speed of switching between polymerisation and depolymerisation allows them their dynamic behaviour.

Microtubule rescue

The change from microtubule depolymerisation to polymerisation is known as microtubule rescue. For many years, the points along microtubules where depolymerisation halted and polymerisation began appeared stochastic, but new research has shown that repaired microtubule defect sites (Dimitrov et al., 2008; Schaedel et al., 2019), CLASP binding (Lawrence and Zanic, 2019; Al-Bassam et al., 2010; Aher et al., 2019), and accumulation of MAP2 (Jr and Williams, 1993; Itoh and Hotani, 1994) can induce microtubule rescue. Microtubule rescue is still dependant on the critical tubulin concentration, and proof of this concept

has been shown *in vitro* where higher concentration of free tubulin induces more rescue events (Tran et al., 1997).

1.3.2 Regulation of microtubules

Microtubules are essential for many different mechanisms in the cells, and are tightly regulated through many pathways in order to allow a diversity of function. These mechanisms include; controlling tubulin concentration, alterations to tubulin structurally through the addition of post transitional modifications, and the interactions of MAPs which can associate with and affect microtubule dynamics.

Post translational modifications

One of the major ways in which microtubules are altered post formation is by post translational modification (PTM) of tubulin. Many of these PTMs occur by enzymes binding the exposed C-terminal tails on tubulin monomers which protrude from the microtubule and are able to change the structural conformation of tubulin and therefore the behaviour of the microtubule as a whole. PTMs can also alter the binding affinity and subsequent recruitment of microtubule associated proteins.

Acetylation

Tubulin acetylation is the best characterised PTM, but is unusual compared to others as its site is within the microtubule lumen (at Lysine 40 of α -tubulin) and therefore inaccessible from the outside (L'Hernaul and Rosenbaum, 1985).

An acetyl group is attached to Lysine(K)40 by the acetyltransferase, α-TAT1 enzyme (Akella et al., 2010; Kalebic et al., 2013) and removed by histone deacetylase 6 (HDAC6) in mammalian cells (Hubbert et al., 2002). Interestingly, recent work on tubulin methylation has shown that the methyl group is also loaded at K40 and therefore competes with acetylation at this site (Park et al., 2016).

Acetylation was thought to stabilise microtubules due to its accumulation on long-lived microtubules, although it has been suggested that it is actually a marker of microtubule age and that microtubules gain more acetylation over time (Garnham and Roll-Mecak, 2012).

Although its exact role in stabilising microtubules is still being elucidated (despite acetylation being a well characterised marker of stable microtubules), acetylation can prevent microtubule damage expansion and therefore increases microtubule survival as detailed in section 1.3.3.

Microtubules in neurons and cilia are hyper acetylated and as many as 100% of microtubules in both can be acetylated, indicating their high stability and longevity (LeDizet and Piperno, 1987).

MAPs; Microtubule associated proteins

Microtubule associated proteins (MAPs) are any proteins which are able to associate with microtubules. Many have been identified and some directly affect microtubule organisation, dynamics or stability. Others associate with microtubules as part of their function but do not affect microtubule behaviour, e.g. microtubule motor proteins (section 1.3.4). These MAPs are in turn regulated via their expression or activation state by other signalling pathways as well as by tubulin isoform or PTM binding preference, allowing a complex network of regulation.

MAPs which stabilise microtubules tend to bind sections across multiple tubulins for long periods, acting as crosslinkers across tubulin monomers and protofilaments (e.g.CLASP2α) and/or preferentially binding tubulin in its straight conformation. Destabilising MAPs provide energy via ATP hydrolysis to bring microtubules closer to their depolymerisation conditions e.g. kinesin-13 (Walczak et al., 1996).

Microtubule severing

Microtubule depolymerisation is specific to the end of the microtubules, where the final β-tubulin undergoes hydrolysis and catalyses depolymerisation from the plus end. Hydrolyzed tubulin monomers in the microtubule shaft are locked within the tight lattice by surrounding tubulin monomers, preventing depolymerisation from these points.

Microtubule severing enzymes circumvent this and can release tubulin monomers from anywhere along the microtubule by cutting microtubules orthogonally. This exposes tubulins and can result in the depolymerisation of the rest of the microtubule from this point.

Microtubule severing enzymes bind the C-terminal tails of tubulin and pull them out of the microtubule lattice (Roll-Mecak and Vale, 2008). An increase in the negative charge of the tails by certain PTMs, including acetylation and polyglutamylation, increases the binding of these positively charged enzymes, leading to more severing of certain microtubules (Lacroix et al., 2010; Sudo and Baas, 2010). This spatially constrains severing enzymes to certain microtubules and these enzymes are tightly regulated through their transcription and activation due to their capability to destroy the microtubule network.

There are 3 known microtubule severing enzymes; katanin (McNally and Vale, 1993), spastin (Hazan et al., 1999) and fidgetin (Cox et al., 2000). All of them fall within a subfamily of the AAA (ATPase associated with diverse cellular activities) ATPases, which all contain the highly conserved AAA protein domain which encodes the ATPase. There is also a fourth member of this family, Vsp4, which contains this domain but has no reported microtubule severing function (Frickey and Lupas, 2004; Sharp and Ross, 2012).

Katanin

Katanin is made up of two sub-units, p60 (KATNA1) which contains the ATPase activity and p80 (KATNB1) which acts as a regulatory unit and localises

to the centrosome. Both have a cytosolic pool in over expressing cells although this hasn't been confirmed in endogenous cells (K.P. McNally, O.A. Bazirgan, 2000).

An active katanin complex is formed of 6 katanin proteins arranged in hexameric structure which forms a complete ring upon ATP binding (Zehr et al., 2017). This ring has 6 radial spokes which harbour katanin's microtubule binding domain, necessary for the binding and subsequent severing of microtubules. Whether katanin binds as a wheel orthogonally to the microtubules, or lies on its side when removing tubulin monomers is still unknown (Sharp and Ross, 2012).

Tubulin C-terminal tails are threaded through the central AAA pore causing the disassembly of proteins, although how this local loss of single monomers propagates to complete microtubule severing is still unknown.

Katanin is highly expressed in neurons, and has a preference for acetylated microtubules found in abundance in neurons. But, this is balanced by high expression of Tau in these tissues, which protects microtubules from katanin severing (Qiang, 2006). It has been hypothesised that the relocalisation of hyperphosphorylated Tau in Alzheimer's disease (AD) from microtubules causes the associated loss of microtubule mass as microtubules are vulnerable to katanin severing which leads to further dysfunction in these cells (Qiang, 2006; Sudo and Baas, 2010).

Katanin has well characterised functions in mitoisis, cilia generation and degradation, and neuronal function. During mitosis, it localises to the centrosome and kinetochores in order to induce microtubule shortening during spindle separation (Rogers et al., 2005), and is involved in midbody separation during cytokinesis (Errico et al., 2002). In neurons, it is responsible for the severing of microtubules from MTOCs, releasing short microtubule lengths necessary for new microtubule seeding in axonal branching and neurite outgrowth (Kapitein and Hoogenraad, 2015). Katanin has an unusual involvement in cilia biogenesis where it is necessary for the creation of the central doublet in motile cilia (Dymek et al., 2004) but also specifically severs the outer doublets when over-

expressed in cilia, whilst the middle doublet remains unaffected (Sharma et al., 2007). It is also necessary for the deciliation of cells upon mitosis initiation, where it severs cilia microtubules at the transition zone, just above the basal body (Sharp and Ross, 2012).

Katanin regulation is key to microtubule homeostasis due to its strong activity and severing effects in microtubules. Whilst some of these regulatory pathways have been identified (Tau binding, oligomerisation, ATP binding, tubulin PTMs), several questions remain surrounding katanin activity. These include how katanin selects microtubule areas to sever, how katanin is targeted to these regions, and how it binds there. Katanin has few known binding partners (including katnip), is expressed natively at low levels and is difficult to image (due to overexpression causing microtubule network disintegration), making these questions difficult to answer.

Spastin

Spastin has been researched due to its involvement in familial hereditary spastic paraplegia (HSP). Disregulated spastin severs a subset of microtubules in long axons causing loss of function in legs over time (Hazan et al., 1999). HSP provides good evidence that the microtubule severing enzymes require tight regulation as both downregulation and upregulation of spastin has been linked to HSP pathogenesis (Evans et al., 2005; Solowska et al., 2014). It is likely that loss of regulation of spastin is particularly problematic in neurons due to its increased expression in neuronal tissues and preferential severing of polyglutumylated microtubules, which are abundant in neuronal microtubules (Lacroix et al., 2010).

1.3.3 Microtubule damage

Microtubule defects

During the polymerisation process, microtubules have defects incorporated into their structure by mistake. These manifest as changes in the regularity of the

lattice, such as changes in the protofilament number throughout their length (Chretien et al., 1992), incomplete tubulin monomer integration resulting in gaps in the lattice, and possibly, GDP-tubulin monomer incorporation (rather than GTP-tubulin) (Dimitrov et al., 2008). GDP-tubulin monomers are also incorporated into microtubules through repair mechanisms, but whether they are also incorporated by mistake during polymerisation is unknown.

Both changes in protofilament numbers and holes in the lattice can abrogate microtubule trafficking, as motors that 'walk' along single tubulin protofilaments will either halt or disassociate off the microtubule if the protofilament is disrupted (Liang et al., 2016; Ray et al., 1993; Yildiz et al., 2004). The decision to either pause or dissociate is dependent on the number of motors connected to the cargo; cargo with fewer motor attachments are more likely to dissociate, whereas cargo with many attachments are more likely to pause due to attachment to surrounding protofilaments (Liang et al., 2016).

In vitro, the error rate during microtubule polymerisation can be altered by changing the polymerisation conditions, including the salt concentration, free tubulin concentration, speed of polymerisation, and the presence of certain microtubule associated proteins (Chretien et al., 1992; Aumeier et al., 2016; Gramlich et al., 2017). There is a general trend towards rapidly polymerised microtubules containing more defects. Doublecortin and EB1, both of which bind to microtubule ends to stabilise them, have been reported to only bind and stabilise microtubules with 13 protofilaments, and therefore act as a form of selection towards microtubules formed of the correct number of protofilaments (Vitre et al., 2008; Bechstedt and Brouhard, 2012).

Microtubule damage triggers

Microtubule defects can worsen through stressing triggers to become microtubule damage, where larger sections of the microtubule lattice around the defect is depolymerised. Due to the lack of specific microtubule damage markers and effective protocols to induce microtubule damage *in vivo*, much of the work on microtubule damage is limited to *in vitro* studies and hypotheses.

It is hypothesised that defects can worsen due to the propensity of tubulin to depolymerise at points where the lattice lumen is exposed. How exactly these holes propagate into the surrounding lattice is unknown currently. It may be that the reduction in regularity of the lattice results in fewer connections between adjacent protofilaments, allowing the local hydrolysis of β-tubulin from these points.

One trigger hypothesised is mechanical stress; both bending of the microtubules (Schaedel et al., 2015; Aumeier et al., 2016) and force exertion on microtubules (Chretien et al., 1992; Hawkins et al., 2010) have been investigated *in vitro*. Both these processes occur naturally in the cells due to microtubule function, including buckling under microtubule motor forces generated as they move along the microtubule (Triclin et al., 2018), rearrangement of microtubules and fluid flow (especially in cilia (Schaedel et al., 2015)). It has been hypothesised that spindle microtubules also accumulate microtubule damage during anaphase due to the labelling of GTP-tubulin, a possible marker of microtubule damage and/or repair, along anaphase microtubules (Dimitrov et al., 2008). This may be due to the large forces experienced by these microtubules when pulling chromosomes into the new daughter cells. Increased GTP-tubulin incorporation has also been observed at sites of microtubule crossover and bundling, indicating that these two organisations may induce local microtubule damage, possibly due to mechanical stress (Zhang et al., 2013; Aher et al., 2019).

Microtubule bending has been shown to damage microtubules *in vitro* as lattice stiffness and recovery is reduced with incremental rounds of bending (Schaedel et al., 2015) and the lattice eventually becomes unable to return to its original straight conformation. Bending of lattice materials concentrates forces at areas of pre-existing holes i.e. microtubule defects. Concentrated forces may be able to overcome the threshold maintaining microtubule lattice organisation specifically at defects, whilst the rest of the lattice is unaffected, and induce local depolymerisation (Chretien et al., 1992).

Oxidative damage via laser ablation has also been used in *in vitro* microtubule damage experiments and is hypothesised to induce local microtubule

lattice damage (Schaedel et al., 2015; Aumeier et al., 2016), although this has not been observed at the lattice level. Very high levels of laser have been used to artificially sever microtubules (which can be observed when the plus end of microtubule dissociate away from the lasered site), so the use of less powerful lasers is hypothesised to induce breakages replicating local microtubule damage.

Protection of microtubules from damage

The addition of acetyl groups to the C-terminal tails of tubulin (acetylation, section 1.3.2) has been shown to prevent the spread of microtubule damage and protect microtubule integrity *in vitro*. Acetylation increases the flexibility between adjacent tubulin monomers, which is hypothesised to protect them from damage by making them more resistant to forces applied, and less brittle (Portran et al., 2017; Garnham and Roll-Mecak, 2012).

Acetylation is an interluminal post-translational modification catalysed by acetyltransferase α-TAT1 enzyme (α-tubulin N-acetyltransferase) which requires access to the microtubule lumen (Coombes et al., 2016). Areas of damage gain more acetylation as α-TAT1 has increased access to the lumen, selectively protecting areas of microtubule defects/damage and preventing damage from further propagation (Portran et al., 2017; Szyk et al., 2014).

As further evidence of acetylation's protective affect against microtubule damage, increased microtubule breakages were observed in hTERT RPE-1 cells which were depleted of α-TAT1 (Xu et al., 2017). *C. elegans* lacking the α-TAT1 enzyme orthologue resulted in loss of microtubule organisation and eventual complete loss of microtubule function (Topalidou et al., 2012; Cueva et al., 2012). This could be due to increased microtubule damage in cells lacking acetylation, although this was not directly tested. These studies suggest that microtubule acetylation is required for both maintaining correct microtubule organisation and resistance to microtubule damage.

Katanin's role in microtubule damage

An overview of katanin's role as a microtubule severing protein is detailed in

section 1.3.2. How katanin chooses sites to sever is unknown, but in both models and *in vitro* experiments, katanin has a preference to sever at microtubule defects (especially protofilament number shifts)(Díaz-Valencia et al., 2011; Davis et al., 2002). Models of katanin severing were only compatible with biological data when regular defects were added to microtubules, and therefore katanin may require defects for severing (Davis et al., 2002).

It has been hypothesised that katanin is only able to sever from the inside of the microtubule lumen. This would spatially constrict katanin to sites of exposed lumen including microtubule damage, where the lattice is broken and katanin can enter (K.P. McNally, O.A. Bazirgan, 2000).

Katanin has also been reported to sever at the GDP-tubulin/GTP-tubulin interface, this combination is only found at the ends of capped microtubules and at areas of repaired microtubule damage (Díaz-Valencia et al., 2011).

Katanin also preferentially severs at points of microtubule crossovers and bundles, both of which have previously been reported to exacerbate microtubule damage (Mao et al., 2017; Aumeier et al., 2016).

Microtubule repair

In many cells, microtubule damage will naturally be removed by the constant turnover of microtubules via dynamic instability and mitosis. However, post-mitotic cells with long lived microtubules, including neurons and cilia, do not undergo this regular removal and therefore accumulate microtubule damage over time.

It was hypothesised by Schaedel et al. (2015) that cells must have processes to restore their microtubule's material integrity, otherwise these long lived microtubules would gain excessive microtubule damage and lose functionality over time.

The first experimental evidence for microtubule repair was the finding that resting periods (100 seconds minimum) between bending cycles resulted in microtubules regaining their stiffness whereas immediate continuous bending cycles resulted in material fatigue (Schaedel et al., 2015). Importantly, in *in vitro* stud-

ies, repair only required the presence of free tubulin. It has been suggested that GTP-tubulin is naturally attracted to and incorporated into these damaged areas by exposed interluminal tubulin (Dimitrov et al., 2008; Aumeier et al., 2016). It may be that this replacement process is the time factor which allows microtubules to regain structure integrity (Schaedel et al., 2015).

This agrees with previous data which showed that free tubulin incorporates at points of microtubule crossover, bending and bundling, all known to be initiators of microtubule damage (Aumeier et al., 2016). Dimitrov et al. (2008) had previously reported the existence of GTP-tubulin patches throughout microtubules, rather than just the ends, where expected. Although unknown at the time, these are now thought to highlight areas of microtubule damage, where GTP-tubulin has been incorporated as part of the repair process. This may be a similar mechanism to the recruitment of a GTP-tubulin cap during microtubule growth (section 1.3.1).

Although microtubule self-healing only requires free tubulin to be present *in vitro* (Schaedel et al., 2015), it is likely that the process is regulated by a variety of MAP proteins in the cellular environment. Very high levels of free tubulin were used in *in vitro* microtubule repair experiments, and MAPs may be required to repair under normal conditions. Very little is known about this process, but it could be regulated similarity to microtubule polymerisation, which similarly only requires free tubulin *in vitro* but is known to have many regulating MAPs *in vivo*.

Potential candidates include the CLASP family of proteins; microtubule nucleators which have recently been shown to bind GTP-tubulin patches along the microtubules. They contain 3 TOG2 domains, a low affinity microtubule binding domain, which has been shown to be sufficient to stimulate microtubule repair at points of oxidative microtubule damage. *In vitro* microtubules also appeared to soften less in the presence of CLASP2a when exposed to oxidative damage (Aher et al., 2020).

Once repaired, the areas of damage would theoretically be homogeneous to the rest of the microtubule lattice; but the resistance of repaired areas to

depolymerization suggests otherwise.

Points of microtubule damage which underwent rescue are less likely to subsequently depolymerize, resulting in repaired microtubules having longer lifetimes compared to native microtubules (at least 5x as long (Aumeier et al., 2016)). Microtubules were observed to depolymerise to the point of repair and then start repolymerising from this point, suggesting that there is some form of 'memory' in repaired patches compared to the rest of the microtubule (Schaedel et al., 2015). This somehow catalyses the repair of microtubules from these points; this could be structural or protein binding based.

1.3.4 Functions of microtubules

Microtubules have many diverse functions and therefore have many distinct organisations adapted for each function. The dynamic nature of microtubules, as well as their complex regulation, means they can quickly be remodelled for different functions dependent on the cell needs.

Trafficking

Microtubules are necessary for the trafficking of cargo around the cytoplasm in multiple pathways. Included in this is the movement of extracellular cargo packaged into endocytic vesicles and autophagosomes towards lysosomes for degradation either for nutrients or sensing the extracellular environment.

Trafficking along microtubules is constant during interphase, and therefore default organisation of microtubules in interphase is suited to this function. Microtubules are nucleated radially from the centrosome, across the cytoplasm for efficient capture of cargo. Most mammalian cells have a single MTOC at the centrosome and all cargo captured by microtubules ultimately arrives at the perinuclear region where lysosomes are clustered (Korolchuk et al., 2011).

Cargo for microtubule trafficking is attached to adaptor and linker proteins which then load cargo onto the microtubule motor proteins, kinesin and dynein. Motor proteins walk along single protofilaments of microtubules in an antero-

grade (towards plus end, cell periphery) or retrograde (towards minus end, perinuclear region) fashion (figure 1.8).

Due to the energy necessary to drive kinesin and dynein stepping along the microtubules, force is dissipated along the microtubule as motors move (16kT per step for kinesin (Kawaguchi, 2008; Block, 2007)).

Kinesins and dyneins are essential to position organelles within the cell, and mutations cause localization defects in many organelles including lysosomes, Golgi and mitochondria, and affect the function of these organelles (Korolchuk et al., 2011).

Mature neurons rely heavily on microtubules for trafficking due to their long extensions and large size (Maday and Holzbaur, 2014). Evidence of this can be seen in the range of neurodegenerative and neuroinflammatory diseases which are caused or propagated by the disregulation of microtubules and reduced trafficking (Millecamps and Julien, 2013; Sorbara et al., 2014; De Vos et al., 2008).

Kinesins

Kinesins move along the microtubules in a stepping fashion through the hydrolysis of GTP into energy. In mammals, there are 45 kinesin genes (kif genes), some functioning as motor proteins and others acting as MAPs affecting microtubule dynamics (section 1.3.2). Cargo is bound to kinesin through adaptor proteins, e.g. SKIP, which is responsible for the binding of lysosomes to kinesin for anterograde transport (Sanger et al., 2017).

Dyneins

The dynein superfamily consists of 32 different proteins encoding the heavy, immediate, light immediate and light chains which are all necessary for the assembly of a functional dynein monomer. These are separated into axonemal dynein, specific to cilia and flagella, and cytoplasmic dynein. Axonemal dyneins have an essential role in the positioning of cilia microtubule doublets via dynein linking arms (King, 2012).

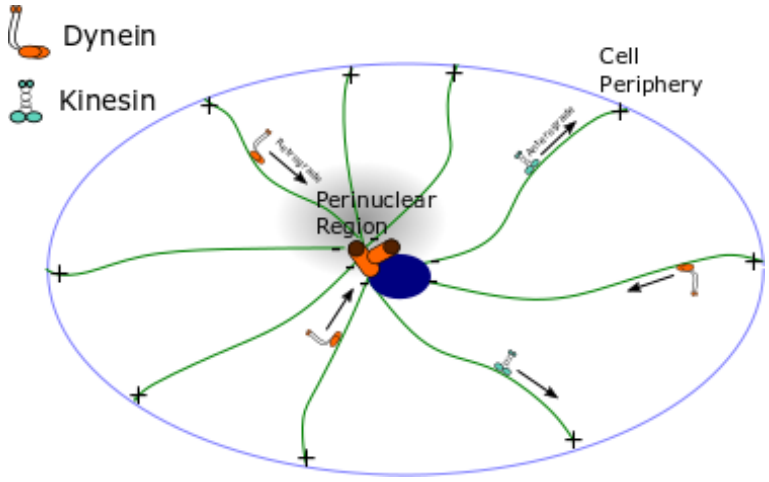

Figure 1.8: **Microtubule organisation for intracellular trafficking**

Under normal interphase conditions, microtubules radially stretch across the cell's cytoplasm from their origin, the MTOC, which they remain tethered to. This allows them to cover the cytoplasm and come in to contact with cargo which requires microtubule trafficking. Cargo is attached to microtubules through either of the microtubule motor proteins, kinesin and dynein. Kinesins move in the anterograde direction, towards the cell periphery and microtubule plus ends. Dynein moves in the retrograde direction, towards the cell's MTOC and microtubule minus ends. Lysosomes are clustered at the perinuclear regions adjacent to the MTOC so cargo for degradation is trafficking via dynein to this area to increase contact with lysosomes.

Microtubules in autophagy

The requirement of microtubules for the trafficking and subsequent degradation of autophagosomes has been investigated using the microtubule depolymerising drug Nocodazole. In both Koch et al. (2006) and, Aplin et al. (1992), reduced autolysosome formation, accumulation of mature autophagosomes in the cytoplasm, and reduced autophagic flux was observed upon loss of microtubules. Under these conditions, autophagosomes cannot be trafficked along microtubules and cannot come into contact with lysosomes to be degraded, leaving them to

accumulate in the cytoplasm and failing to break down cargo.

Further evidence pointed to the necessity of microtubules in autophagy when several microtubule associated proteins were linked to autophagy defects in neurodegenerative diseases (reviewed in Guo et al. (2018)). It is likely that these microtubule associated protein mutants affect many cells and processes, but neuronal cells are especially sensitive due to the large distance across which they are required to transport autophagosome and lysosomes across (Maday and Holzbaur, 2014).

The autophagosome/microtubule interaction is mediated by Rab7, LC3/Atg8 and Atg5 on the autophagosomal membrane, which recruits the adaptor RILP which further complexes with dynein to load autophagosomes onto microtubules (Nakamura and Yoshimori, 2017). Although known to be essential for the loading of autophagosomes onto microtubules, RILP has also recently been shown to be essential for autophagosome biogenesis in neuronal cells, further suggesting that microtubules have a role in autophagosomes formation as well as their transport and subsequent degradation (Khobrekar et al., 2020). One hypothesis is that microtubules facilitate the delivery of certain proteins and complexes to the omegasomes (section 1.1.3).

Recent discoveries have suggested that autophagosomes are spatially concentrated on a subset of microtubules carrying the detyrosination post translation modification (where the final tyrosine is removed of the C-terminal tails of tubulin (Mohan et al., 2019))). Both lysosomes and autophagosomes were preferentially loaded on these microtubules which was hypothesised to increase the likelihood of contact and fusion events.

Microtubules in other lysosomal trafficking pathways

In addition to their role in autophagy, microtubules are also important in both phagocytosis and macropinocytosis.

Vesicle fusion events are facilitated by microtubule trafficking as macropinosomes and phagosomes are loaded onto microtubules via RILP and dynein and move in an anterograde fashion to contact lysosomes (Harrison et al., 2003; Jordens et al., 2001).

This loading onto microtubules also allows them to come into contact with other smaller vesicles which deliver vacuolar ATPase (v-ATPase) and lysosomal enzymes which also faciliate cargo degradation (Vines and King, 2019; Clarke et al., 2002; Gotthardt et al., 2002).

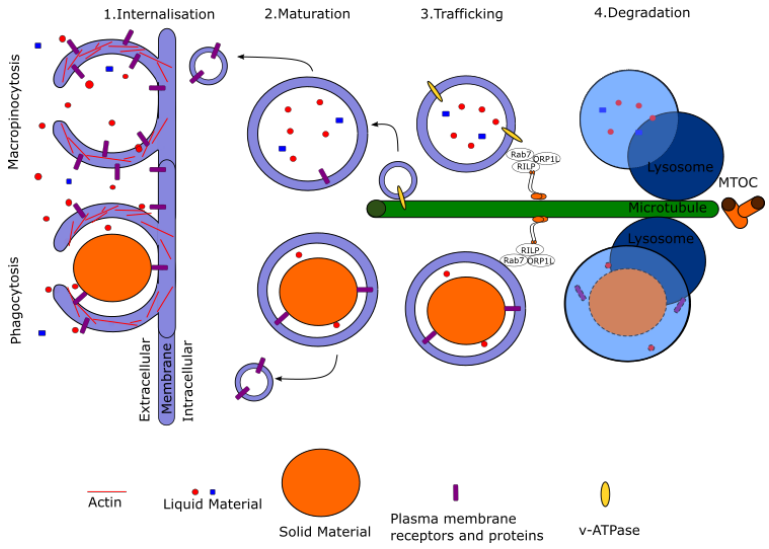

Figure 1.9: **The major steps of macropinocytosis and phagocytosis**

Major steps of macropinocytosis and phagocytosis internalisation, maturation, trafficking and lysosomal degradation. Macropinocytosis pathways use membrane ruffling and actin remodelling to form plasma membrane protrusions externally to capture liquid material. Phagocytosis remodels plasma membrane upon solid material binding to surface receptors to draw cargo inwards. Both phagosomes and macropinosomes are attached to microtubules via dynein

and its associated adaptor proteins before retrograde trafficking. Both vesicles fuse with lysosomes to degrade contents which is either loaded onto MHC complex for immune presentation, used for nutrients, or expelled from the cell.

Cilia

Cilia are specialised cell protrusions important for cell signalling and fluid flow. There are two types, non-motile (or primary cilia) and motile cilia, which move in a coordinated wave-like motions with surrounding cilia to 'beat' fluid in certain directions. Primary cilia are important for their role in signalling transduction although specialised types of sensory cilia are found in the eyes and nose. In addition to signalling, motile cilia are also important to for generating fluid flow in the central nervous system, Fallopian tubes and respiratory tract.

Ciliopathies are a group of diseases with different causes but similar phenotypes resulting from aberration of cilia function. These include Joubert's syndrome, a multivariant ciliopathy which katnip lacking humans suffer from.

Centrioles relocalise to the plasma membrane to induce cilia growth during interphase through the creation of an axoneme. The axoneme, formed of microtubule doublets, extends out from a centriole whilst the other is attached orthogonally and is known as the basal body. The area which separates the cilia from the cell cytoplasm is known as the transition zone.

Primary cilia have 9 microtubule doublets (the A tubule which is complete, and the B tubule which is attached and partially complete) arranged in a circle. Motile cilia, which are capable of lateral movement, have these doublets with a further 2 central doublets (figure 1.10).

In motile cilia, the microtubules slide past each other allowing the cilia to move from side to side (Satir, 1968). This movement is dependent on dynein arms attached to the outside microtubule doublets (Gibbons and Rowe, 1965). Microtubule doublets within the same horizontal plane are attached by nexin bridges preventing them from moving vertically and becoming too long.

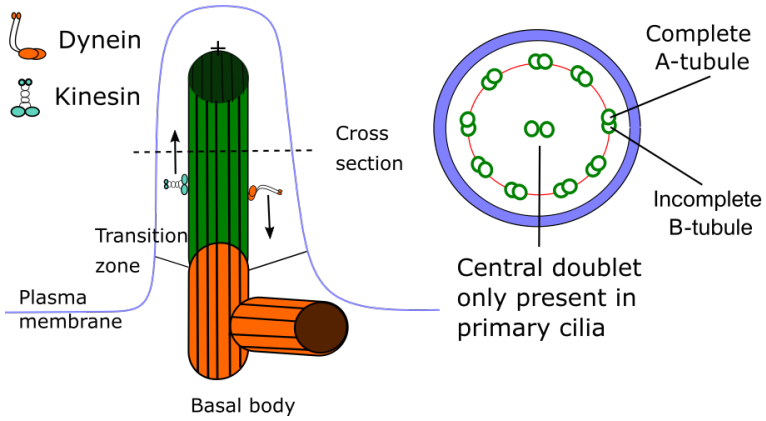

Figure 1.10: **Microtubule organisation in cilia**

During interphase, cells which form cilia relocate their MTOC towards the plasma membrane. This is called the basal body at this location, and polymerises out a specialised microtubule structure called the axoneme to form a cilia. This include 9 doublets in a ring and a central doublet only present in motile cilia. Doublets contain an A-tubule which is a full microtubule, and a B-tubule with is an incomplete microtubule which attaches the A-tubule. Kinesin and dynein motors along with cilia specific IFT proteins catalyse the transport of cargo along axoneme's microtubules.

Mitosis

One of the most well characterised functions of microtubules is in the spindle during mitosis. The spindle includes specialised mitotic microtubules which grow out from duplicated centrosomes to form a spindle. Due to the essential function of microtubules for cell division, spindle microtubules are tightly regulated, and the loss of their function is linked to many cancers due to unsuccess mitosis producing aneuploidy and increased apoptosis.

Microtubules grow out from the duplicated centrosomes and attach to the kinetochores on the centre of the chromosomes in order to organise and separate the chromosomes into the two new daughter cells.

Stages of mitosis

Mitosis is a highly regulated process, which many distinct phases which can be identified through microtubule and DNA organisation.

Upon entry into mitosis (prophase), all interphase microtubules are released from the MTOC and depolymerised. The DNA begins condensing into chromosomes, the centrosome duplicates and the nuclear envelope begins to break down to allow microtubules access to DNA.

During prometaphase, centrosomes are orientated to opposite sides of the cell, and microtubules begin to extend and form stable attachment to either the opposite centrosome (interpolar microtubules) or kinetochore (K-fibres microtubules). Chromosomes begin to orientate onto the metaphase plate (the spindle centre) due to the force generated by the attachment of K-fibres.

When chromosomes are aligned on the metaphase plate ready for separation and all kinetochores are attached to K-fibres, metaphase begins. Several biological checks are completed which can stall mitosis in metaphase if conditions are not met. This checkpoint is known as the spindle assembly checkpoint (SAC) and is important for maintaining chromosome number and DNA amount in the daughter cells (Zirkle, 1970). Factors which require passing including no lagging or misaligned chromosomes, no early or inappropriate spindle microtubule shortening (Hoyt et al., 1991) or failure to attach K-fibres to kinetochores (Wang and Burke, 1995). If any of these conditions are not met, the cells will postpone anaphase entry by preventing the activation of anaphase promoting complex (APC) which controls microtubule shortening in anaphase (Musacchio and Salmon, 2007).

Anaphase is the mitotic stage when K-fibres begin to depolymerise. Anaphase can be further separated into two stages; Anaphase A, where the chromosomes are pulled towards the static centrosomes, and Anaphase B, where the centrosomes begin to move further away from each other (further toward daughter cells), pulling chromosomes with them.

After chromosomes have been pulled into daughter cells, telophase begins

when the mitotic spindle begins to break down, releasing free tubulin ready to be utilised for building a new radial interphase microtubule array in the daughter cell and DNA begins to decondense and package back into the nuclear envelope.

Cytokinesis is the final stage of mitosis and is not dependent on the spindle; it involves cleavage furrow formation and plasma membrane separation so daughter cells are no longer attached.

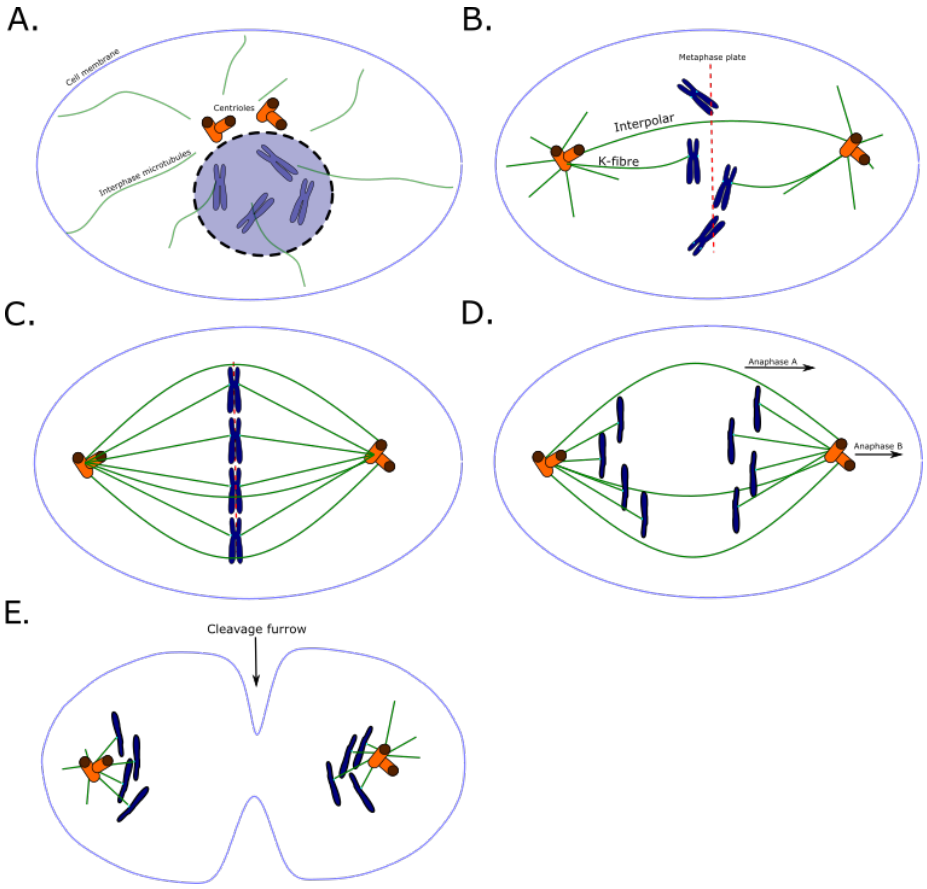

Figure 1.11: **The stages of mitosis in mammalian cells**

Major stages and organisation of microtubules during mitosis. Plasma membrane is represented by purple line, microtubules in green and chromosomes in blue. A. Prophase, B. Prometaphase, C. Metaphase, D. Anaphase (both anaphase A and B) and E. is telophase/cytokinesis.

1.3.5 Microtubules in *Dictyostelium discoideum*

The microtubule cytoskeleton of *Dictyostelium discoideum* has been previously studied to investigate the functionality of kinesins (McCaffrey and Vale, 1989; Koonce, 2000; Kollmar and Glöckner, 2003), unusual centrosome architecture and duplication (Ueda et al., 1999), and microtubule array organisation (Brito et al., 2005; Tikhonenko et al., 2016).

Dictyostelium discoideum shares many similar microtubule functions with higher eukaryotic cells (e.g. microtubule-based mitosis, vesicle trafficking), but has a reduced genetic redundancy, for example the *Dictyostelium discoideum* genome contains only one dynein (Koonce, 2020; McIntosh and Koonce, 1989). *Dictyostelium discoideum* also have reduced redundancy of tubulins including only 2 α-tubulin proteins and 1 β and 1 γ-tubulin and have no non-centrosomal microtubules. Its genome is also fully sequenced (Eichinger et al., 2005), and all the microtubule motors have been identified and functionally characterised (Kollmar and Glöckner, 2003; Koonce, 2020).

Although many protists have cilia for migration, *Dictyostelium discoideum* has lost them and migrate by crawling instead. As *Dictyostelium discoideum* has no cilia, it lacks all of the specialised cilia proteins (Koonce, 2020) but still contains katnip, and therefore katnip must have a role outside of cilia.

Tubulin in *Dictyostelium discoideum*

Dictyostelium discoideum tubulin shares high levels of genetic similarity (α-tubulin has 79% similarity and β-tubulin has 82% similarity to mammalian orthologues (Trivinos-Lagos et al., 1993)), but has a much lower isoeletric point (White et al., 1983). The C-terminus of *Dictyostelium discoideum* tubulin contains local variability in its genetic sequence and is more neutral than mammalian tubulin, which is negatively charged in this area (Ponstingl et al., 1981). This deviation is likely the cause of both taxol and calcium binding not affecting *Dictyostelium discoideum* microtubules, as both have sites within the C-terminus (Solomon, 1977). This is specific to *Dictyostelium discoideum* as

other amoeba and yeast have taxol binding sites (Entwistle et al., 2008; Lataste et al., 1984).

Apart from taxol, and subsequent taxol based drugs, *Dictyostelium discoideum* microtubules respond to other microtubule poisons similarly to mammalian cells. *Dictyostelium discoideum* microtubules are depolymerised by Nocodazole, but only up to a point; hyper-resistant stubs always remain at the plus ends of microtubules upon treatment (own data, figure 4.10, (Koonce and Khodjakov, 2002)). These may be due to protection by the protein rich corona surrounding the centrosome, or due to a separate pool of hyper stable tubulin used for these microtubules.

Tubulin post-translational modification in *Dictyostelium discoideum*

A major pathway for regulating microtubule dynamics is the addition or subtraction of post translational modifications to tubulin sub units (section 1.3.2). In addition to affecting dynamics, acetylation is a marker of microtubule age and therefore stability. Unfortunately, despite several attempts at optimisation with 3 different antibodies, no antibodies which recognised tubulin acetylation were found to work on *Dictyostelium discoideum* microtubules. Whether this is due to the natural variation of *Dictyostelium discoideum* tubulin to mammalian tubulin which the antibodies were created against (section 1.3.5) or the lack of PTMs in *Dictyostelium discoideum* is unknown. Yeast species, which sit evolutionary between human and *Dictyostelium discoideum* , have lost all microtubule PTMs and therefore prove microtubule networks can function without PTMs (Drummond et al., 2011). Although *Dictyostelium discoideum* have much more complex microtubule network than yeast, similar to those found in mammalian cells, some other protosa still lack some or all of the tubulin PTMs (Gull, 2001).No PTM in *Dictyostelium discoideum* have been previously reported and in order to identify if tubulin contains any tubulin PTMs, *Dictyostelium discoideum* tubulin could be purified and PTMs identified through mass spectrometry.

Microtubule organisation in *Dictyostelium discoideum*

Dictyostelium discoideum have approximately 30-70 microtubules during interphase (Moens, 1976) which spread across their cytoplasm from a tri-layered centrosome which is externally tethered to the nucleus (Omura and Fukui, 1985; Ueda et al., 1999) . These microtubules spread out towards the cortex where they are connected to the actin matrix by dynein (Koonce and Knecht, 1998). Microtubules are usually longer than the distance between the centrosome and the cortex, so commonly bend and buckle (Koonce and Khodjakov, 2002). Bends which are seen in microtubules are not due to general cytoplasmic movement, as microtubules are seen to move independently via fluorescence microscopy (Brito et al., 2005). Bends are the product of tension from cortex attachment (Koonce and Khodjakov, 2002) and the force related from microtubule motor walking (figure 1.12).

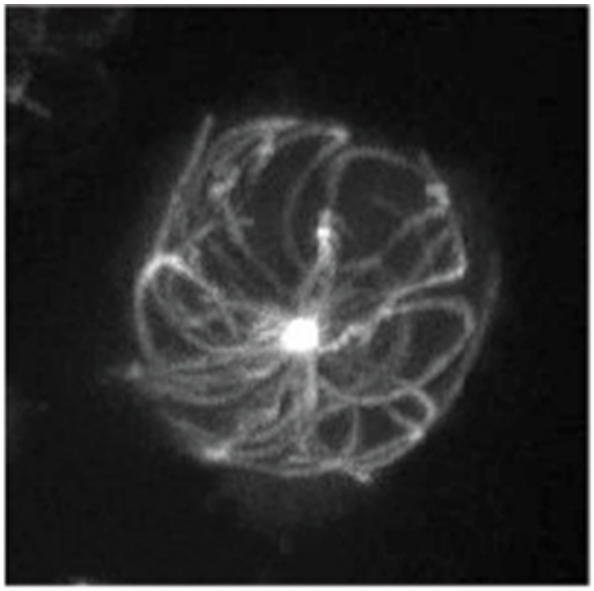

Figure 1.12: **Microtubule organisation in *Dictyostelium discoideum***

Live image of *Dictyostelium discoideum* cell expressing GFP-tubulin. Image taken by Jason King.

Binucleate *Dictyostelium discoideum* synctia are also commonly seen, and *Dictyostelium discoideum* remain functional with two nuclei and two microtubule arrays. In such cells, the two microtubule arrays occupy completely separate spaces of the cytoplasm, with the help of Ase1 (ortholgue of PRC1)(Tikhonenko et al., 2016), which recognises microtubules of different polarities.

Dictyostelium discoideum microtubules have a significantly faster polymerisation and depolymerization rate, polymerising at 14.4μm /min compared to 11.5μm /min in mammalian cells and depolymerising at 16.8μm /min compared to 13.1μm /min (Roos et al., 1987).

The microtubules in *Dictyostelium discoideum* are also very stable and are more resistant to depolymerisation by cold treatment both *in vivo* and *in vitro* than mammalian cells (Roos et al., 1987; White et al., 1983). This may be due to high stabilisation of tubulin via PTM or MAP binding, or to their innately different tubulin. *Dictyostelium discoideum* microtubules are less dynamic than their mammalian counterparts and have much longer lifetimes as they do not undergo microtubule catastrophe.

Microtubule dependent trafficking in *Dictyostelium discoideum*

As previously stated (section 1.1.4), *Dictyostelium discoideum* have more vesicles trafficking at any one time than higher eukaryotic cells and therefore may have a higher amount of force on their microtubules due to increased motor movement (Roos et al., 1987; Koonce, 2000). *Dictyostelium discoideum* kineins also move up to 4 times faster than their mammalian counterparts, at an average of 2μm a second (Roos et al., 1987; Koonce, 2000).

Although no research has previously been published on autophagosome movement along microtubules in *Dictyostelium discoideum* specifically, their microtubules have been shown to be essential for the transport and subsequent clearance of other lysosomal pathways, including phagosomes (Rai et al., 2016; Welin et al., 2018) and endocytic vesicles (Pollock N, Koonce MP, de Hostos EL, 1998).

Mitosis in *Dictyostelium discoideum*

One of the major differences between higher eukaryotes and *Dictyostelium discoideum* microtubules is their centrosomes and therefore, mitotic process. *Dictyostelium discoideum* centrosomes are made up of 3 distinct layers, all of which are similar to elements found in mammalian centrosomes but in a different structure.

During interphase, the centrosome is a rectangular shape consisting of an inner core layer of CP91 protein (Putzler et al., 2016) surrounded by two layers of outer core structures on the longest sides (Ueda et al., 1999). This rectangular complex is then surrounded by an amorphous matrix known as the corona (Ueda et al., 1999), which consists of a sparse protein 'cloud'. It is this layer which contains the γ-tubulin responsible for the microtubule nucleation, and is functionally equivalent to the pericentriolar matrix in higher eukaryotic cells (Euteneuer et al., 1998).

Upon mitotic entry, interphase microtubules are depolymerised along with the disassembly of the corona and inner core. The nuclear membrane of *Dictyostelium discoideum* also remains partially closed throughout mitosis, unlike mammalian cells where the nuclear membrane is completely broken down. The centrosome enters the nucleus (Kitanishi et al., 1984) and its outer core layer separates to expose microtubule nucleation surfaces on the inner (previously buried) side.

Approximately 140 microtubules extend from the outer core to connect to the 6 duplicated chromosomes (12 in total) (McIntosh and Koonce, 1989). These form a single line like structure, rather than the spherical spindle seen in mammalian cells, which pulls the chromosomes in to the two new daughter cells. The centrosomes fold in such a way that the outer core nucleating surfaces are reversed, so they lie on the exposed side ready to nucleate interphase microtubules (Ueda et al., 1999; Putzler et al., 2016). During late telophase, the centrosome is removed from inside the nucleus, tethered to the nuclear envelope and the corona is re-established.

1.4 Aims of the project

1.4.1 Gap in the literature

Katnip is a highly conserved protein which contains 3 repeats of a unique domain of unknown function, DUF4457.

Katnip is known to interact with tubulin and may be able to bind to microtubules when overexpressed. Katnip is a regulator of microtubule organisation in cilia, and mutations in the gene cause cilia defects resulting in Joubert's syndrome and have also been linked to Alzheimer's and brain tumours. However, the relationship between katnip and microtubules is still unknown, and its function in interphase microtubules has not been researched. Previously unpublished work using *Dictyostelium discoideum* indicates that loss of katnip may result in an autophagy defect, but its function in this context and underlying cause of the observed defects is unknown.

I hypothesis that katnip's function may not just be limited to cilia but may also affect microtubules in the cytoplasm of the cell, resulting in a trafficking defect. Microtubules are essential for the delivery of autophagosomes to lysosomes, and I speculate that this could result in the autophagy defect. This thesis presents data investigating the role of katnip in autophagy and other microtubule-based trafficking pathways to investigate the severity and range of the katnip$^-$ defect and its role in regulating non-cilia microtubules in both *Dictyostelium discoideum* and mammalian cells.

1.4.2 Aim 1: Understand the role of katnip during autophagy

Although the role of Katnip in autophagy in *Dictyostelium discoideum* cells has already been identified, no information is known on the severity, cause or stage at which the defect is based. Investigation has been limited to indirect functional assays and autophagosome formation has never been investigated. The assays in the thesis will assess the dynamics of autophagy and observe different autophagy stages in katnip mutants to answer these questions. There are many well established autophagy assays available in *Dictyostelium discoideum* which will therefore be used to complete this aim.

1.4.3 Aim 2: Investigate if loss of katnip affects other lysosomal trafficking pathways

Many of the machinery used in autophagy pathways are also required in other trafficking pathways, including microtubule trafficking. In order to see if the defect in katnip mutants is specific to autophagy or affects these other pathways, changes in macropinocytosis and phagocytosis will be monitored. Again, due to the large amount of trafficking assays established, *Dictyostelium discoideum* was used to investigate this aim.

1.4.4 Aim 3: Identify the function of katnip on microtubules

As both the microtubule organisation function of katnip and the autophagy function of Katnip were functionally connected through microtubules, the final aim of my project was to understand the underlying function of katnip on microtubules. I hypothesise that it may be a conserved regulator of microtubules which causes a secondary effect on autophagy and so microtubules will be investigate both in *Dictyostelium discoideum* cells and human cells.

Chapter 2

Methods

2.1 Molecular biology

2.1.1 Cloning

Polymerase chain reaction (PCR)

All template DNA used was from previous lab plasmids stocks (table 2.2). Template DNA was linearlised with suitable restriction enzymes (single site in the plasmid outside the PCR region) by digesting for 15 minutes at 37^oC (subsection 2.1.1). Resulting linear template DNA was added to x2 PrimeStarMax DNA polymerase (Tanaka) mixed to a final concentration of x1 with 100pmol of relevant forward and reverse primers (table 2.1 and water to make a 20μL reaction. DNA was amplified using cycling protocol as shown below.

Table 2.1: Polymerase chain reaction steps

Step	Temperature	Length	
1	94^oC	3 minutes	
2	94^oC	30 seconds	
3	55^oC	1 minute	Repeat x34
4	72^oC	5 seconds per kilobase product	
5	72^oC	10 minutes	
6	4^oC	Hold	

Agarose gel electrophoresis

DNA (digested plasmid,subsection 2.1.1) or PCR product (subsection 2.1.1) was loaded on to a 1% agarose gel (agarose powder (Fisher Bioreagents) mixed with TAE (1M Tris free base, 1M EDTA, 1M glacial acetic acid) with 1μL of midori green advance DNA stain (Geneflow). Samples were mixed with x6 purple gel loading dye (NEB) to give a final concentration of 1x. 10μL of quick-load purple 1kB plus ladder (NEB) was used as a size reference. Loaded gel was covered with 1xTAE buffer and run at 100 volts for 40 minutes. Gels were imaged on an EZ imager gel doc (Bio-Rad) using SYBR safe stain plate to visualize bands. For subcloning, correct bands were visualized for extraction on a Fast-Gene LED illuminator (Nippon Genetics) and extracted using a scalpel. DNA from extracted gel segment was purified using ZymoClean gel DNA recovery kit (Cambridge Bioscience) and eluted in 10μL elution buffer.

TOPO ligation

Purified PCR products were ligated into 0.5μL blunt ended Zero blunt TOPO vector (Thermo Fisher Scientific) with 0.5uL provided salt solution and 1.5uL of DNA in a total volume of 5μL . Reaction was incubated at room temperature for 30 minutes to ligate.

DNA digestion

All plasmids used were from previous stocks (table 2.2) or from plasmid stocks created by Douwe Veltman (Veltman et al., 2009). 20μL of plasmid (concentration varied) was digested by 10 units of restriction enzymes (all from NEB except BglII and BcuI/SpeI from Thermo Fisher) along with suitable buffer and water in a 20μL reaction. Reactions were incubated at 37^oC for 1 hour.

Plasmid ligation

Vector and insert DNA was mixed at a 3:1 insert:vector ratio along with 20 units T4 DNA ligase (Thermo Scientific), x6 ligase buffer to a final concentration of x1, and water to make 10μL reaction. Reaction was incubated at room temperate between 30 minutes and 3 hours. Ligation reactions were then transformed as in subsection 2.1.1.

Making competent cells

A single DH5α colony grown on an antibiotic free LB plate (Miller LB agar; 10g tryptone, 5g yeast extract, 10g NaCl, Fisher Scientific Ltd) was picked and grown in 3mL SOB (0.5% yeast extract, 2% tryptone, 10mM NaCl, 2.5mM KCl, 20mM $MgSO_4$) overnight at 37^oC . After 18 hours incubation, 500μL of overnight culture was transferred to 250mL of SOB in an autoclaved 2L flask. Culture was incubated at room temperature with shaking until OD600 = 0.6 (approximately 18 hours). Culture was cooled on ice for 10 mins before centrifuged at 1670g for 15 minutes at 4^oC . Pellet was resuspended in 83mL of ice cold TB buffer (10mM PIPES, 15mM $CaCl_2$, 250mm KCl, 55mM $MnCl_2$, pH 6.7) and incubated on ice for a further 10 minutes. Solution was centrifuged at 1670g for 15 minutes at 4^oC and pellet resuspended in 20mL ice cold TB. 1.4mL DMSO was added and cells incubated on ice for 10 minutes before aliquotting 100uL into pre cooled 500uL tubes on dry ice and flash freezing. Aliquots were stored at -80^oC .

Bacterial transformation

Ligation reactions were cooled on ice for 5 minutes and 50μL of thawed competent DH5α cells (lab made, subsection 2.1.1) added. For retransformations, 1μL of DNA was used. Mix was incubated for 5 minutes on ice then placed at 42^oC for 42 seconds before placing on ice for a further 5 minutes. 250μL of LB broth (Fisher) was added and reaction placed at 37^oC for an hour. Reaction was plated out on to Agar plate (with antibody if necessary) and incubated overnight at 37^oC .

Plasmid check digest

Bacterial colonies were selected and grown up in 3mL of LB (with antiboitic if necessary) overnight at 37^oC . DNA was purified from culture using GeneJet plasmid miniprep kit (Thermo Fisher). To check plasmids, 10μL of miniprepped DNA was digested as before (subsection 2.1.1) and run on a gel as before (subsection 2.1.1). If expected positive DNA bands were observed, 500μL of bacterial culture was mixed with 500uL of glycerol (Fisher) and stored at -80^oC . Resulting miniprep DNA was stored at -20^oC for use and remade via retransformation and miniprepping when needed.

List of plasmids

Table 2.2: List of plasmids used

Plasmid ID	Plasmid name	Description	Species expressed	Made by	Gene ID	Number
pJSK560	katnip	katnip with internal BgLII sites removed	Human	JSK	KIA0556	pDM368
pJSK572	GFP-katnip	GFP-katnip with internal BgLII removed	Human	JSK	KIAA0556	pDM707
pJSK584	GFP-dlkatnip	full length katnip from KIAA0556 *Dictyostelium discoideum* *lacteum* tagged with GFP	*Dictyostelium discoideum*	JSK	KIAA0556	pDM448
pJSK526	GFP-ddkatnip	Conserved C-terminus (3348bp) of katnip from *Dictyostelium discoideum* *Dictyostelium discoideum* tagged with GFP	*Dictyostelium discoideum*	JSK	DDB_*G0275861*	pDM448
pJSK336	GFP-α-tubulin	GFP tagged α-tubulin A2	*Dictyostelium discoideum*	JSK	DDB_*G0281889*	pDM448
pDM430	GFP-Atg8A	GFP tagged Atg8A	*Dictyostelium discoideum*	DV	DDB_*G0286191*	

Plasmid ID	Plasmid name	Description	Species expressed	Made by	Gene ID	Number
pGPS3	GST-ddDUF4457R1	First DUF4457 repeat from *Dictyostelium discoideum* DDB_*G0275861* tagged with GST	E.coli	GPS	DDB_*G0275861*	pGEX-6P-1
pGPS4	GST-hsDUF4457R1	Second DUF4457 repeat from *Dictyostelium discoideum* tagged with GST	E.coli	GPS	DDB_*G0275861*	pGEX-6P-1
pGPS5	GST-hsDUF4457R2	Second DUF4457 repeat from Human *katnip* tagged with GST	E.coli	GPS	KIAA0556	pGEX-6P-1
pGPS13	GST-hsDUF2-HisTag	Second DUF4457 repeat from Human *katnip* tagged with GST and HisTag	E.coli	GPS	KIAA0556	pGEX-6P-1
pGPS17	KIAA556 CRISPR KO	For CRISPR knockout of *katnip* Primers 49 and 50	Human	GPS	KIAA0556	pSpCas9 (BB)-2A Puro

JSK, Jason King.DV, Douwe Veltman.GPS, Georgina Starling. KIAA0556 is human katnip and DDB_*G0275861* is *Dictyostelium discoideum* katnip.

2.2 Cell culture

2.2.1 *Dictyostelium discoideum* methods

Dictyostelium discoideum axenic growth

Dictyostelium discoideum cells were grown in axenic adherent culture in sterile HL5 media (Formedium powder in dH20) at 22^oC . WT strain denoted in this thesis is axenic strain 2 (Ax2, table 2.3). Cells tranfected with antibiotic resistance plasmids were selected with either 20μg /L hygromycin (Invitrogen), 10μg /mL G418 (Sigma) or 10μg /mL blasticidin (Meldford) in water. Cells were grown in 10cm petri Dishes (Thermo Fisher) and split 1/5 to 1/10 everyday.

List of *Dictyostelium discoideum* cell strains

Table 2.3: *Dictyostelium discoideum* strains

Name	Parent	Genotype	Source	Strain ID
Ax2	Ax1 (DBS0237979)	*axeA2, axeB2, ax2C2,*	Robert Kay	DBS0235521
Katnip clone 1	Ax2 (DBS0235521)	Katnip$^{-(1)}$ */DDB_G0275861*	Jason King	JSK14
Katnip clone 2	Ax2 (DBS0235521)	Katnip$^{-(2)}$ *DDB_G0275861*	Jason King	JSK15
Atg1^{-}	Ax2 (DBS0235521)	*Atg1*$^{-}$*/DDB_G0292390*	Jason King	JSK12

Dictyostelium discoideum freezing and thawing

A confluent 10cm plate of cells (approximately 30x10^6 cells) in exponential growth phase was resuspended and pelleted at 100g for 2 minutes. Cell pellet was resuspended in 1mL of freezing buffer (HL5 media with 10% DMSO) and aliquotted out into 200μL aliquots and placed in a cell freezer at -80^oC . For thawing, an aliquot was removed from -80^oC storage box, thawed at room temperature and placed in 10mL of HL5 in 10cm petri dish. 24 hours after thawing, antibodies were added if selection was necessary.

Dictyostelium discoideum axenic growth curve

Cells were seeded at 0.5x10^6 cells/mL in either HL5 or SIH in 6 well plates with a final volume of 2mLs. At time indicated, cells were counted by resuspending cells and loading 10μL culture into Neubauer haemocytometer and counting 3x 1mm^2 boxes. Doubling time was calculated by fitting growth to the exponential growth curve equation on GraphPadPrism Version 7. Statistical significance was calculated by T-test between average doubling time across 3 repeats.

Dictyostelium discoideum survival of amino acid starvation

To assess their ability to survive starvation, cells were washed in SIH - Arg/Lys (from power, Formedium) twice before resuspending at 5x10^5/mL in 10mL in sterile 50mL conical flask. Cultures were shaken at 175rpm on a SSL1 Stuart orbital shaker. Cells were harvested by added 10uL of culture to 450uL SIH -Arg/Lys and 30uL spread on to duplicate SM agar plates with 200uL LB inoculated with *Klebseilla aerogenes* culture from a plate. Cells were harvest at day 0, 2, 4, 6 and 8 days before seeding. Protocol adapted from Otto et al. (2003).

Dictyostelium discoideum growth on bacteria

Cells were counted using a heamocytometer and diluted to give a final concentration of 1 cell per 1uL. A loop of *Klebseilla aerogenes* bacteria grown on a SM (Formedium) agar plate was mixed with 1mL of LB. 100μL of this was then mixed with 100μL (equivalent to 100 cells) or 10μL (equivalent to 10 cells) of 1 cell/μL culture and spread on a SM agar plate. Plates were kept in the dark at room temperature for 5 days and then imaged on Gel Doc EZ imager to measure plaque diameter. T- tests were then performed on the plaque sizes between WT and katnip$^-$ plates.

Dictyostelium discoideum transformation

Dictyostelium discoideum cells were resuspended and 6x10^6 cells were pelleted at 100g for 2 minutes. Cell pellet was resuspended in 400μL of chilled E buffer (10mM KH_2PO_4 at pH6.1, 50mM sucrose) and placed in a chilled 2mm gap electroporation cuvette on ice. For extrachromosomal plasmids, 5μg of DNA was added. Culture was mixed by pipetting the cuvette and electroporated using a 5Ω resistor in series with a Bio-Rad Gene Pulser II set to 3μF capacitance and 1.2kV resulting in a time constant of approximately 0.3ms. The electroporated cells were immediately transferred to 10mL of HL5 in 10cm dish and 10 μg/mL Doxycycline was added. After 24 hours, antibiotics for selection were added if necessary and cells grown for 1 week and then cultured as normal.

Folate chemotaxis assay

Chemotaxis towards folate was performed under agar as previously described (Laevsky and Knecht, 2001). P60 petri dishes (Thermo Scientific) were filled with 8mL of 0.75% agarose in HL5. Agarose was left to set at room temperature in a humidifying chamber for 16 hours. After setting, 3 parallel wells of 2mm x 39mm were cut into agarose 50mm apart using a razor blade. Cells were resuspended at $5x10^6$ cells/mL and 200μL of culture added to top and bottom wells. 200μL of 0.1mM folate was added to middle well. Plates were incubated in a humidified chamber for an hour and then imaged using a LD A-plan x20 air objective on Zeiss Axiovert widefield microscope with a Hamamatsu Orca ER camera running uManager software (Edelstein et al., 2010, 2014). Cells were observed at the folate side of the top or bottom wells and images captured at 30 seconds intervals for 1 hour. Each cell which could be seen for the whole hour on screen was traced using Image J plug in Trackmate. 'Total distance' was calculated by adding all all of the X and Y distances and 'net directionality' is the final XY position minus the initial XY position and represents the total net movement towards the gradient. 'Directionality' was 'net drectionality' divided by 'total distance'. T-test was performed between WT and katnip$^-$ cell 'directionality' across 3 repeats.

Phagosome proteolysis assay

Phagosome proteolysis protocol was altered from Sattler et al. (2013) along with the preparation of lab made beads. Its uses DQ-BSA which gets brighter upon unqueching in acidifc conditions. When loaded into phagosomes, DQ-BSA unquenches upon phagosome proteolysis and increases in brightness.

Cells were washed in Lo-Flo media (Formedium) twice by pelleting at 100g for 2 minutes and seeded in Lo-Flo into a glass bottom 96 well plate (Greiner) at $3x10^5$ per well in triplicate. After cells had attached (minimum 30 minutes), 10μL of $1.5x10^7$ BSA and Alexa594 coupled beads (lab made) were added to each well except 3 which were kept as control wells. Plates were spun for 800g for 10

seconds in a Heareus Megafuge 1.0R centrifuge with plate holder to synchronize bead uptake. All media was removed, cells washed twice and Lo-Flo added back to remove unphagocytosised beads. Plates were immediately loaded into Synergy Mx. Biotek plate reader and excited at 480nm (DQ-BSA green) and 560nm (DQ-BSA red) and measured at 510nm and 620nm respectively every 2 minutes for 2 hours. Fluorescence from control wells was subtracted from the sample wells to remove background fluorescence. Signal was normalised for bead uptake by dividing the 480nm signal by 580nm signal (480nm reflects the proteolysis, 580nm represents the number of beads). Average fluorescence from triplicate samples wells was normalised by subtracting time 0 from all other time points. Average graph was made by averaging normalized fluorescence at each time points across 4 repeats and plotted errors bars and S.D.

Total proteolytic activity (TPA)

Total proteolytic activity was performed as previously published in Buckley et al. (2019). 4x10^6 cells were resuspended and washed in 150mM potassium-acetate twice before freeze thawed in liquid nitrogen to lyse them. Lysates were pelleted 50g at 4^oC for 5 mins and 100uL of supernatant added to glass bottom 96 well plate (Greiner). 1.23x10^5 beads were added to each well along with 5uL of HALT protease inhibitor (Thermo Fisher) to control wells. Media has been optimised to be the same as lysosome pH (around pH4.0) to maintain optimal pH for enzyme activity. Experiment was then performed and analysised as above in subsection 2.2.1.

Visualising macropinosomes

WT and katnip$^-$ cells were seeded in 35mm glass dishes at appromatively 0.5x10^5 in 2mL of HL5 with 0.4mg/mL FITC Dextran (Sigma) and 2mg/mL TRITC Dextran (Sigma) and left for 16 hours. Cells were imaged using Airyscan confocal microscope. Macropinosomes width was measured using measure function on ImageJ.

Phase chase of macropinosomes

WT cells expressing GFP-α-tubulin, (from now on called GFP-tubulin), were seeded into 35mm glass bottom dishes (MatTek) at 70-80% confluency and left to settle. All media was removed and replaced with 150μM Nocodazole in HL5 and incubated for 5 mins. Nocodazole was removed and 20uL concentration TxRed Dextran was added for 2 minutes and washed off with HL5. Cells were imaged using Perkin-Elmer Ultraview VOX spinning disk confocal microscope running on Olympus Ix81 body at x60 oil immersion objective and captured by Hamamatsu C9100-50 EM CCD camera using Volocity software every 2 mins to observe Dextran positive vesicles (macropinosomes) along microtubules.

Autophagy induction and lifetime

To both improve imaging and induce autophagy via mechanical stress induction, cells were compressed under agar (King et al., 2011). Cells expressing GFP-Atg8 were seeded at 70-80% confluency in 35mm glass bottom dishes (MatTek) and left for a minimum of 1 hour to adhere. 10mL of 1% agarose gel was made with HL5 in a 10cm petri dish (ThermoFisher) and let to set. Once set, 3mL of HL5 was poured over the top to keep it moist. Before imaging, a small square (approximately 1cm^2) was cut out of the 1% agarose HL5 gel. Media was poured off glass bottom dishes with cells and agar square placed on top. Residual media was removed by filter paper touching the agarose square. Cells were left for 5 minutes and imaged using 488nm laser with 1μm intervals on Perkin-Elmer Ultraview VOX spinning disk confocal microscope at x60 oil immersion objective every 10 seconds for 10 minutes. Autophagosomes were tracked manually from first frame present to last frame present. Autophagosome cup closure was defined as the brightest timepoint for each autophagosome. Autophagosome size and number was measured manually on Image J.

Photodamaging cells

Cells expressing GFP-dlkatnip seeded at 70-80% confluency in 35mm glass bottom dishes (MatTek) were imaged on Perkin-Elmer Ultraview VOX spinning disk confocal microscope with a x100 1.4NA oil immersion objective using 488nm laser excitation. To induce photodamage, shutters were disabled and cell exposed to 50% 488nm laser for 30 minutes and total cell imaged with 1μm intervals obtained every 10 minutes.

Microtubule depolymerization assay

In order to assess the dynamics of microtubule depolymerisation, cells were treated with microtubule depolymerising drugs and microtubule spread over time assessed. WT and katnip^{-} cells expressing GFP-tubulin were seeded in 35mm glass bottom dishes (MatTek) at 2x10^5 cells per mL and left to settle for an hour before imaging. Cells were imaged on a Perkin-Elmer spinning disk confocal microscope at x100 objective with 0.5μm z-stacks. All media was then removed from the dish using an extended tip Pasteur pipette (Samco Scientific) and 200μL was immediately added of either 10μM or 30μM Nocodazole (Acros Organic) in HL5. Cells were imaged every 5 minutes for 30 minutes (new field of view for every time point). After 30 minutes with nocodazole incubation, media was removed, cells washed with HL5 twice carefully as to not wash off cells and 200μL HL5 was added back on. Cells were immediately imaged every 5 minutes for a further 30 minutes for nocodazole wash out time points.
Images were analyzed from maximum internsity projections (using ImageJ Z-project function) and adjusting contrast to identify plasma membrane clearly on Image J. Cell area and the area covered by microtubules was drawn around following the ends of the microtubules. The area in μ metres^2 covered by microtubules was then divided by the total cell area in μ metres^2 to give the fraction of cell which was covered by microtubules. This was calculated for all (complete) cells in the field of view for each time points and the mean fraction from each time point across 3 biological repeats was plotted on a graph. Significance

was calculated between different cell lines at each time point by T-test against the mean fraction.

Mitosis imaging

WT and katnip^{-} expressing GFP-tubulin were seeded in HL5 at 0.5x10^{5} in 35mm glass dishes and left overnight. A minimum 16 of hours after seeding, cells were imaged on brightfield every 30 seconds for 2 hours on a LD A-plan x20 air objective on Zeiss Axiovert widefield microscope with a Hamamatsu Orca ER camera running uManager software (Edelstein et al., 2010, 2014). Any cells undergoing mitosis were timed from when cells rounded up until no membrane contacts could be seen between resulting daughter cells.

To image microtubules during mitosis, after a minimum of 16 hours, cells expressing GFP-tubulin were imaged under brightfield and 488 laser every 10 seconds for 10 to 40 minutes on Perkin-Elmer Spinning Disk Confocal microscope with a x60 oil immersion objective. Any cells undergoing mitosis were timed from when interphase microtubules began depolymerisation until no contact can be seen between resuling daughter cells. Total mitosis time of each cell was plotted for each cell line and a T-test performed between cell lines.

Metaphase was measured from the beginning of mitosis (cell rounding up) until all interphase microtubules were depolymerised. Anaphase was measured from when centrosomes started to move apart until centrosomes parted no more. Telophase and cytokinesis were measured from the end of anaphase until to end of mitosis. Mitotic stages including prometaphase and separating telophase and cytokinesis were not measured due to inability to define exact time due to the speed of these stages. Distance between centrosomes was measured during anaphase manually using ImageJ . Distance was measured from the furthest edge of the first centrosomes to the furthest edge of the second along the microtubule spindle.

Autophagy flux assay

The ability of cells to degrade autophagosomes (i.e. flux) was measured based on the lysosomal cleavge of GFP-Atg8, as described in (Cardenal-Muñoz et al., 2017). WT, katnip^{-} and *Atg1*$^{-}$ cells expressing GFP-Atg8 were seeded at 4x10^{6} cells in 3mL of HL5 in Nunclon 6 well TC plates (Fisher). Cell lines were seeded in triplicate and placed on orbital shaker at 180 rpm at 22^{o}C . After 2 hours, 2.5μM AR-12 (OSU-03012, ApexBio techonology) was added to one well and incubated for a further hour to induce autophagy. Then, x42 COMPLETE mini protease cocktail inhibitor tablets in water (Roche) was added to relevant well and incubated for another hour. After incubation, cells were counted by transferring 10μL to Neubauer haemcytometer , 50μL was transferred to a cloning ring on a 35mm glass bottomed dish (MatTek) for microscopy analysis and the rest of the culture was pelleted at 50g for 5 mins and supernatant removed. Cell pellets were flash frozen in liquid nitrogen and stored at -20^{o}C until lysis. Cells in cloning rings were imaged using FITC laser on Perkin-Elmer spinning disk confocal microscopy at x20 oil immersion objective with 0.5μm z intervals. Images were z-projected on ImageJ and number of autophagosome counted on manually. Cell pellets were resuspended in pre-heated 95^{o}C x4 Laemelli sample buffer (3.5M Tris-HCL pH8.0, 10% SDS, 10% glycerol, 5% B-mercaptoethanol, 0.05% bromophenol blue) diluted to 1% in solution to give a final volume of 1x10^{8} cells per mL. 5μL of each sample was electrophoresed by 12.5% SDS-PAGE (subsection 2.3.1) and bands quantified by measured fluorescence on Licor Studio Lite Ver 5.2.

Ultracold methanol fixation

For improved sample preservation, *Dictyostelium discoideum* were fixed in ultracold methanol (-80^{o}C) as described in Hagedorn et al. (2006). 13mm round glass coverslips (VWR) were acid-washed with 50% $NH0_3$ for 5 minutes and washed 3 times with tap water and a final wash with distilled water. Cells were seeded at 2x10^{5} on to 3 treated non-overlapping coverslips in a 6 well plate

(Nunclon) and left to adhere (20 minutes minimum). Coverslips with cell side up were transferred at a 15^oC angle into a vertical coverslip rack submerged in -80^oC methanol and incubated for 30 minutes. Coverslips were removed and submerged 9 times into PBS to wash before a final wash in distilled water to remove salt. Coverslips were then mounted in Prolong Gold with DAPI (Invitrogen) cells face down on to glass slides if no antibody staining was required.

Immunofluorescence staining (IF)

Coverslips were transferred cell face down on to a 50μL drop of 3%BSA in PBS for 30 minutes to block. Coverslips were transferred to a 50μL drop of primary antibody (table 2.4) diluted in 3%BSA in PBS (3% P/BSA) for 30 minutes. Coverslips were washed in PBS 9 times and incubated with secondary antibody (table 2.5) diluted in 3% P/BSA. Coverslips were washed in PBS 9 times and distilled water 3 times before mounted with Prolong Gold (Invitrogen) with DAPI or without DAPI onto a 76mm x 26mm microscope glass slides (Fisher). Slides were left overnight to harden and imaged on Perkin-Elmer spinning disk confocal microscope using x100 oil immersion objective or Zeiss Airyscan confocal microscope at x60 oil immersion objective.

HEMS lysis for tubulin fractionation

Tubulin fractionation for total tubulin quantification

Protocol altered from Kimble et al. (2000). One confluent 10cm plate (approximately 2x10^6/mL) of cells were spun down at 50g for 2 minutes, supernatant removed and resuspended in 1mL KK_2. Resuspended cells were spun at 50g for 2 minutes again and supernatant removed. Pellet was resuspend in room temperature 200μL HEMS buffer (50mM HEPES (Sigma Aldrich), 2mM EGTA, 5mM Mg-acetate (Fisher), 10% Sucrose (Fisher) , 2% Triton X-100 (Fisher), at pH7.4) with 1% added HALT (Thermo Fisher) and incubated for 2 minutes at room temperature. 30μL of lysate was removed for 'total tubulin' fraction, samples were then centrifuged at 2700g (max) for 1 minutes to pellet and separate

the polymerised microtubules from the free tubulin supernatant.

2.2.2 Mammalian cell culture methods

Mammalian cell culture

NSC-34 cells were a gift from Mark Collins, CMIAD. HeLa-M were a gift from Andrew Peden, CMIAD. hTERT RPE-1 cells were a gift from Kai Erdmann, CMIAD. SHSY-5Y cells were a gift from Kurt de Vos, SITRAN.
All cells were grown in adherent culture in DMEM (Gibco) supplemented with 1x L-glutamine and 10% FBS. HeLa-M and NSC-34 were grown in flat sterile TC treated 10cm plates (Fisher). hTERT RPE-1 and SHSY-5Y cells were grown in T75 flasks (Fisher). Media was changed every 2-3 days and cells were split 1 in 10 when confluent (every 3-5 days). NSC-34 and hTERT RPE-1 were resuspended by pipetting/trituration and SHSY-5Y and HeLa-M cells were resuspended by washing once in PBS and incubating with 1mL 0.25% trypsin for 3 minutes to resuspend. Cells were supplemented with 500 units of Penicillin-Streptomycin (Pen/Strep, Fisher) when cultured.

Freezing and thawing of mammalian cell lines

Confluent cell were resuspended and spun at 50g for 4 minutes. Pellet was resuspended in freezing media; 90% DMEM supplemented with L-glutamine and FBS and 10% DMSO (AnalaR). Cells suspension was aliquotted out into 1mL aliquots in 1mL cryovails (StarLabs). Aliqouts were transferred to a cell freezer at -80^oC for 24 hours before transferring to storage box.
For thawing aliquots, cells were removed from -80^oC and thawed in a 37^oC water bath and placed in a T25 angled flask (Fisher) with warmed DMEM media supplemented with L-glutamine, FBS and Pen/Strep. Media was replaced after 24 hours and cells were transferred to T75 angled flask 48 hours after thawing.

Transfection of mammalian cell lines

30,000 cells/cm^2 were seeded 1 day in advance for HeLa-M, and SHSY-5Y or 2 days in advance for hTERT RPE-1 and NCS-34 to allow cells to adhere and be 70% confluent for transfection. Cells were either seeded on to NHO_3 treated sterile coverslips in 24 or 6 well plates for immunofluorescence or 6 well plates for harvesting protein for western blotting.

NSC-34 , HeLa-M and hTERT RPE-1 cells were transfected using a one to 3 DNA:PEI transfection reagent (ThermoFisher Scientific) mix using 2μg DNA per mL of culture. SHSY-5Y cells were transfected 24 hours after seeding using 1μL FuGene (Promega) or Lipofeactmine 3000 (Thermo Fisher) with 1μg DNA. DNA and transfection reagent was incubated for 5 minutes before 100μL of Optimem (Gibco) per mL of culture was added, incubated for a further 15 minutes and then added to wells drop by drop. HeLa-M were incubated for a 1 day and hTERT RPE-1 and NSC-34 were incubated for 48 hours to allow protein expression. SHSY-5Y were incubated for 6 hours with reagent before media was replaced and cell harvested 18 hours later.

PFA fixation of mammalian cell lines

Half of DMEM media was removed from wells and replaced with equal volume of PBS, mixed and half the volume removed. An equal volume of 8% PFA was then added to wells and incubated at 15 minutes at room temperature. All liquid was removed from wells and washed with PBS 3 times. PFA was quenched using an equal volume of 0.1M glycine in PBS for 15 mins at room temperature and then washed 3 times with PBS.

Immunofluorescence of mammalian cell lines

Cells were permeabilised with 0.1% Triton X-100 in PBS for 10 minutes and then washed 3 times in PBS. Same protocol was then followed as stated in subsection 2.2.1.

Lysing mammalian Cells by RIPA buffer

A confluent well of a 6 well plate was cooled on ice and all media replaced with 200μL RIPA buffer (10mM Tris-CL (pH8.0), 1mM EDTA, 1% Triton X-100, 0.1% sodium deoxycholate, 0.1% SDS, 140mM NaCl, 1mM PMSF) for 10 minutes. Cells were then scraped from wells using plastic end cell scraper (250mm handle x 18mm head, Fisher) for 2 minutes and RIPA buffer containing lysed cells removed. Lysed cells DNA was either sheered by centrifugation through QIAShredder (Qiagen) and stored at -20^oC for up to a month.

2.3 Protein biochemistry

2.3.1 Western blotting

Precision red protein assay

To measure protein concentration and normalise samples, 10μL of cell lysate was added to 1mL of Precision Red (Cytoskeleton Inc.) in a 1.5mL disposable cuvette. Solution was inverted and incubated at room temperature for 10 minutes. Blank of just Precision Red was used and samples measured at OD600 on Bio-Rad SmartSpec Plus spectrophotometer. OD600 value was then compared to standard curve of BSA concentrations (0.0625mg/mL, 0.125mg/mL, 0.25mg/mL, 0.5mg/mL, 1mg/mL, 2mg/mL) and used to calculate protein concentration in each sample. If necessary, lysates were diluted with relevant lysis buffer used to normalise protein concentration across all samples.

SDS-PAGE

Samples were mixed with x4 Laemelli sample buffer (3.5M Tris-HCl (BioBasic) pH8.0, 10% SDS (Fisher Bioreagents), 10% glycerol (Fisher), 5% B-mercaptoethanol (Fisher), 0.05% bromophenol blue) to give a final dilution of x1 and boiled for 5 minutes at 95^oC . Proteins were resolved on SDS-PAGE gel (10% or 12.5%) in running buffer (25mM Tris, 192mM glycine, 0.1% SDS) at 200V for 40-60 minutes. 5μL Precision Plus Protein Kaleidoscope ladder (Bio-Rad) was loaded as standard.

Wet membrane transfer

Resolved proteins on SDS-PAGE gel were transferred on to Hybond 45μM Nitrocellulose Membrane (Amersham Biosciences) using a transfer sandwich (2 blotting paper, SDS-PAGE gel, nitrocellulose membrane, 2 layers of blotting paper) with transfer buffer (25mM Tris-HCL pH7.6, 12mM glycine, 20% methanol). Sandwich was loaded in to a Mini-Protean pack (Bio-Rad) and run for 200 constant amp for 1.5 hours or 25 volts overnight at 4^oC . Ladder was used to check

if all protein had transferred from gel to membrane.

Coomassie staining

Membranes were washed with water once and then covered (approximately 10mL) with Quick Coomassie solution (Generon) for 90 minutes with shaking. Membranes were washed with water twice and imaged one EZ Gel Doc (Licor) on white plate using default settings.

Western blotting (WB)

Membranes were blocked in 20mL of 5% skimmed milk powder in PBS for 30 minutes with rocking. Membranes were transferred to primary antibody diluted in PBS (dilution in table 2.4) and left on a rollar at 4^oC overnight (18 hours). Membranes were then washed 3 times in PBS before secondary antibody (table 2.5) diluted in 20mL of PBS was added and incubated for 1 hour with rocking at room temperature. Membranes were washed in PBS 3 times for 5 minutes each and imaged on Licor Odyssey 3A. Samples were either normalised to rabbit WASP primary antibody stained with goat anti-rabbit 680, or a conugated strepavidin antibody which binds MCCC1, the only biotinylated protein in *Dictyostelium discoideum* (80 kDa)(Davidson et al., 2013) depending on size of the probed protein. Bands were normalized by manually drawing around and normalizing to the highest reading using Licor Image Studio Lite Version 5.2.

Table 2.4: Primary Antibodies

Antigen	Reactive Species	Host Species	Antibody/ Clone Name	Manufacturer	IF Dilution	WB Dilution
α-tubulin	*Dictyostelium discoideum*	Mouse	12G10	DHSB	1:100	1:100
Detyronsinated α-tubulin	Human/*Dictyostelium discoideum*	Rat	YL1/2	Graf Lab	1:10	N/A
CP224	*Dictyostelium discoideum*	Mouse		Graf Lab	1:10	N/A
Acetylated tubulin	Human	Mouse	6-11B-1	Sigma Aldrich	1:100	N/A
Gamma-tubulin	Human	Mouse		Santa Cruz	1:100	N/A
WASP	Human	Rabbit		Insall Lab	N/A	1:10,000
Katnip	Human	Rabbit	PA5-70906	Thermo Fisher	N/A	1:1000
Katnip	Human	Rabbit	HPA035089	Cambridge Biosciences	N/A	1:1000
GFP	*Dictyostelium discoideum*	Rabbit		Peden Lab	1:1000	N/A
GST	Human	Rabbit	A-5800	Thermo Fisher	N/A	1:10,000

Table 2.5: Secondary Antibodies

Species	Alexa Flouphore	Spectra	Manufacturer	Immunofluorescence Dilution	Western Blotting Dilution
Goat Anti Mouse	594	TRITC	Life Sciences	1:50	
Donkey Anti Goat	680	Far Red	Life Sciences	N/A	1:10,000
Goat Anti Mouse	800	InfraRed	Life Sciences	N/A	1:10,000
Goat Anti Rabbit	680	Far Red	Life Sciences	N/A	1:10,000
Goat Anti Mouse	405	UltraVoilet	Life Sciences	N/A	1:10,000
Chicken Anti Rat	592	TRITC	Life Sciences	1:10,000	1:10,000

2.4 Analysis and presentation of data

Analysis of data

Images were analysed on FIJI, and where possible, blinded. Data inputted into GraphPad Prism version 8 and statisical analysis computed using GraphPad t-test function or manually.

Superplots

Where possible, graphical data was presented as superplots as outlined in Lord et al. (2020). Data points were not coloured by repeats but all shared the same colour consistent across cell type (WT = black, WT expressing GFP-tubulin = grey, katnip$^{-(1)}$ = light green, katnip$^{-(1)}$ expressing GFP-tubulin = dark green and katnip$^{-(2)}$ = light blue.).

Statistical analysis

Where suitable (on Gaussian distributed data), unpaired t.tests were used to calculated significance. Statistical significance was calculated based on average of 3 biological repeats using unpaired t.test and defined by p-value (table 2.6).

P-value range	Denoted star
<0.0001	****
0.0001-0.001	***
0.001 to 0.01	**
0.01 to 0.05	*
≥0.05	ns

Table 2.6: P-values range represented by asterisk on graphs

Chapter 3

Results I
Katnip mutants have a general lysosomal trafficking defect

3.1 Introduction: Katnip is an uncharacterised autophagy protein in *Dictyostelium discoideum*

Autophagy is the endogenous process by which intracellular components are captured and degraded by the lysosomes. It is utilised for the removal of unnecessary and potentially harmful proteins (proteostasis), intracellular pathogens (xenophagy) and for organelle recycling (e.g.mitophagy) (section 1.1.2). Upon autophagy completion, the resulting components are reused by the cell and act as a intracellular nutrient source which is relied upon during extracellular starvation (section 1.1.2).

Autophagy is involved in multiple disease pathologies including neurodegen-

erative diseases and cancers. Therefore understanding this complex process is important for elucidating its role in disease development and potential drug target identification. Many of the essential autophagy proteins are already well characterised (figure 1.3), but many regulatory proteins, which produce less severe phenotypes but are nevertheless important, are still being identified. In order to identify new autophagy regulators, a genetic screen in *Dictyostelium discoideum* was performed to identify genetic mutants which presented with reduced autophagy. From this, katnip, was identified as an possible autophagy regulator. Katnip mutants were initially confirmed to have an autophagy defect through 2 separate experiments; a failure to degrade cytoplasm upon starvation observed via electron microscopy, and increased cell buoyancy assayed by separation on a Percoll density gradient (section 1.1.5).These experiments were performed on mutants generated from an Ax3 background. To independently confirm these results using our standard laboratory strains, two previously generated independent katnip mutants in Ax2 were investigated; katnip$^{-(1)}$ and katnip$^{-(2)}$.

Katnip's protein sequence was investigated for similarity to other proteins as inclusion of known domains or conserved regions can hint at protein function. Not only did the protein bear no resemblance to any *Dictyostelium discoideum* autophagy proteins, it shared no sequence similarly to any proteins (other than Katnip orthologues in other species). However, it does contains 3 repeats of an unique protein domain, DUF4457, although the function of this is currently unknown. Therefore, how katnip functions is unknown including its role in autophagy.

The first aim of my project was to investigate the autophagy defect to identify exactly how, and at what stage, loss of katnip affected autophagy.

3.2 Katnip mutants have autophagosome degradation defects

3.2.1 Katnip mutants have reduced viability under starvation conditions

After the identification of katnip as a possible novel autophagy regulator, its involvement in autophagy was validated by testing if mutants exhibited a defect in surviving starvation.

Under starvation conditions, there is a lack of extracellular nutrients forcing cells to rely on autophagy to generate nutrients from the recycling of intracellular material. Cells with autophagy defects are unable to create these nutrients, and therefore exhibit reduced viability under starvation (section 1.1.2). *Atg1*$^{-}$ is a mutant which lacks the essential Atg1 autophagy protein (figure 1.3) and therefore is unable to survive starvation.

When grown in starvation media (SIH media lacking arginine and lysine), both katnip$^{-(1)}$ and katnip$^{-(2)}$ had significantly reduced viability compared to WT, confirming a role for katnip in surviving starvation (figure 3.1A.). However, when compared to *Atg1*$^{-}$, both katnip mutants have a higher viability at all days (until death at day 6). As the loss of katnip produced a less severe phenotype than loss of Atg1, but is still unable to survive starvation as well as WT, it indicates that loss of katnip results in a partial defect.

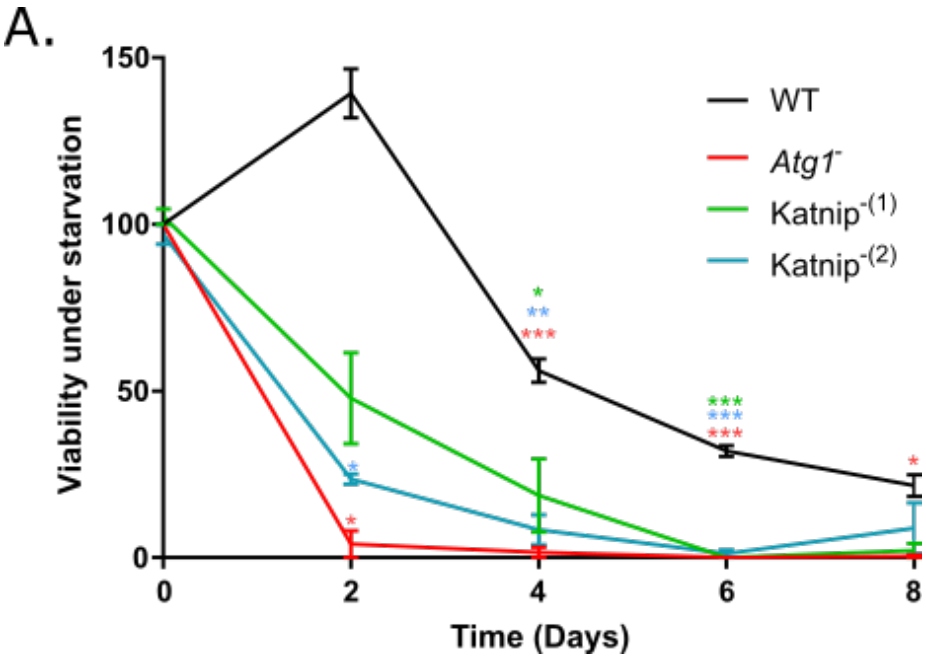

Figure 3.1: **WT and katnip$^{-(1)}$ cell viability after starvation**

A. Viability of WT, katnip$^{-(1)}$, katnip$^{-(2)}$ and *Atg1*$^{-}$ cells grown on *K.aerogenes* bacterial plates after growth in SIH media suspension lacking arginine and lysine over 8 days. N = 3. Unpaired t-test performed on the percentage of colonies across 2 plates compared to Day 0 number (where Day 0 = 100%). Error bars represent SD.

3.2.2 Katnip mutants exhibit reduced autophagic flux

Autophagic flux is the measure of completed autophagy; accounting for the amount of protein turned over by autophagosomes. It can be quantified by the breakdown of GFP-Atg8, (orthologue of mammalian LC3), into free GFP, which is embedded into the autophagosome membrane. Whilst the outer membrane GFP-Atg8 is cleaved off by Atg4 during autophagosome-lysosome fusion, GFP-Atg8 on the inner membrane remains stable (section 1.1.3). GFP is resistant to proteases due to its closed structure and consequently, Atg8 is degraded

upon autophagosome degradation whilst free GFP remains. Therefore, higher levels of free GFP indicate higher levels of autophagosome degradation. This is normalised by calculating free GFP/GFP-Atg8 to account for any changes in number of autophagosomes (when normalised to expression).

AR-12 (also known as OSU-03012) is a celecoxib derivative which downregulates production, increasing the amount of Atg13 available for autophagosome formation (Abdulrahman et al., 2017). It has been previously published as an autophagy inducer in *Dictyostelium discoideum* cells (Cardenal-Muñoz et al., 2017) and was used in this experiment to increase autophagosome numbers.

Protease inhibtiors (PI) inhibit lysosomal proteases preventing the degradation of autophagosomes contents and therefore, the conversion of GFP-Atg8 into free GFP.

Untreated (UT) Katnip$^{-(1)}$ had significantly reduced levels of autophagic flux compared to untreated WT cells (average Katnip$^{-(1)}$ autophagic flux = 0.35, 65% decrease, figure 3.2 A., B.) confirming an autophagy defect in Katnip$^{-(1)}$ cells.

A reduction in autophagic flux can be the result of; 1) a reduction in the number of autophagosomes formed or 2) a reduction in the amount of autophagosomes degraded. In order to ascertain which one of these was the cause of the defect in Katnip$^{-(1)}$, the number of autophagosomes were counted under each condition.

Under AR-12 treatment, neither WT or Katnip$^{-(1)}$ cells had an increase autophagosome number, and no increase autophagosome flux, compared to untreated cells (figure 3.2.2 B., D.). This indicates that AR-12 might not work as a autophagy induction (at least at this concentration), which is conflicting with previously published reports (Mesquita et al., 2013), although matched with past data from our lab .

An increased autophagosome number was observed under PI treatment to the same degree in both WT and Katnip$^{-(1)}$ cells as expected, as autophagosomes build up in cytoplasm when not degraded (figure 3.2.2 B., D.). This is

also reflected in autophagic flux which is reduced in both WT and katnip^{-} cells under PI treatment (figure 3.2.2 A., C.).

Although autophagic flux is reduced in katnip$^{-(1)}$ under all conditions, the same number of autophagosomes were observed in WT and katnip$^{-(1)}$ cells (figure 3.2 C,D). This indicates that katnip$^{-(1)}$ cells have no defect in ability to generate autophagosomes and, therefore, the defect occurs during autophagosome degradation. Similar to their partial defect in surviving starvation (figure 3.1), they exhibit a partial reduction of autophagy flux, as some turnover is still seen in katnip$^{-(1)}$.

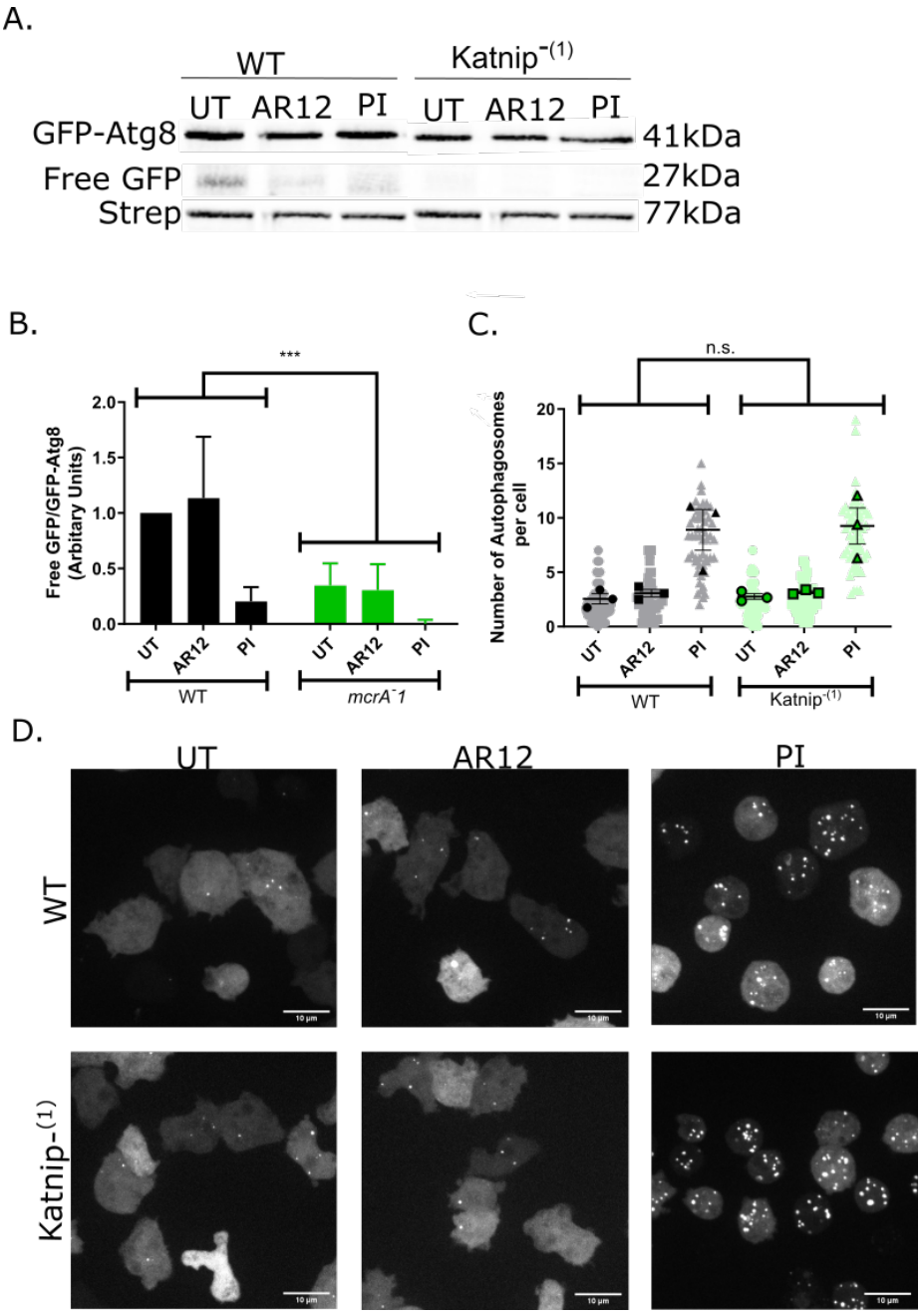

Figure 3.2: **Autophagic flux in WT and katnip$^{-(1)}$ cells**

A. 12% SDS-PAGE gel loaded with lysed WT or katnip$^{-(1)}$ cells expressing GFP-Atg8 ei-

ther untreated (UT), treated with AR12, or treated with x42 Protease Inhibitor (PI). Lysates were probed for anti-GFP and streptavidin as a loading control. B. The ratio between free GFP and GFP-Atg8 levels in WT and katnip$^{-(1)}$ cells either untreated (UT), 2 hour AR-12 treatment (AR12) or 1 hour protease inhibitors (PI) treatment. Representative SDS-PAGE in (A). Levels observed and measured by band intensity from anti-GFP western immunoblotting. WT UT normalised to itself and other conditions were normalised to WT UT fluorescence from relative repeat. N=4.Statistical difference calculated by 2way ANOVA between cells lines across all 4 repeats. Errors bars represent SD. C. Number of GFP-Atg8 positive puncta (autophagosomes) in WT and katnip$^{-(1)}$ cells either untreated (UT), 2 hour AR-12 treatment (AR12) or 1 hour protease inhibitors treatment (PI) in suspension. Representative images in (D). N=3. WT UT cell N = 146, katnip$^{-(1)}$ UT cell N = 149, WT AR12 cell N =144, katnip$^{-(1)}$ AR12 cell N = 199, WT PI cell N = 138, katnip^{-} PI cell N = 152. Counting performed by Ben Phillips. Statistical difference calculated by unpaired t-test between autophagosome number per cell across all cells. Each light grey/green point represent a single cell, darker points indicates average from each repeat. Error bars plotted as SEM from averages. D. Images of WT or katnip$^{-(1)}$ cells expressing GFP-Atg8 imaged after no treatment (UT), AR12 treatment or protease inhibitor treatment (PI). White puncta represent autophagosomes counted in (C).

3.2.3 Katnip mutants have longer autophagosome lifetimes

Previous experiments indicate a defect in autophagosome degradation in katnip$^{-(1)}$, therefore this was investigated further by direct timelapse observation of autophagosome formation and degradation over time. WT and katnip^{-} mutants expressing GFP-Atg8 were compressed and GFP-Atg8 puncta tracked. Compressing *Dictyostelium discoideum* induces autophagy but also allows for the direct observation of different stages of autophagy as previously reported in Mesquita et al. (2017).

Autophagosome formation was determined as the time between when the GFP-Atg8 puncta was first visible (beginning of membrane nucleation) until the completion of a spherical autophagosome, when the signal is brightest. Subse-

quently, degradation can be observed due to the quenching of the GFP fluorescence of GFP-Atg8 puncta upon lysosomal fusion. Quenching was measured as the time between the brightest point of the autophagosome until its disappearance. Quenching is the result of lysosomal fusion and is indicated by the loss of GFP signal due to its proteolysis.

Both katnip^{-} mutants had significantly longer autophagosome formation (WT average = 35 seconds, katnip$^{-(1)}$ average = 136 seconds, katnip$^{-(2)}$ average = 88 seconds) and quenching times (WT average = 55 seconds, katnip$^{-(1)}$ average = 139 seconds, katnip$^{-(2)}$ average = 104 seconds) when compared to WT (figure 3.3 A., B.) indicating both autophagosome formation and degradation were slower. WT autophagosomes had an average lifetime of 90 seconds whereas katnip$^{-(1)}$ mutants, 278 seconds and katnip$^{-(2)}$, 192 seconds (figure 3.3 D.).This, once again, suggests that loss of katnip causes a autophagy defect which affects both autophagosome formation and degradation.

Even though both katnip$^{-(1)}$ and katnip$^{-(2)}$ had reduced autophagy lifetimes, there was variability between the clones, with katnip$^{-(2)}$ have a less severe defect when compared to katnip$^{-(1)}$. This is likely due to genetic variability between cells, similar to the variation of plaques size in figure 3.6.

Autophagosomes in katnip^{-} cells were observed to be larger than WT (figure 3.3 A,B), this may be due to the increased vesicle fusion and membrane delivery to these autophagosomes as they exist for longer (section 1.1.3). Further research would have to be performed in order to understand if this was a genuine defect as results were variable between repeats.

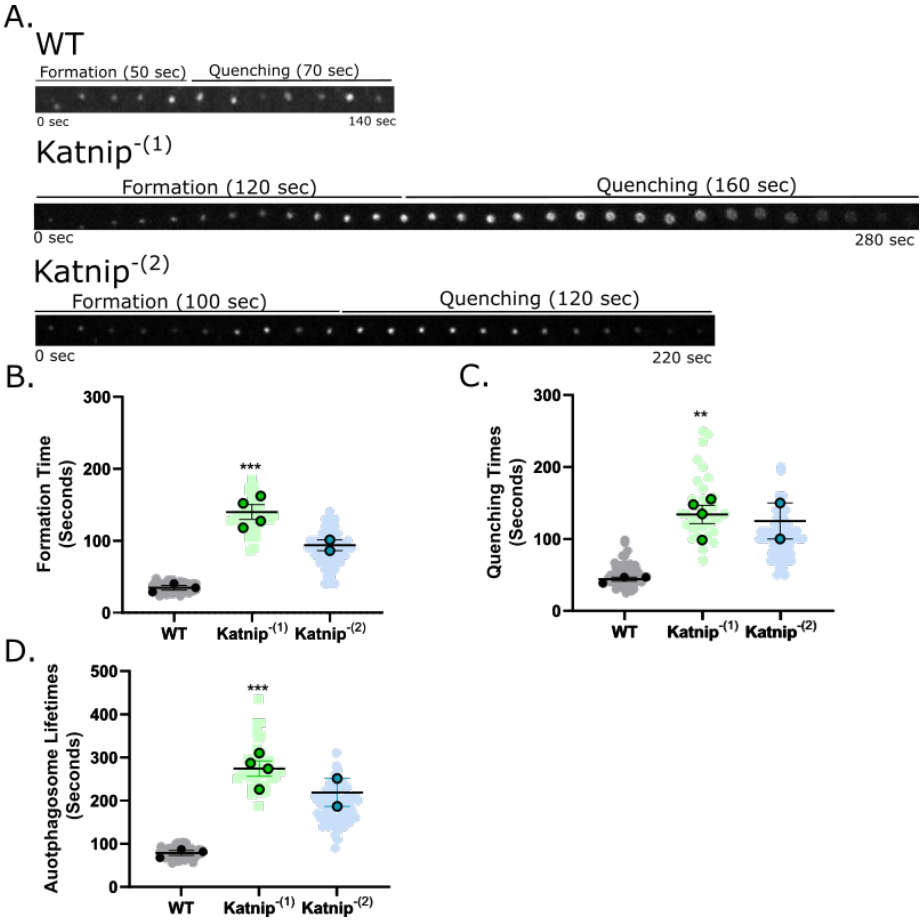

Figure 3.3: **Autophagosome formation, degradation and lifetimes in WT, katnip$^{-(1)}$ and katnip$^{-(2)}$ cells**

A. Example autophagosomes from compressed WT, katnip$^{-(1)}$ and katnip$^{-(2)}$ cells expressing GFP-Atg8. Images were z-stacks to be able to track auophagosomes easily when moving inbetween z-planes which were tracked from the first time point where they were visible, until their brightest point (formation), and from their brightest point, until no longer visible (quenching). Imaged at 5 seconds intervals. Imaged on spinning disk confocal microscope. B. GFP-Atg8 autophagosome formation times of WT, katnip$^{-(1)}$ and katnip$^{-(2)}$ mutants. Unpaired t-test performed. C. GFP-Atg8 autophagosome quenching times of WT katnip$^{-(1)}$ and katnip$^{-(2)}$ mutants. D. Total autophagosome lifetimes of WT, katnip$^{-(1)}$

and katnip$^{-(2)}$ mutants. Both katnip$^{-(1)}$ and katnip$^{-(2)}$. WT N = 209 autophagosomes, 5 repeats. katnip$^{-(1)}$ N = 94 autophagosomes, 4 biological repeats. katnip$^{-(2)}$ N = 96 autophagosomes, 2 biological repeats, no stats where performed due to only 2 repeats. All analysis was blinded.

3.2.4 Katnip mutants can still effectively clear mutant Huntington protein

As the loss of katnip results in autophagosome formation and degradation defects, mutants ability to removed aggregated proteins was assayed as this relies on functional autophagy. A well characterised example of this is the removal of Htt protein aggregates carrying the Q103 mutation associated with Huntington disease development.

Huntington disease is a degenerative neurological disease which develops due to a inherited mutation in the Huntington gene. Disease causing mutations resulting in the inappropriate cleavage of Huntington mRNA and increases its propensity to form toxic aggregates (Wellington et al., 2000). Autophagy defects are associated with Huntington disease progression, as with many molecular neurodegenerative diseases, the cells rely of effective autophagy to remove misfolded proteins before they form toxic aggregates (section 1.1.2). As katnip^{-} cells exhibit a partial autophagy defect, their ability to remove toxic mutant Huntington protein was observed to assess if autophagy defect was severe enough to cause build up of aggregates.

GFP-HttQ103 was over expressed in WT, katnip$^{-(1)}$ and *Atg1*$^{-}$ cells and the percentage of cells with observable GFP positive aggregates was counted. In WT cells only 4.5% (6/133 cells) of cells exhibited GFP positive puncta and in *Atg1*$^{-}$ cells expressing GFP HttQ103, 100% (80/80) of cells had GFP positive aggregates due to *Atg1*$^{-}$ cells' total loss of autophagy (binucleate cells were not counted due to inability to tell between aggregates or secondary nucleus). In katnip$^{-(1)}$ cells, only 3.5% of cells (4/114 cells) had GFP positive aggregates, comparable to WT levels (figure 3.4). This suggests that although

katnip^{-} have a partial autophagy defect, cells are still able to degrade mutant Huntington proteins via autophagy at a high enough level to prevent aggregates accumulating in the cytosol.

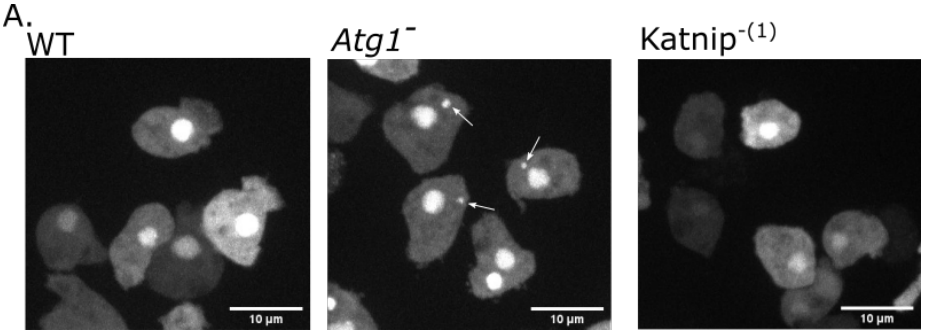

Figure 3.4: **WT, katnip$^{-(1)}$ and *Atg1*$^{-}$ cells expressing HttQ103 protein**

A. WT, *Atg1*$^{-}$ or katnip$^{-(1)}$ cells expressing GFP-HttQ103 mutant proteins. Cells imaged at x60. Arrows points to GFP-HttQ103 aggregates which are observed in *Atg1*$^{-}$ cells. GFP-HttQ103 also slightly accumulates in the nucleaus seen in all cell lines. Imaged on spinning disk confocal microscope.

3.3 Katnip mutants exhibit a phagosome degradation defect

After identifying that loss of katnip causes a partial defect in autophagosome degradation, phagocytosis was investigated to observe if this degradation defect is specific to autophagy or affects other trafficking pathways.

Autophagic degradation is dependent on the fusion of autophagosomes to lysosomes along microtubules. Upon contact, they fuse to form an autolysosome and cargo is degraded by the catabolic enzymes in the lysosome. Other trafficking pathways also rely on these mechanisms for the degradation of their vesicles; these pathways are collectively known as the lysosomal trafficking pathways and include phagocytosis and macropinocytosis.

Phagocytosis is the specific uptake of solid material from the extracellular environment. It is used to remove apoptoic and necrotic cell corpses to prevent local inflammation and by immune cells to remove extracellular pathogens (Rosales and Uribe-Querol, 2017). Phagocytosis is dependent on surface receptor binding to pathogenic material (e.g.lipopolysaccharide bacterial coat)(Wilson et al., 2015) or apoptotic protein markers (e.g. ATP) (Nagata et al., 2016). After internalisation, phagosomes undergo a similar process to autophagosomes, where they are loaded on to microtubules and transport to come into contact, and fuse with, lysosomes. Once phagosomes are degraded, material is either expelled from the cell or used for nutrients.

3.3.1 Katnip mutants have a phagosomal proteolysis defect

As katnip$^-$ cells have defects in their autophagosome degradation, phagosomal degradation was assessed to see if this defect also affected phagocytosis by measuring proteolysis in phagosomes. As *Dictyostelium discoideum* are professional phagocytes, there are well established assays to measure phagosome proteolysis.

By loading the cells with DQ-BSA BODIPY/Alexa 594 beads, phagosome proteolysis can be directly measured. The BSA bead coating degrades upon proteolysis, releasing BODIPY from its self quenching form and allowing it to fluoresce. Each bead is also labelled with Alexa 594, allowing the number of beads in cells to be normalised. The ratio between DQ-BSA BODIPY and Alexa 594 is calculated to give 'proteolytic activity' and an increase in this measure signifies increased proteolysis of phagosomes.

Both katnip$^-$ mutants had significantly reduced proteolytic activity (84.3% reduction) compared to WT cells (figure 3.5 A., C.) and therefore, katnip$^-$ cells have a defect in phagosomal proteolysis.

In order to test if this defect could be rescued, the proteolysis of katnip$^-$

mutants expressing GFP tagged katnip constructs was assessed. Unfortunately, due to the excessive AT-richness and repetitive sequence of the N-terminus of *Dictyostelium discoideum* katnip (688 of its 2516aa are asparagines), only the sequence from base 1561 to the sequence end was amplified (includes 4395bp of the total 5956bp, uniprot code: O60303).

This construct was GFP-tagged and named GFP-ddkatnipΔN. As a full length alternative, katnip sequence from *Dictyostelium lacteum*, a close relative to *Dictyostelium discoideum* which lacks the polyN repeats in katnip, was amplified, GFP-tagged and named GFP-dlkatnip. Both of the cell lines expressing these plasmids still had a reduced phagosomal degradation compared to WT suggesting that this phenotype cannot be rescued by these constructs (figure 3.5 B.). Neither of these constructs are the full length *Dictyostelium discoideum* katnip gene and this may be the reason the constructs didn't fully rescue. Although I was unable to rescue the knockout by extrachromosomal overexpression, identical phenotypes were observed in both independent mutants.

As both katnip$^-$ clones have defective phagosomal proteolysis, katnip$^-$ mutants have a general degradation defect affecting the degradation of both autophagosomes and phagosomes.

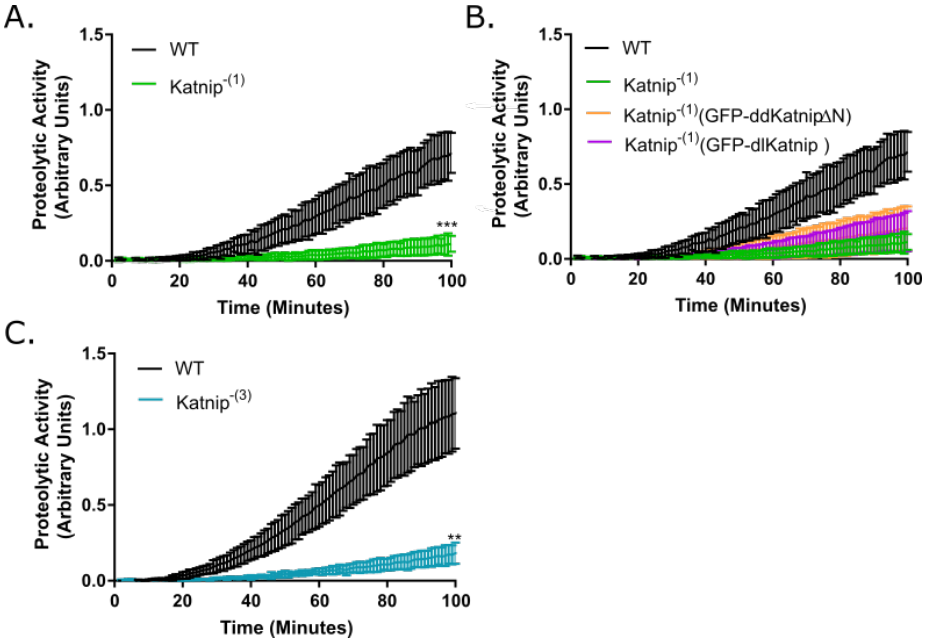

Figure 3.5: **Phagosome protelysis in WT, katnip$^{-(1)}$ and katnip$^{-(2)}$ cells**

A. Proteolytic activity (DQ-BSA/Alexa 594 fluorescence) within phagosomes in WT and katnip$^{-(1)}$ cells. B. Proteolytic activity assessed by the degradation of DQ-BSA Biodipy beads in WT (blue), katnip^{-} (green), katnip^{-} cells expressing GFP-ddkatnipΔN plasmid (dark blue) and katnip^{-} cells expressing GFP-dlkatnip plasmid (blue). C. Proteolytic activity within phagosomes in WT and katnip$^{-(2)}$ cells by assessed proteolysis of DQ-BSA Biodipy beads. A.,B. and C. all N = 4. Plotted as normalised mean (time = 0) and standard deviation across all repeats. T-test against means at time = 100. Unpaired T-test performed at 100 minutes to calculate significance.

3.3.2 Loss of katnip results in reduced growth on bacteria

Klebsiella aerogenes bacteria is a Gram-negative rod-shaped bacteria naturally phagocytosised and degraded by *Dictyostelium discoideum* for food. To test whether the phagosome proteolysis defect observed above is physiologically important for the growth of katnip^{-} cells, WT and katnip$^{-(1)}$ cells were spread on a lawn of *Klebsiella aerogenes* and the plaques formed by clearing of bacteria were imaged and measured after 5 days of growth. During this time,

cells phagocytosed and cleared surrounding bacteria in order survive, forming plaques.

During growth on bacteria, *Dictyostelium discoideum* cells aggregates together and form fruiting bodies in order to reach new area of nutrients (section 1.1.4). As the plaques grow larger, cells in the centre are starved due to lack of nutrients and begin their developmental pathway and form fruiting bodies (which appear as white spots in the dark grey plaques, examples pointed to by red arrows, in Figure 3.6). All WT plaques contain multiple fruiting bodies whereas none are observed in katnip$^{-(1)}$ plaques. The formation of a fruiting bodies relies on autophagy (section 1.1.4) and therefore, this phenotype may be caused by the reduced autophagic capability of Katnip^{-} cells.

Although there was no significant different between WT and katnip$^{-(1)}$ mutant plaques sizes, katnip$^{-(1)}$'s plaques had more variable size and shape within the population. This may be due to genetic variability between the populations.

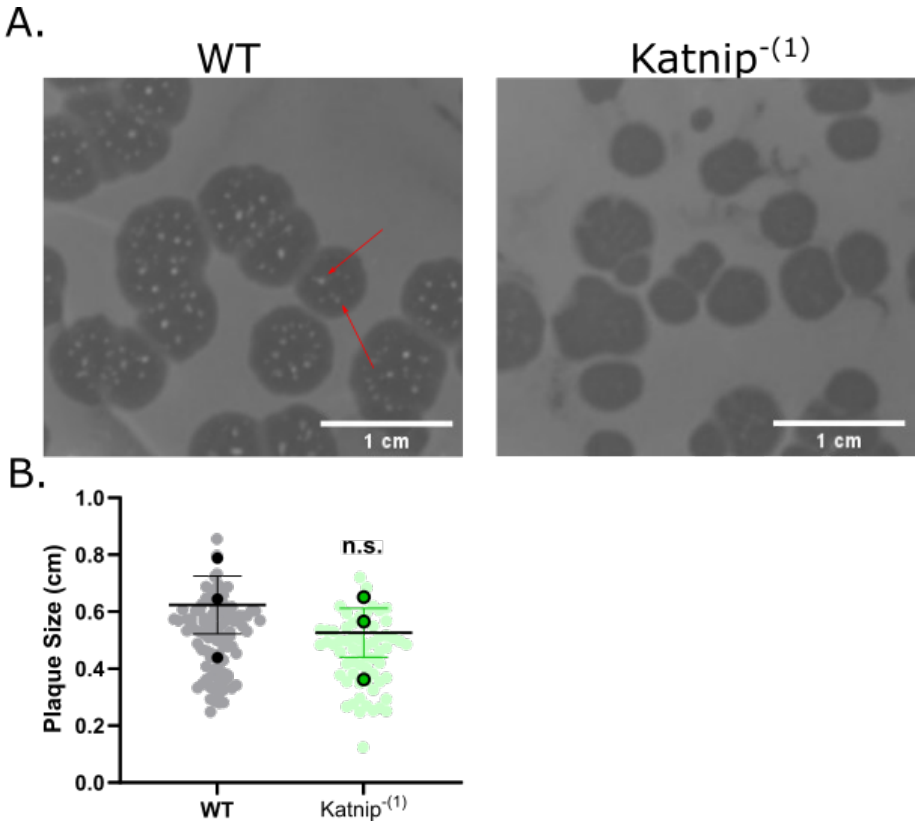

Figure 3.6: **WT and katnip$^{-(1)}$ growth on bacterial plates**

A. Image of WT and katnip$^{-(1)}$ plaques on a *Klebsiella aerogenes* lawn on SM agar plates 5 days after 100 cells were spread. Red arrows point to examples of fruiting bodies, which appear as white spots on within the dark background on the plauque were the bacteria has been eaten away. B. Plaques size of WT and katnip$^{-(1)}$ plaques on *Klebsiella aerogenes* lawns after 5 days growth. Representative images in (A). N = 3. WT plaques counted = 115, katnip$^{-(1)}$ plaques counted = 166. Analysised by paired T-test.

3.3.3 Katnip mutants exhibit a chemotaxis defect

Because katnip^{-} cells produce smaller plaques on bacteria, chemotaxis was measured as small plaques may be due to defective migration towards bacteria. *Dictyostelium discoideum* endogenously chemotax towards a folic acid gradient by

sensing through a folate acid G-coupled receptor on their cell surface (Pan et al., 2016). This behaviour has evolved in order to sense and move towards folate secreting bacteria in the soil which they phagocytose and degrade for nutrients.

When incubated with a folate acid gradient, all WT cells moved towards the folate acid source and all had a positive directionality (ending position was closer to the folate acid source than the beginning position) (figure 3.7 A.).

Katnip^{-} cells travelled the same total distance as WT cells (figure 3.7 C.) but exhibit an almost complete loss of directionality (figure 3.7 D.). This indicates that Katnip^{-} cells can move at WT levels but not in the direction of folate acid.

In conjunction with other data, one hypothesis is that the cause of the chemotaxis defect is due to the inability to traffic and recycle the folate acid receptor once they have bound and been internalised. Katnip^{-} cells may suffer from a general trafficking defect which affects all trafficking processes, including the recycling of plasma membrane receptors. This has larger implications for signalling processes and receptor mediated cargo internalisation. Alternatively, this may be due to loss of polarity in these cells, a function which requires correct microtubule organisation.

The cheomtaxis defect may also be the cause of the lack of fruiting bodies observed in Figure 3.6 as cells chemotax towards each other along a cAMP gradient in order to form the fruiting bodies.

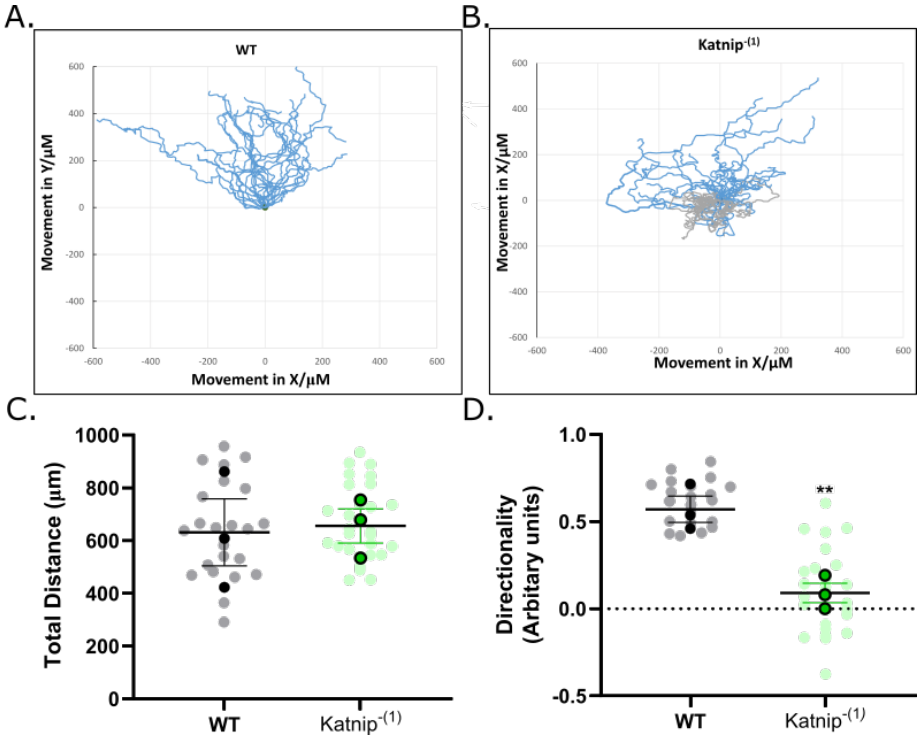

Figure 3.7: **WT and katnip$^{-(1)}$ chemotaxis along a folate acid gradient**

A. Graphical representation of each WT cell movement towards a 0.1mM folate acid gradient (at top of graph) over 1 hour. Total cell N = 28. B. Graphical representation of each katnip$^{-(1)}$ cells towards a 0.1mM folate acid gradient (at top of graph) over 1 hour. Blue lines representative cells with positive directionality (N = 18) whereas grey lines represent cells with negative directionality (N=10). Total cell N = 28. C. Average total distance travelled by WT and katnip$^{-(1)}$ cells over 1 hour. WT N=28 cells, katnip$^{-(1)}$ N = 28 cells. P value = 0.8705. Biological repeats N=3. D. Mean directionality (defined as the total distance travelled by the cells over net distance) of WT and katnip$^{-(1)}$ cells over 1 hours. WT N = 28, katnip$^{-(1)}$ N = 28. N = 3. P-value = 0.0070.

3.4 Katnip mutants display disrupted macropinocytosis

3.4.1 Katnip mutants have reduced growth in minimal media

As katnip^{-} cells have defects in both autophagosome and phagosome degradation, another lysosomal trafficking pathway, macropinocytosis, was investigated to see if it shared a similar defect.

Macropinocytosis is the non-selective bulk uptake of extracellular liquid by large plasma membrane cups which can be up to 5μM in size (Swanson and Watts, 1995; Lim and Gleeson, 2011).

This process is non-selective, meaning that no surface receptor binding is required for initialisation. Although cargo binding isn't required, overall levels of macropinocytosis are increased in response to growth factor binding and immune cell activation (Haigler et al., 1979; Kerr and Teasdale, 2009).

In liquid (axenic) culture, *Dictyostelium discoideum* rely on macropinocytosis to gain nutrients from the extracelluar environment to survive and grow. *Dictyostelium discoideum* are grown in rich media (HL5) which has an overabundance of nutrients and therefore cells require very little of this media in order to gain enough nutrients to survive.

Alternatively, minimal media (SIH) has a much reduced amount of nutrients meaning the cells have to uptake and process more media in order to gain enough nutrients to survive. Under minimal media growth, cells with even subtle aberrations to macropinocytosis cannot gain enough nutrients and therefore exhibit growth defects.

Under rich media growth (HL5), katnip$^{-(1)}$ exhibited no growth defects (figure 3.8 A., B). But, under minimal media growth, katnip$^{-(1)}$ cells exhibited a growth defect (figure 3.8 C.) and have an increased doubling time (although didn't reach significance) (figure 3.8 D.). As they can grow under rich media and minimal media (albeit at a slower rate), this suggests they can gain some

nutrients from macropinocytosis but, due to the reduced growth rate in minimal media, do have some form of reduced macropinocytosis.

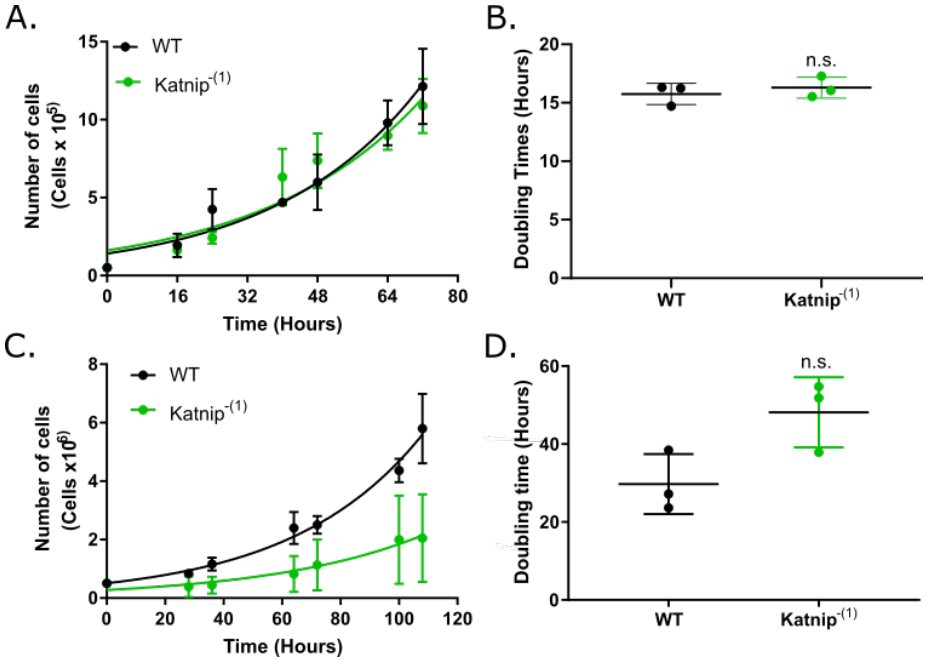

Figure 3.8: **WT and katnip$^{-(1)}$ growth in minimal media**

A., C. Number of WT and katnip$^{-(1)}$ cells measured at 8 or 16 hours interval for 3 days under either HL5 (A.) or minimal media (SIH) (C.). N = 3. B., D. Doubling time of WT and katnip$^{-(1)}$ in HL5 (B.) or SIH (D.) media. N=3. P value = 0.0547.

3.4.2 Macropinosomes are smaller in katnip mutants

After identifying a partial defect in the axenic growth of katnip^{-} cells, the number of macropinosomes in the cells were measured to see if this was a defect in macropinosome creation or degradation. The maturity of macropinosomes was also observed by loading cells with TRITC (red) and FITC (green) Dextran. Immediately after internalisation, macropinosomes fluoresce yellow as both TRITC and FITC Dextran fluorese in neutral pH. Macropinosomes quickly undergo maturation, shrinkage and acidification, the last of which causes the quenching

of the FITC protein (it is still present but doesn't fluoresce under these conditions). This leaves only the TRITC behind causing mature macropinosomes to appear red. Post-maturation, macropinosomes can be repackaged for exocytosis, re-neutralising and regain the FITC fluorescence, appearing as yellow again. These post-lysosome fused yellow macropinosomes can be differentiated from early yellow macropinosomes as they are more concentrated.

Both katnip^{-} mutants had more mature (red) macropinosomes (although it did not reach significance in katnip$^{-(2)}$)(figure 3.9 A., D.), suggesting a defect in the clearance of mature macropinosomes. These mature macropinosomes were significantly smaller than WT cells (figure 3.9 A., E.).

There were similar numbers of post-lysosomal (yellow) macropinosomes (figure 3.9 A., B.) between WT and katnip^{-} mutants and they were significantly smaller in the katnip^{-} mutants (figure 3.9 A., C.). This shows katnip^{-} 's macropinosomes do mature into post-lysosome macropinosomes although further analysis would be required to tell if the rate of which was different. Due to the build up of mature macropinosomes, it may be that the fusion of mature macropinosomes with lysosomes is reduced leaving mature macropinosomes to build up in the cytoplasm.

These results suggest that loss of katnip results in macropinosomes disruption, affecting both immature and mature macropinosomes size and number although these results are variable between clones.

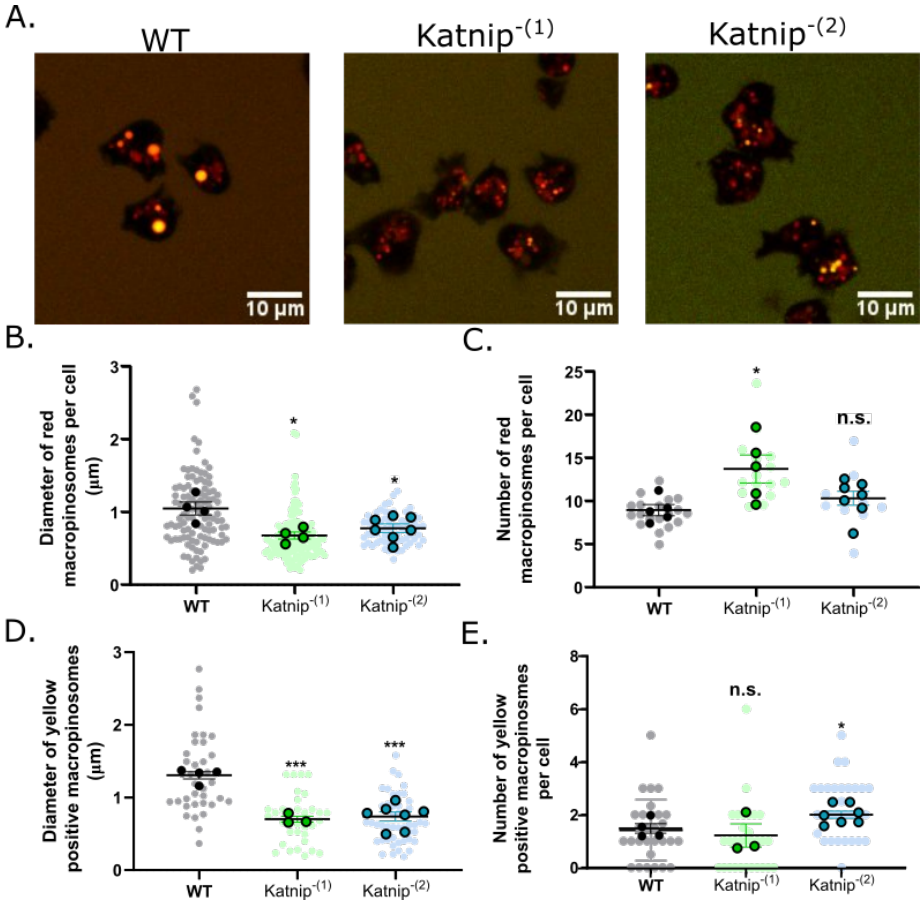

Figure 3.9: **Cytoplasmic macropinosomes in WT and katnip$^{-(1)}$ and katnip$^{-(2)}$ cells**

A. Images of WT, katnip$^{-(1)}$ and katnip$^{-(2)}$ cells incubated in 2mg/mL TRITC Dextran and 0.4mg/mL FITC Dextran in HL5 media for 18 hours. Red macropinosomes represent mature macropinosomes which have been acidified as FITC signal has been quenched. Imaged on spinning disk confocal microscope. B. Number of TRITC positive macropinosomes in WT, katnip$^{-(1)}$ and katnip$^{-(2)}$ cells. WT cell N = 51 , katnip$^{-(1)}$ cell N = 34, katnip$^{-(2)}$ cell N = 44 cells. C. Width of TRITC positive macropinosomes in WT, katnip$^{-(1)}$ and katnip$^{-(2)}$ cell lines. WT N = 56, katnip$^{-(1)}$ N = 37, katnip$^{-(2)}$ N = 81. D. Number of FITC/TRITC positive macropinosomes per cells in WT, katnip$^{-(1)}$ and katnip$^{-(2)}$ cell lines. N = 3. WT

N = 68 cells, katnip$^{-(1)}$ N = 62 cells, katnip$^{-(2)}$ N = 48 cells. E. Width of FITC/TRITC positive macropinosomes in WT, katnip$^{-(1)}$ and katnip$^{-(2)}$ cell lines. N = 3. WT N = 248, katnip$^{-(1)}$ N = 358, katnip$^{-(2)}$ N = 237. WT N = 4 repeats, katnip$^{-(1)}$ N = 4 repeats, katnip$^{-(2)}$ N = 7 repeats. Significance calculated from unpaired t-test against repeat averages. Bars represent SEM between repeat averages.

In conclusion, I have shown that 3 lysosomal degradation pathways are disrupted indicating a general role of katnip in the vesicle-lysosome fusion.

3.5 Katnip appear to have functional lysosomes

3.5.1 Katnip mutants have WT levels of cathepsin D

Autophagy, phagocytosis and, to some extent, macropinocytosis share a degradation defect in katnip^{-} cells. In order to assess if these degradation defects are caused by lower levels of lysosomal enzymes, the levels of cathepsin D, a major lysosomal protease, were quantified.

A small decrease in the amount of cathepsin D was observed between WT and katnip^{-} but this did not reach significance (figure 3.10 A., B.). Cathepsin D is used to assess the measure of lysosomal proteins in the cells, as WT and katnip^{-} mutants had a similar amount, this indicates that they share similar levels of this enzyme, but there are many other lysosomal enzymes in *Dictyostelium discoideum* and they may still have defects in packaging of lysosomes.

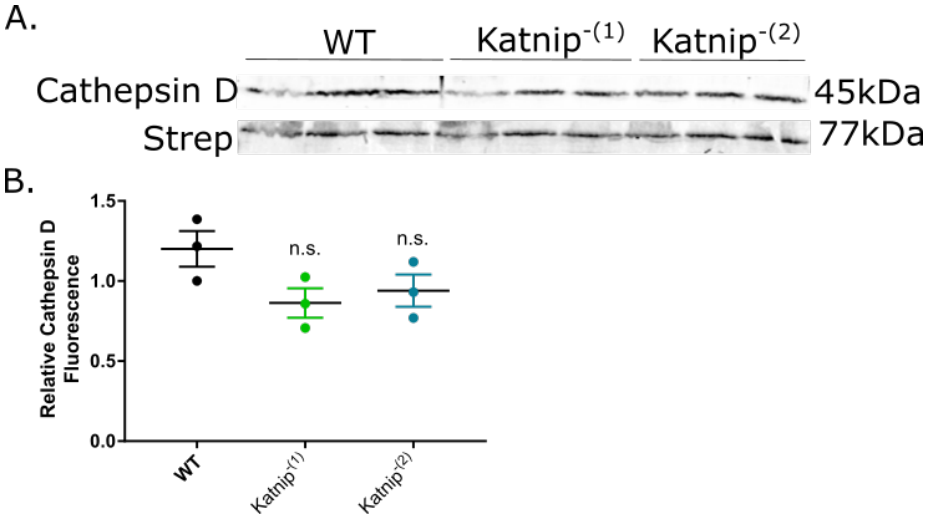

Figure 3.10: **Loss of katnip doesn't affect cathepsin D amount**

A. Western Blot of RIPA lysed WT and katnip$^{-(1)}$ cells probed for cathepsin D and for the loading control, streptavaidin (Strep). 3 repeats loaded on the same blot. N=3. B. Cathepsin D fluorescence normalised against strepavaidin loading control and divided by normalised cathepsin fluorescence of WT repeat 1. N=3. Bars represent SD between repeats.

3.5.2 Katnip mutants exhibited no defects in total proteolytic activity

After identifying that the WT and katnip^{-} mutants had the same amount of cathepsin D, the total proteolytic activity of cells was measured using a DQ-green/Alexa 594 beads proteolysis assay (same beads as used in section 3.3.1) on whole cell lysate.

By lysing cells, the localisation and packing of proteases is removed and therefore cargo, in this case DQ-green/Alexa 594 beads, degraded without the necessity for lysosomal and vesicle trafficking, and is therefore independant from microtubules.

As a control, protease inhibitors were used to block proteolytic activity. WT, katnip$^{-(1)}$ and katnip$^{-(2)}$ exhibited no difference in proteolytic activity

both with and without protease inhibitors (figure 3.11 A.).This indicates that the ability to degrade the material is the same between WT and katnip^{-} cell lines. Loss of katnip therefore does not affect the cells capacity to degrade material.

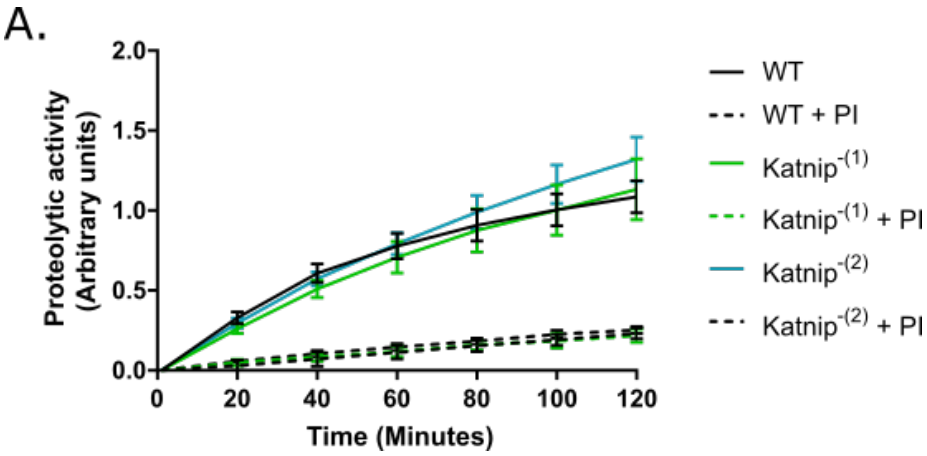

Figure 3.11: **Total proteolytic activity of WT and katnip$^{-(1)}$ and katnip$^{-(2)}$ cells**

A. Total proteolytic activity, measured by levels of DQ-BSA to Alexa594 levels on silica beads normalised to readings at time = 0. PI = 1:20 protease inhibitors. Bars represent SD across repeats. N=3.

3.6 Discussion: Loss of katnip results in a general lysosomal degradation defect

3.6.1 Katnip mutants have reduced autophagy but are still able to prevent HttQ104 aggregates

Loss of katnip produces a 65% decrease in autophagic flux and a 261% increase in autophagosome lifetimes. Despite these defects, katnip$^{-(1)}$ cells are still able to prevent HttQ104 protein aggregates forming (Malinovska et al., 2015). *Dic-*

tyostelium discoideum are known to be especially effective at removing polyQ proteins as their genome has many polyQ tracks, with katnip itself containing 220 glutamine (Q) residues. Therefore, whilst the autophagy defect in katnip$^-$ cells doesn't reach great enough severity to prevent HttQ104 clearance, in other species, including mammals, katnip mutants may not be able to remove HttQ104 aggregates, especially in long lived cells like neurons.

3.6.2 Phagosome proteolysis defects in katnip mutant cells cannot be rescued using GFP-dd katnipΔN or GFP-dl katnip

Katnip$^-$ cells expressing GFP-ddkatnipΔN or GFP-dlkatnip only exhibited a very small increase (10% increase) in phagosome proteolysis compared to katnip$^-$ cells. As the GFP-ddKatnipΔN did not contain the first 1561bp of katnip's sequence, it may be that this sequence is required for its function. Whilst there are no identified protein domains or highly conserved regions within this section, it may be necessary for the correct protein folding. GFP-dlkatnip did not rescue either; although the *Dictyostelium lacteum* genome is similar to *Dictyostelium discoideum* , dlkatnip may be different enough to not be able to rescue katnip$^-$ cells. The gene is also a different size to ddkatnip, being 5956bp whereas the dlkatnip is 7350bp and therefore may be missing certain elements required for katnip function and disallowing katnip$^-$ rescue.

3.6.3 Macropinocytosis is less reliant on lysosomal transport

The macropinocytosis data indicates that the macropinocytosis degradation defect is less severe than the autophagy and phagocytosis degradation defect in katnip$^-$ cells. This suggests that macropinocytosis is less sensitive to the loss of katnip and therefore, hypothesised to be less reliant on lysosomal transport for degradation. This may be due to the acidification of macropinosomes through

early fusion with mature acidic macropinosomes catalysing their degradation in a indirect manner.

Even though macropinocytosis seems less sensitive to the loss of lysosomes/vesicle contact, they still interact with microtubules as shown in figure 3.12.

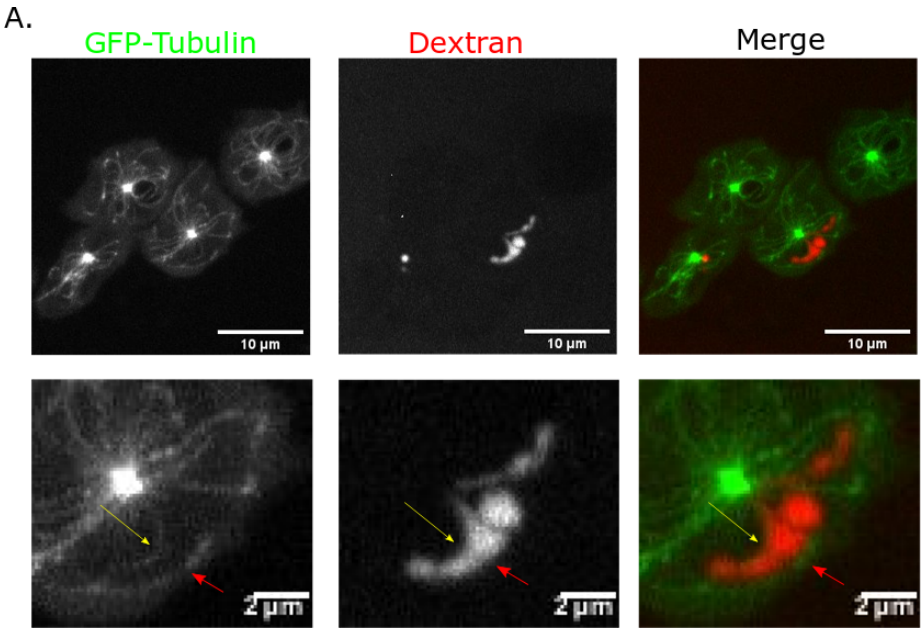

Figure 3.12: **Macropinosome movement along microtubules**

A. GFP-tubulin expressing WT cells treated with 100μM Nocodazole and pulse chased with 2mg/mL TRITC Dextran. Arrows indicates points at which macropinosomes which are attached to microtubules. Imaged on spinning disk confocal microscope.

Other knockouts in the lab which exhibit a complete blockage in phagosome degradation have also been observed to have little to no defects in their macropinocytosis pathways, such as PIKfyve mutants (unpublished lab data). This suggests that macropinosomes degradation works through a separate pathway for degradation to phagosome and autophagosomes. This may be the cause of the differences in defect severity between katnip$^-$ phagocytosis compared to macropinocytosis.

3.6.4 Katnip functions in maintaining lysosomal transport and/or fusion

Katnip was originally identified as being required for the autophagy-dependent change in cell density upon starvation but the molecular mechanisms underpinning this defect were completely unknown. The dynamics of 3 lysosomal trafficking pathways; autophagy, phagocytosis and macropinocytosis were investigated using 2 independent katnip$^-$ mutants and all were found to be disrupted, with cells able to form these vesicles but share defective degradation.

As the defect in katnip$^-$ cells affects the degradation of vesicles across all lysosomal trafficking pathways, loss of katnip must affect the lysosome-dependant degradation machinery shared by all the pathways.

As previous reports of katnip implicate its role in cilia microtubule organisation (Sanders et al., 2015), the cause of the lysosomal transport defect observed in this chapter may be due to defective microtubules.

Vesicles and lysosomes are transported along microtubules to come into contact with each other. As lysosomes were functional (as shown by their total proteolytic activity, section 3.11), but lysosomal degradation defective, a possible explanation is that loss of katnip affects the transport of lysosomes and vesicles along microtubules. This could be due to a role in katnip in loading lysosomes and vesicles onto microtubules, or maintaining microtubule function and/or organisation.

Further investigate in to lysosomal functionality and activity was limited by lack of lysosomal assay and difficulties imaging lysosomes in *Dictyostelium discoideum* . There are no specific markers of lysosomes in *Dictyostelium discoideum* and many of the common markers used in mammalian cells also mark macropinosomes in *Dictyostelium discoideum* which covered large portions of the cell volume. Lysosomal defects could arise from incorrect lysosomal package or enzyme production, incorrect positioning or defective pH affecting lysosomal enzyme activity. In relation to the degradation of vesicles, lysosomal loading on to microtubules or the fusion betwen lysosomal and vesicles could also be

defectives, accounting for the degradation defects seen in *katnip* cells. Future work should be focus around the creation of a katnip knockout in a suitable mammalian cells line to aid investigate into lysosomes.

The requirement for microtubules in autophagy (and other vesicles) degradation has been well reported but, the involvement of microtubules in autophagy formation has been previously investigated with contradicting results (Köchl et al., 2006), (Aplin et al., 1992). Data looking at autophagosome lifetimes in figure 3.3 suggests that katnip and therefore microtubule function is necessary for the efficient formation of autophagosome due to the elongated formation time observed in both katnip^{-} mutants (figure 3.3). This may be due to microtubules trafficking autophagy proteins and membrane to the omegasome during autophagy but, more research needs to be performed to confirm microtubule's exact involvement in autophagosome formation.

Chapter 4

Results II
Katnip is a centrosomal protein responsible for tolerating microtubule damage

4.1 Introduction: Katnip mutant cells have cilia microtubule organisation defects

No papers have previously reported on katnip function in *Dictyostelium discoideum* and only one on the function of katnip function in humans at the beginning of this PhD. Sanders et al. (2015) stated that the loss of katnip caused microtubule organisation defects in the cilia (a loss of A-tubule number and microtubule doublet organisation).

Interestingly, *Dictyostelium discoideum* are not able to form cilia but still have the katnip gene. Therefore katnip is likely to have cilia independent roles in microtubule organisation otherwise the gene would of been loss through evolution.

Although Sanders et al. (2015) work focuses on cilia, they did state that GPF-katnip localised to 'filamentous cytoskeletal structures' in the cytoplasm. I hypothesised that these 'filamentous cytoskeletal structures' were interphase microtubules and therefore katnip may be able to localise and potentially affect these microtubules.

In order to further understand katnip's role interphase microtubules, the function katnip in *Dictyostelium discoideum* microtubules was investigated using two separate katnip$^-$ clones, katnip$^{-(1)}$ and katnip$^{-(2)}$.

4.2 Katnip is a centrosomal protein which can bind to microtubules

4.2.1 GFP-katnip localises to the centrosome

In order to identify where katnip localised to, GFP-ddkatnipΔN was expressed in WT and katnip$^{-(1)}$ cells (section 3.3.1 for more details on plasmid).

GFP-ddkatnipΔN localised to the centre of the tubulin network, likely the centrosome. Staining overlapped the nucleus itself which may be due to the incorrect folding of the truncated protein causing accumulation in the nucleus. Previous use of this construct had proven insufficient for rescue (figure 3.3.1) and therefore the full length *Dictyostelium lacteum* fusion protein was imaged to see the missing N terminus of GFP-ddkatnipΔN altered the localisation.

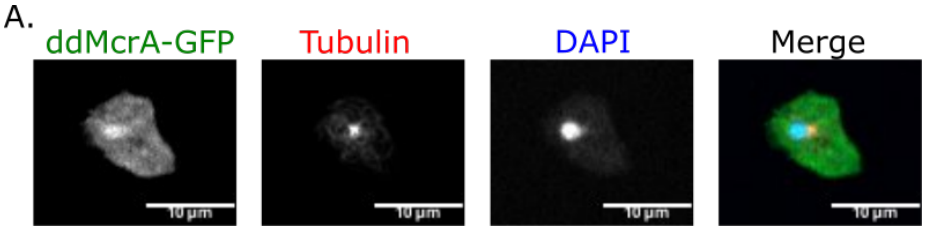

Figure 4.1: **GFP-ddkatnipΔN localises to the centrosome and nucleus**

A. Ultra cold methanol fixed WT cells on coverslips expressing GFP-ddkatnipΔN (green), stained with anti-tubulin (red) and mounted in Prolong Gold with DAPI (blue). Slides imaged on airyscan microscope at x100 with 0.5μM z-stacks, images airyprocessed and then max-projected. Merge between all 3 channels.

In order to confirm that katnip was localising at the centrosome, GFP-dlkatnip expressing cells were fixed and stained with CP224, a centrosomal marker (which also partially stains the end of microtubules),(Samereier et al., 2011). In both interphase (figure 4.2 A.) and mitotic cells (figure 4.2 B.), GFP-dlkatnip overlaps with CP224 as well as having a relatively high cytoplasmic background, potentially indicative of a free pool of the protein.

Both of these localisations (centrosomal and cytoplasmic) are similar to GFP-katnip expression in mammalian cells, where proteins was observed to localise to the basal body and had high cytoplasmic expression. In mammalian cells, the centrosome is also the basal body of cilia upon translocation. Therefore centrosomal localisation is conserved between *Dictyostelium discoideum* and mammalian cells. GFP-katnip localises along the microtubule spindle in mitosis, this may be due to the overlap with centrosomal proteins as shown by CP224 staining, or it may have a role in mitosis.

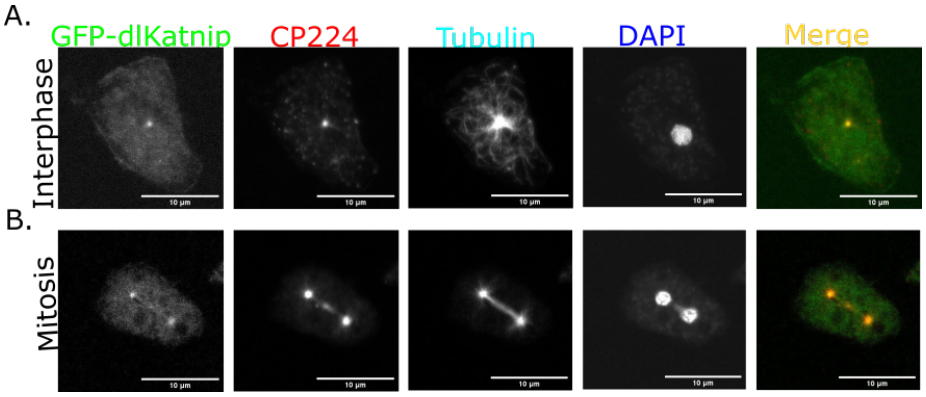

Figure 4.2: **GFP-dlkatnip localises to the centrosome**

A. Interphase WT cells and, B. mitotic WT cells on coverslips expressing GFP tagged *Dictyostelium lacteum* katnip (green), ultracold methanol fixed and stained with anti-tubulin (cyan) , anti-CP224 (a centrosomal and microtubule end marker,red) mounted in Prolong Gold with DAPI (blue). Merge between GFP-dlkatnip (green) and CP224 (red) to show centrosomal localisation. Slides image at x100 on airyscan with 0.5μM z-slices, airyscan process and max-projected.

4.2.2 GFP-katnip relocalises to microtubules under oxidative stress

To further understand the role and dynamics of katnip, GFP-dlkatnip expressing cells were observed by time laspe microscopy. Interestingly, during time courses with high laser power, a relocalisation of the GFP-dlkatnip from cytoplasic pool on to filamentous cytoplasmic structures was observed (figure 4.3 A.). Background cytoplasmic fluorescence decreased as GFP-katnip puncta were seen to relocalise onto motile puncta near the plasma membrane first (hypothesised to be the ends of microtubules), before decorating whole fibres emanating from the centrosome.

In order to confirm if these structures were microtubules (without the necessity of GFP-Tubulin expression which can affect microtubule binding), cells were treated with Nocodazole, a microtubule depolymerising drug. Treatment with Nocodazole shortens microtubules and therefore would expect GFP-katnip relo-

calise to smaller structure if these were microtubules, although doesn't remove all microtubule as stated in Section 1.3.5. By reducing the length of microtubules, GFP-katnip would be more densely concentrated along the lengths as well. After Nocodazole treatment and photodamage, GFP-dlkatnip once again relocalised from the cytoplasm onto filamentous structures (figure 4.3 B.).

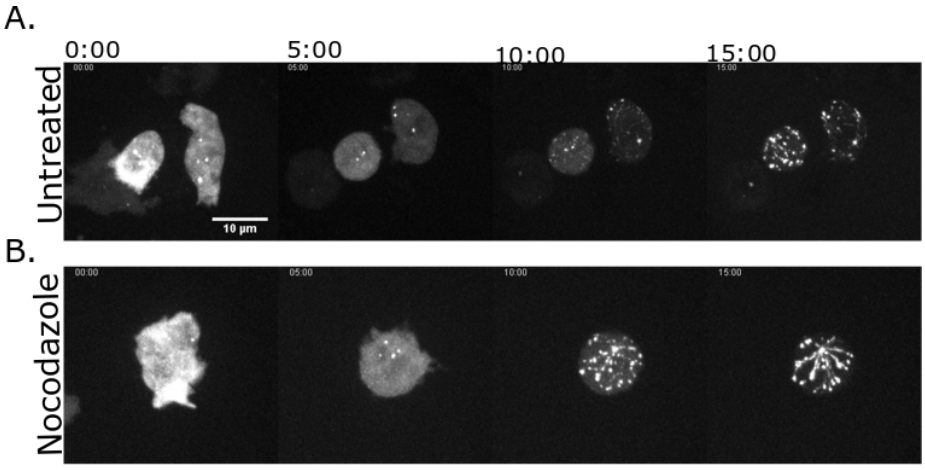

Figure 4.3: **GFP-dlkatnip relocalises to microtubules upon photodamage**

A. Live time laspe of untreated GFP-dlkatnip expressing WT cells exposed to 50% power FITC laser over 15 mins. Time stamps in minutes above images. Imaged on spinning disk confocal at x64 with 0.5 μm z-slices, images max-projected. B. Time lapse of GFP-dlkatnip expressing WT exposed to 50% power FITC laser after 20 minutes incubation with 100μM Nocodazole to depolymerised unstable microtubules. Imaged on spinning disk confocal at x64 with 0.5 μm z-slices, images max-projected.

Photodamage occurs due to the light-induced production of reactive oxygen species (ROS), which causes cellular damage due to local oxidation and membrane permeabilisation. The photodamaging dependent relocalisation of GFP-katnip may be a direct response to ROS damage. To confirm if this relocalisation was an ROS specific response, cells were imaged after hydrogen peroxide treatment, which acts as a source of free radicals in the form of superoxide (O_2^-) (figure 4.4). In WT cells expressing GFP-dlkatnip, relocalisation

after hydrogen peroxide treatment in to distinct puncta was seen, replicating the photodamaging phenotype and confirming GFP-katnip relocalisation is ROS dependent.

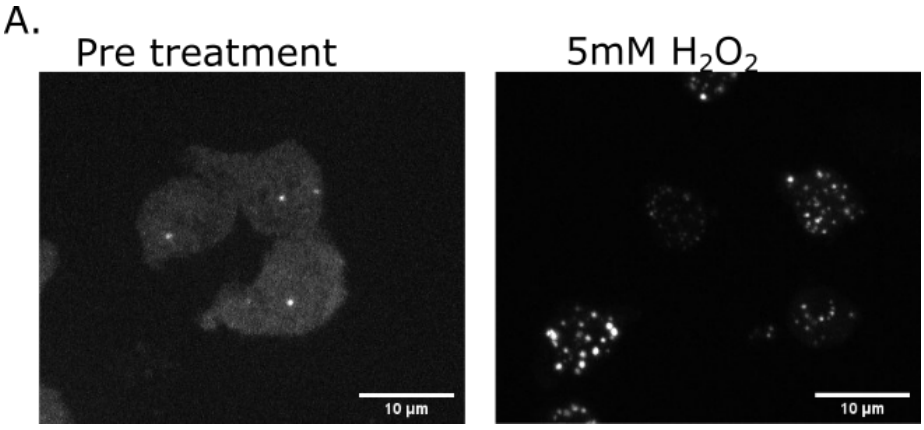

Figure 4.4: **GFP-dlkatnip relocalises upon hydrogen peroxide treatment**

A. Live WT cells expressing GFP-dlkatnip before and after 25 minute treatment with 5mM hydrogen peroxide (H_2O_2). Imaged on spinning disk confocal at x64 with 0.5μm z-slices, images max projected.

4.3 Katnip mutants have interphase microtubule organisation defects

Previous studies in mammalian cells have shown that GFP-katnip localises to the basal body and affects cilia microtubule organisation. As katnip localises to the centrosome, a structure very similar to the basal body which also controls microtubule organisation, katnip may also affect interphase microtubule organisation from the centrosome.

To test this, WT and katnip$^-$ cells expressing GFP-tubulin were imaged to observe their microtubule network. WT cells had normal microtubule networks, with a central centrosome and a large number of microtubules which

evenly cover their cytoplasm (figure 4.5 A.). Whereas, both katnip$^{-(1)}$ and katnip$^{-(2)}$ cells had disorganised microtubule network. Commonly seen in these cells were microtubules in thick circular bundle-like formation but also loss of microtubule connection to the plasma membrane (example zoom 2), where the microtubules didn't appear to reach the plasma membrane on all sides. Microtubules in katnip^{-} cells do not have an even coverage of the cytoplasm and there are observable large sections of the cytoplasm without microtubules. The loading of vesicles on to microtubules in these ares, both formed at the plasma membrane (macropinosomes and phagosomes) and throughout the cytoplasm (autophagosomes) may be reduced, reducing the amount of lysosomal contact, and in turn, be the cause of the lysosomal degradation defect report in Results I. To further confirm this phenotype severity and deleterious affect on cells, I found that cells with microtubule tangles were selected against, with older cell lines exhibit reduced numbers of microtubule tangles, although this has not be quantified at the time.

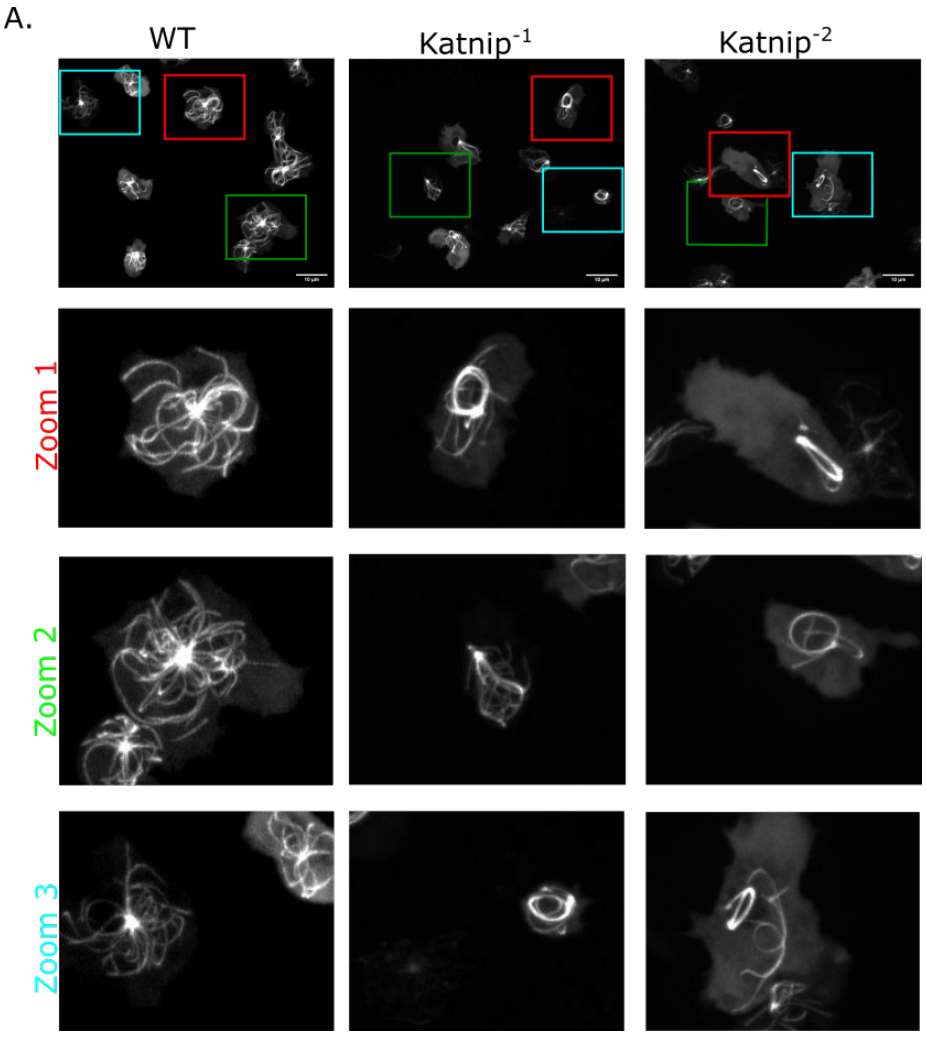

Figure 4.5: **Interphase microtubule organisation in WT, katnip$^{-(1)}$ and katnip$^{-(2)}$ cells**

Live WT, katnip$^{-(1)}$ or katnip$^{-(2)}$ cells expressing GFP-tubulin. Imaged on spinning disk confocal microscope at x64 at 0.5μm z-slices and images max projected.

In order to quantify the number of cells exhibiting this defect, WT, katnip$^{-(1)}$ and katnip$^{-(2)}$ cells expressing GFP-tubulin were imaged and percentage of cells with clear tangles counted. On average, around 30% of katnip^{-} cells had ob-

servable microtubule tangles whereas only 2.4% of WT cells exhibited tangles (4.6).

It may be this loss of microtubule organisation in katnip^{-} cells which leads to the trafficking defect investigated in Chapter 3, as the microtubules cannot come into contact with vesicles. The tangles may be an extreme phenotype of the loss of Katnip and this may be caused by a defect which is only observable at the molecular level e.g. abnormal protofilament number or incorrect microtubule seeding.

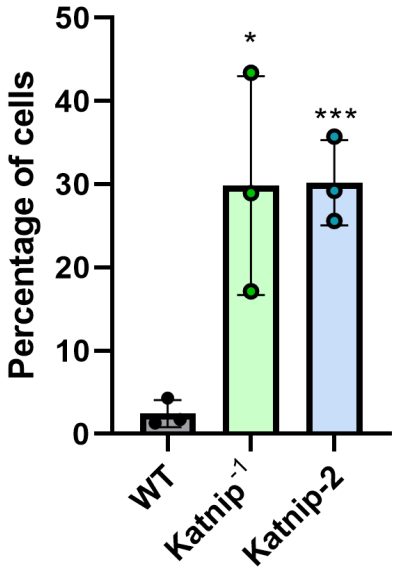

Figure 4.6: **Katnip$^{-(1)}$ and Katnip$^{-(2)}$ cells exhibit more microtubule tangles than WT cells**

Graph showing the percentage of WT, katnip$^{-(1)}$ and katnip$^{-(2)}$ cells expressing GFP-tubulin with observable microtubule tangles, from z-stack images of cells images at x64 on spinning disk confocal, examples in Figure 4.5. N=3. WT cell N = 438, katnip$^{-(1)}$ cell N = 331, katnip$^{-(2)}$ cell N = 361.

In order to assess if the loss of microtubule organisation in katnip^{-} cells caused reduced trafficking of vesicles, the movement of autophagosomes were measured. Autophagosomes move along microtubules to contact lysosomes for degradation and the loss of microtubule function and organisation would impact their transport, and therefore be the cause of reduced degradation. Using previous time laspe data used to assess autophagosome lifetimes (figure 3.3), autophagosomes were tracked and speed calculated. Katnip$^{-(1)}$ had a significantly lower average autophagosome speed compare to WT (WT mean = 0.079 μm/second, katnip$^{-(1)}$ mean = 0.049 μm/second), and whilst katnip$^{-(2)}$ did not reach significance, it had a similar mean to katnip$^{-(1)}$ (katnip$^{-(2)}$ mean = 0.053 μm/second) and a third repeat may increase statistical power (figure 4.7 A.). This indicates that the ability of autophagosomes to transport is reduced in katnip^{-} cells and may be due to defective microtubules. Tangles observed may be a secondary defect to a role of katnip in maintaining microtubule function.

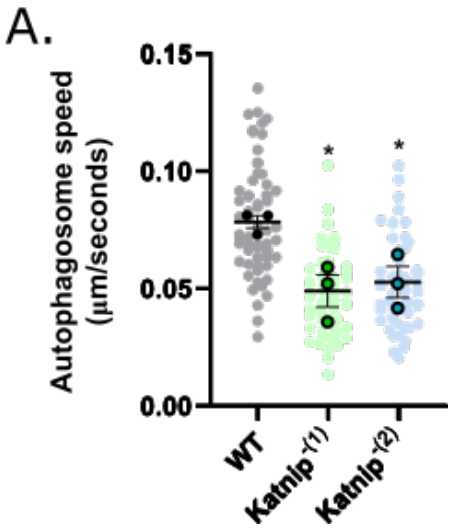

Figure 4.7: **Katnip$^{-(1)}$ cells autophagosome exhibit reduced speed**

A. Speed of autophagosomes (during formation and quenching) from WT, katnip$^{-(1)}$ and katnip$^{-(2)}$ cells expressing GFP-Atg8 imaged on spinning disk confocal examples in Figure 1.1.3. Autophagosomes were tracked manually using Trackmate plug-in on ImageJ and speed calculated from distance/time. Stats calculated viva T-test. All cell lines N = 3.

4.4 Microtubule dynamics and volume aren't affected by loss of katnip

Based on microtubule tangles observed in katnip^{-} cells, it was hypothesised that these tangles could be the result of hyper stable microtubules due to similarity with tangles observed in highly acetylated neuronal microtubules (Sanchez-Soriano et al., 2009).

If loss of katnip^{-} caused more stable microtubules, they would be more resistance to depolymerisation, and therefore more tubulin would be incorporated in the microtubules rather than existing freely in the cytoplasm. In order to measure this, cells were lysed in a microtubule stabilising buffer (HEMS) and

centrifuged to separate polymerised tubulin from free tubulin.

Fractions were then run on a western blot and immunostained using tubulin antibody. A slightly higher polymerised tubulin amount was measured in katnip^{-} but it was not significant (figure 4.8 A., B.).

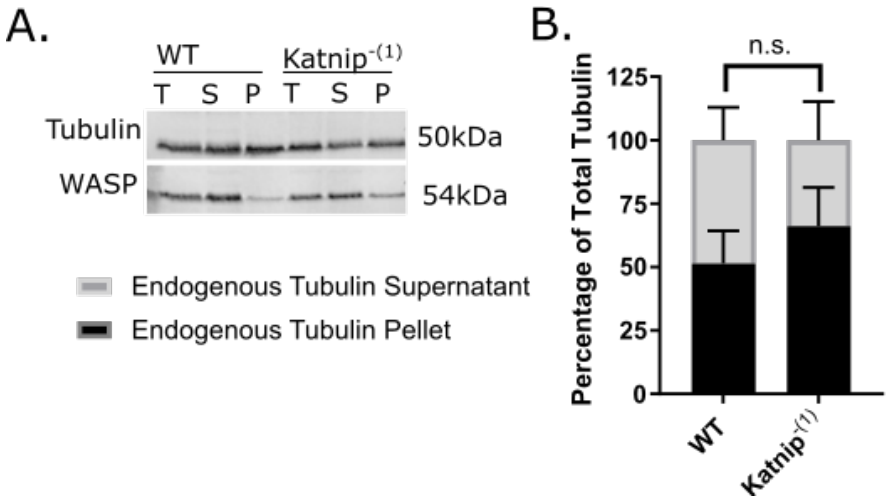

Figure 4.8: **Incorporation of tubulin in to microtubules in WT and katnip$^{-(1)}$ cells**

A. Western blot loaded with HEMS lysed WT and katnip$^{-(1)}$ cells, probed with antibodies against α-tubulin and the soluble protein WASP as a loading control. T = total tubulin, S = supernatant (free tubulin fraction) and P = pellet (polymerised tubulin fraction). B. Quantification of tubulin fraction in total (T), supernatant (S) and pellet (P) from (A). Quantified manually using Licor Lite software. Fraction normalised to 100% tubulin, which was calculated by adding supernatant and pellet fraction together. WT pellet = 51.44%, supernatant = 48.56%. katnip$^{-(1)}$ pellet = 48.56%, supernatant = 39.60%. N=4. Statistical significance calculated using unpaired T-test across averages.

As expression of GFP-tubulin may exacerbate the mutant microtubule tangle phenotype, levels of both endogenous and GFP-tubulin were also assessed (GFP-tubulin expressing cells have a total of 4 tubulin pools as including free and polymerised pools of both endogenous and GFP-tagged tubulin).

Consistent with previous reports on GFP-tubulin incorporation (Kimble et al., 2000), less GFP-tubulin was incorporated into microtubules than untagged tubulin protein in both cells types. Only around a quarter of GFP-tubulin pool was incorporated into microtubules compared to, around 50% of available untagged. This is identical to previous data reported by Kimble et al. (2000) in *Dictyostelium discoideum* (figure 4.9 A., B., C.)).

However, no significant difference in either GFP-tubulin or endogenous tubulin polymerisation was observed (figure 4.9 A., B) nor the GFP-tubulin expression levels between WT and katnip$^{-(1)}$ cells (figure 4.9 C), suggesting that loss of katnip doesn't affect the amount of tubulin incorporated into microtubules, nor do katnip^{-} cells incorporate GFP-tubulin less efficiently. This indicates that the amount and stability of microtubules are not affect by loss of katnip and differences in GFP-tubulin incorporation are not the cause of katnip^{-} 's sensitivity to GFP-tubulin expression.

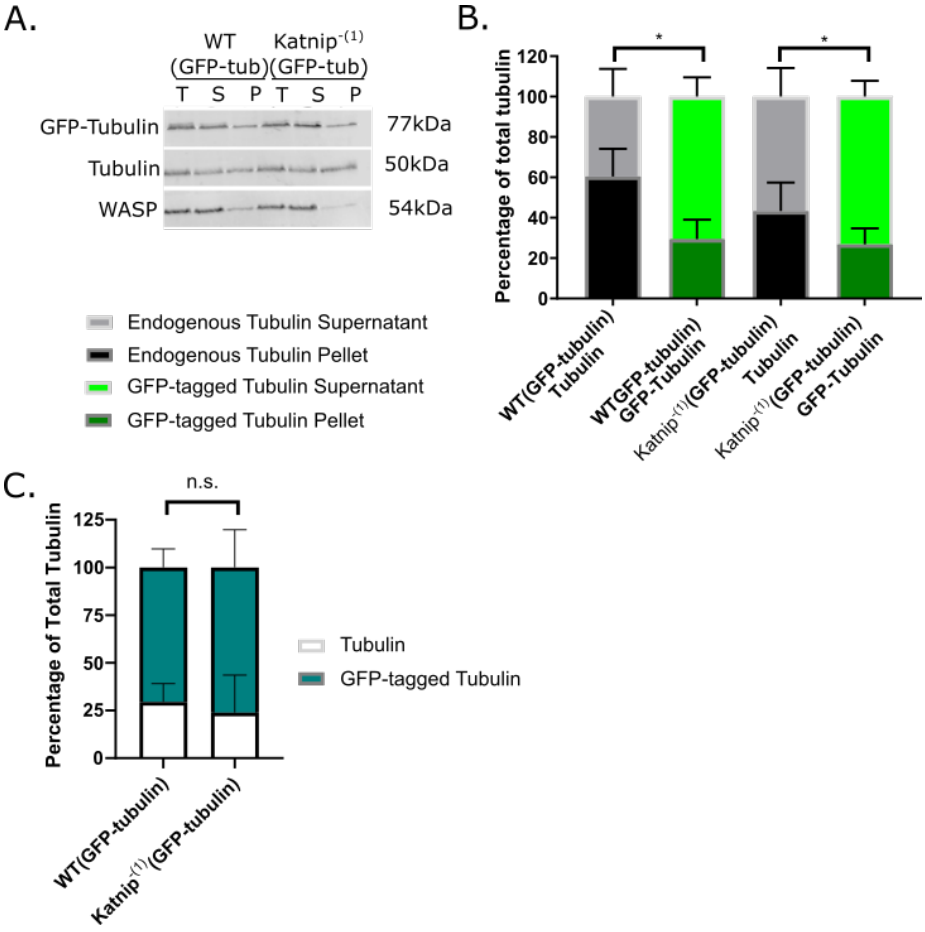

Figure 4.9: **Incorporation of tubulin into microtubules in WT and katnip$^{-(1)}$ cells expressing GFP-tubulin**

A. Western blot loaded with HEMS lysed WT and katnip$^{-(1)}$ cells expressing GFP-tubulin, probed with antibodies against α-tubulin and the soluble protein WASP as a loading control. T = total tubulin, S = supernatant (free tubulin fraction) and P = pellet (polymerised tubulin fraction). B. Quantification of tubulin fraction in total (T), supernatant (S) and pellet (P) from (A). Fraction normalised to 100% tubulin, which was calculated by adding supernatant and pellet fraction together with WT and katnip$^{-(1)}$ cells expressing GFP-tubulin. WT(GFP-tubulin) tubulin pellet = 51.44%, supernatant = 48.56%. WT(GFP-tubulin) GFP-tubulin pellet = 29.45%, supernatant = 70.55%. katnip$^{-(1)}$ (GFP-tubulin) tubulin pellet

= 43.33%, supernatant = 53.37%. katnip$^{-(1)}$ (GFP-tubulin) GFP-tubulin pellet = 26.87%, supernatant = 73.13%. C. The total amount of tubulin compared to GFP-tubulin expression in lysed WT(GFP-tubulin) and katnip$^{-(1)}$ (GFP-tubulin) cells from (A). Calculated by percentage of total tubulin expression. N = 3. WT(GFP-tubulin) tubulin expression = 29.43%, GFP-tubulin expression = 70.5645. katnip$^{-(1)}$ (GFP-tubulin) tubulin expression = 23.84%, GFP-tubulin expression = 76.16%.

In order to assess microtubule stability directly, an assay was created based on stabilised microtubule's resistance to Nocodazole. Nocodazole sequesters tubulin monomers, inhibiting microtubule polymerisation; therefore stable microtubules which don't undergo dynamic instability are less sensitive to treatment. WT and katnip$^{-(1)}$ cells were treated with Nocodazole, and microtubule response measured by the area of the cell covered by microtubules (more details in section 2.2.1, figure 4.10 A.)

No difference was seen between WT and katnip$^{-(1)}$ in the proportion of the cell covered by microtubules nor rate of depolymerisation or polymerisation after addition, or subsequent removal of 30μM Nocodazole (figure 4.10 B.). In both cell lines, microtubules shortened to the same length at the same rate. In order to see if the rapid depolymerisation due to 30μM Nocodazole treatment was masking any subtle defects in depolymerisation, the experiment was repeated with a lower Nocodazole concentration (10μM, figure 4.10). Once again, no difference in area covered, depolymerisation nor recovery of microtubules was seen. This suggest that loss of katnip causes no major changes in microtubule stability or dynamics.

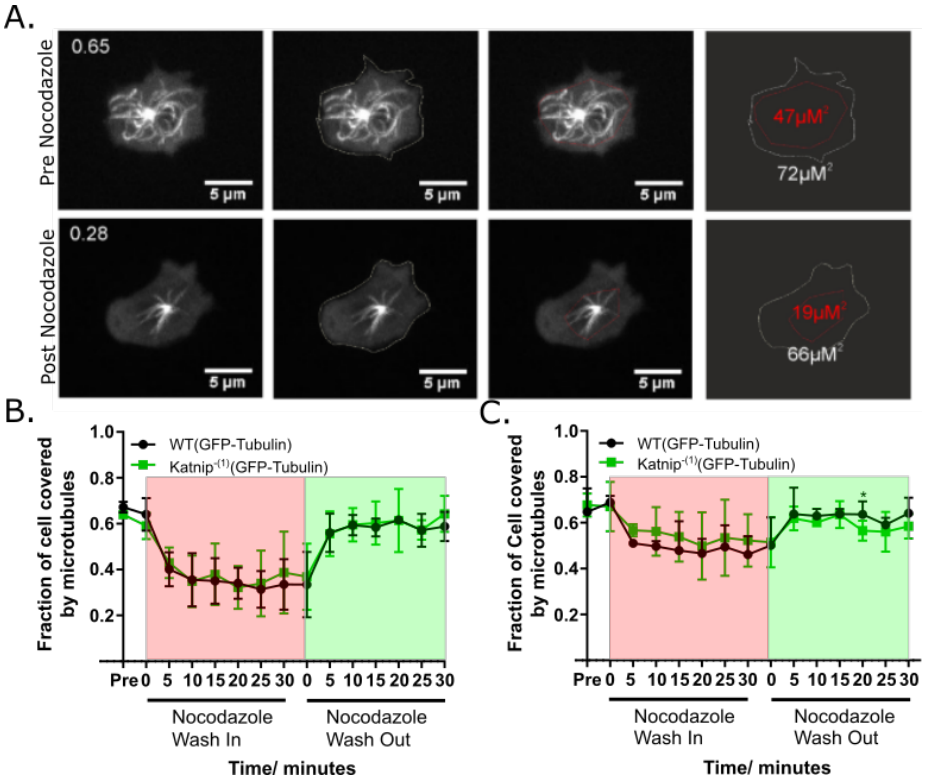

Figure 4.10: **Loss of katnip does not result in an increased sensitivity to Nocodazole**

A. Example images of WT cells pre and post 30μM Nocodazole treatment for 30 minutes. White dotted line and number indicate whole cell area and red dotted line and number indicate microtubule area. Number at the top left of first panal is the fraction of cell covered by microtubules. Imaged on spinning disk confocal microscope at x64 with 0.5 μm z-slices and max projected. B. Graph depicting the change in average fraction of cells covered microtubules in WT and katnip$^{-(1)}$ cells throughout 30μM Nocodazole treatment during 30 minutes wash in (depolymerisation) and 30 minutes wash out (repolymerisation/recovery). N=3, error bars represent SD. C. Same as (B.) but with 10μM Nocodazole treatment. N=3, error bars represent SD.

4.5 Katnip mutant cells have a sensitivity to GFP-tubulin

4.5.1 Katnip mutants expressing GFP-tubulin have reduced growth

After finding that loss of katnip did not alter microtubule dynamics nor stability, the question still remained of how loss of katnip caused microtubule organisation defects and affected trafficking. Whilst growing cells, it was observed that katnip^{-} cells expressing GFP-tubulin grew more slowly, but WT cells expressing GFP-tubulin grew at a normal rate. To quantify this, a growth curve was performed on WT and katnip$^{-(1)}$ cells with and without GFP-tubulin expression. Interestingly, whilst loss of katnip alone had no effect on growth rate, expression of GFP-tubulin in katnip$^{-(1)}$ exhibited a reduced growth, with a doubling time of 48 hours compared 15 hours for all other cell lines (figure 4.11 A., B.).
Cell growth requires the creation of a robust microtubule spindle for DNA separation (section 4.5.2). As GFP-dlkatnip localised to the mitotic spindle, I hypothesised katnip may have a function during mitosis, but katnip$^{-(1)}$ had no mitosis defect and therefore, loss of katnip alone is insufficient to disrupt mitosis. But, katnip$^{-(1)}$ expressing GFP-tubulin has a severe defect in growth, suggesting that katnip may be require to tolerate GFP-tubulin expression. Loss of katnip sensitises cells to GFP-tubulin, and this may be due to katnip functioning to tolerate the increased microtubule damage and breakages upon GFP-tubulin over expression (Kimble et al., 2000).

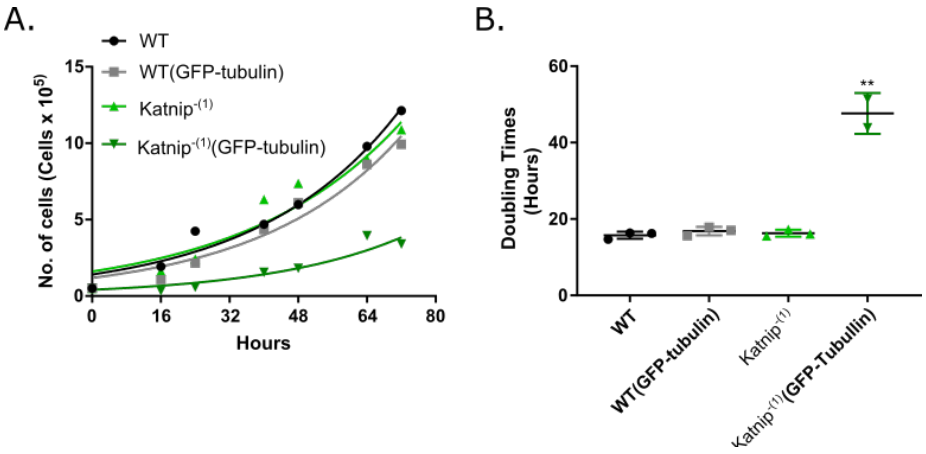

Figure 4.11: **Katnip$^-$ cells expressing GFP-tubulin exhibit a growth defect**

A. Growth curve of WT and katnip$^{-(1)}$ cells with and without GFP-tubulin expression. N = 3. B. Doubling times of WT and katnip$^{-(1)}$ cells with and without GFP-tubulin expression. WT, WT expressing GFP-tubulin and katnip$^{-(1)}$ N = 3. Katnip$^{-(1)}$ expressing GFP-tubulin N = 2. Statistical difference calculated using unpaired T-test. Error bars represent SD across repeats.

A possible function of katnip which could result in mitosis defects is an aberration of cytokinesis. Cytokinesis is the final stage of mitosis where the plasma membrane and conjoining cytoplasm of the two daughter cells is severed, freeing the two independent daughter cells (section 1.3.5). Both microtubules and actin are required for cytokinesis and therefore, katnip might be required for the correct organisation of microtubules and complete cytokinesis. In order to assess this, katnip$^-$ cells were fixed and stained with DAPI to observe nuclei. Cells which fail to complete cytokinesis don't separate and instead result in one cells with multiple nuclei. Both WT, katnip$^{-(1)}$ and katnip$^{-(2)}$ have the same occurrence of cells with multi nuclei and therefore, loss of katnip does not produce multi nucleated cells and a cytokinesis defects is not the cause of the reduced growth rate observed in these cells.

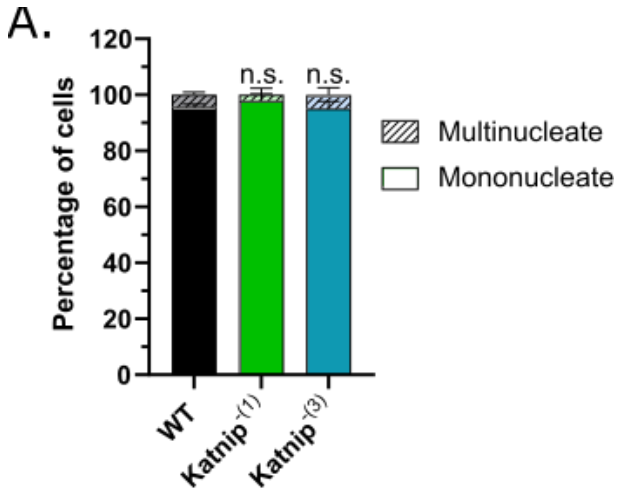

Figure 4.12: **Neither katnip$^{-(1)}$ or katnip$^{-(2)}$ have increased rates of multinucleation**

A. Percentages of cell with multiple nuclei counted from ultra cold methanol fixed cells mounted in Prolong Gold. N = 3 repeats. Ax2 N = 119 cells, katnip$^{-(1)}$ N = 130 cells, katnip$^{-(2)}$ N = 295 cells. Unpaired T-test across 3 repeats used to calculate significance. Imaged on spinning disk confocal microscope at x64.

4.5.2 Katnip mutants expressing GFP-tubulin have anaphase specific mitosis defect

As katnip$^{-(1)}$ cells expressing GFP-tubulin exhibited a severe growth defect, mitosis in these cells was investigated to observe if this was the cause of the defect.

WT, WT expressing GFP-tubulin and katnip$^{-(1)}$ cells all took the same amount of time to complete mitosis (WT = 502 seconds/8.4 minutes), but katnip$^{-(1)}$ cells expressing GFP-tubulin exhibited a significantly longer and more variable mitosis time, with an average of 839 seconds/14 minutes (figure 4.13 A., B.). This pattern reflects the growth curve data and therefore

may partially account for the reduced growth of katnip^{-} cells expressing GFP-tubulin. Once again, as this mitosis defect is only observed when GFP-tubulin is expressed in katnip^{-} cells, the loss of katnip sensitises cells to an effect of GFP-tubulin expression.

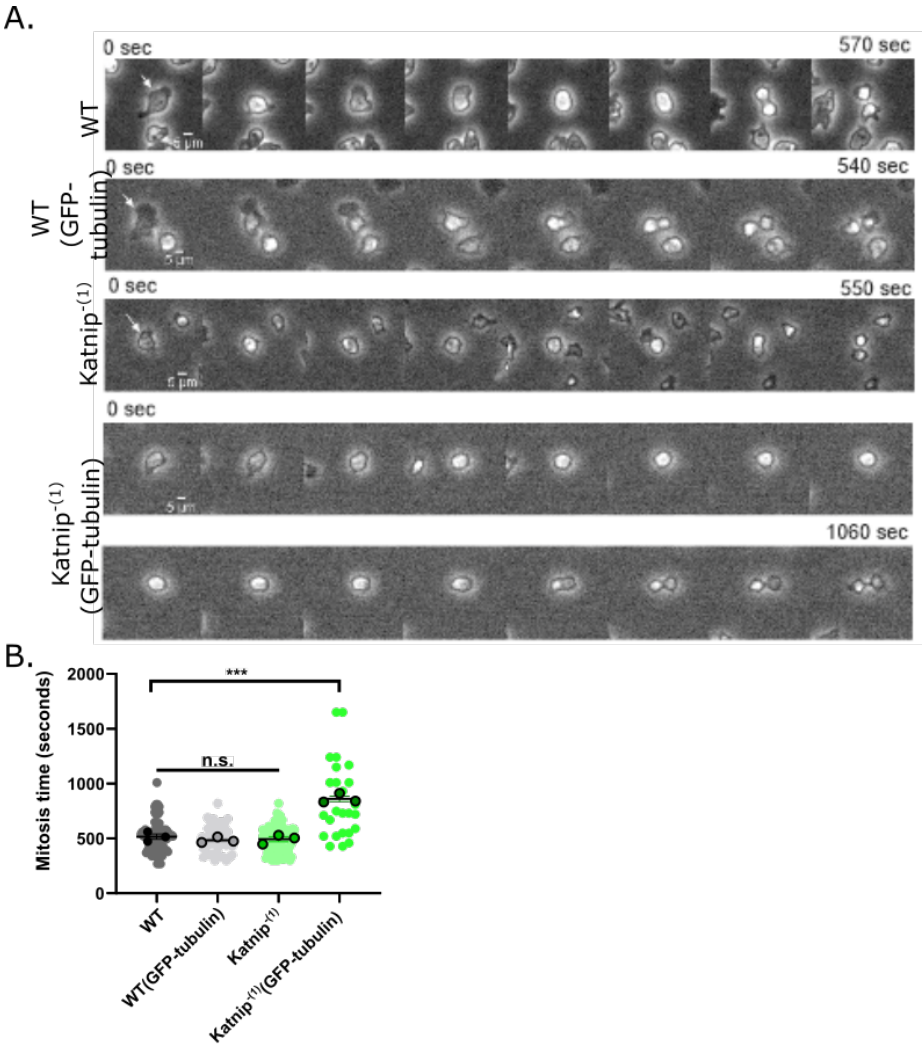

Figure 4.13: **Katnip^{-} (GFP-tubulin) exhibit mitosis elongation**

A. Example brightfeild montage of WT and katnip$^{-(1)}$ cells with and without GFP-tubulin expression. Imaged on confocal brightfield at x20. B. Time in mitosis of WT and

katnip$^{-(1)}$ cells with and without GFP-tubulin. Counted from when cell rounded to when no membrane connections were seen by eye from brightfield images, examples in (A). N=3. WT cell N = 75, WT(GFP-tubulin) cell N = 51, katnip$^{-(1)}$ cell N = 90, katnip^{-} (GFP-tubulin) cell N = 26. Error bars represent SEM across repeat averages.

In order to understand where this mitosis defect manifested, the stages of mitosis where investigated for delays through time laspe microscopy. In order to observe these stages in more details, WT and katnip$^{-(1)}$ GFP-tubulin expressing cells were imaged undergoing mitosis by time lapse fluorescence microscopy (figure 4.14 A., B.). After quantifying the time spent in each mitotic stage, anaphase is the only stage which was significantly longer in katnip$^{-(1)}$ compared to WT when both expressing GFP-tubulin (figure 4.14 C.). Anaphase is the stage where force is generated on microtubules to separate the centrosome and pull DNA into the new daughter cells (section 4.5.2). To measure anaphase progression, distance between centrosomes were tracked over time in the two cell lines (figure 4.14 D.). WT cells (black lines) began centrosome separation at the same time, all separated at the same rate and finished at the same time. In contrast, katnip$^{-(1)}$ cells were much more variable; the cells which managed to separated their centrosomes all began later than WT and at different times. At several points, (labelled with black arrows in figure 4.14 D.), a reduction between centrosomes was recorded and frequent stalling of centrosome separation was observed. In several cases, centrosomal separation never even initiated and cells and remained in anaphase until imaging was stopped (maximum 35 minutes). The times measured here are consistent with the above growth curve and brightfield mitosis data and together shown that katnip^{-} cells have a GFP-tubulin dependent defect in anaphase whereby centrosomes are less efficiently and robustly separated by spindle microtubules.

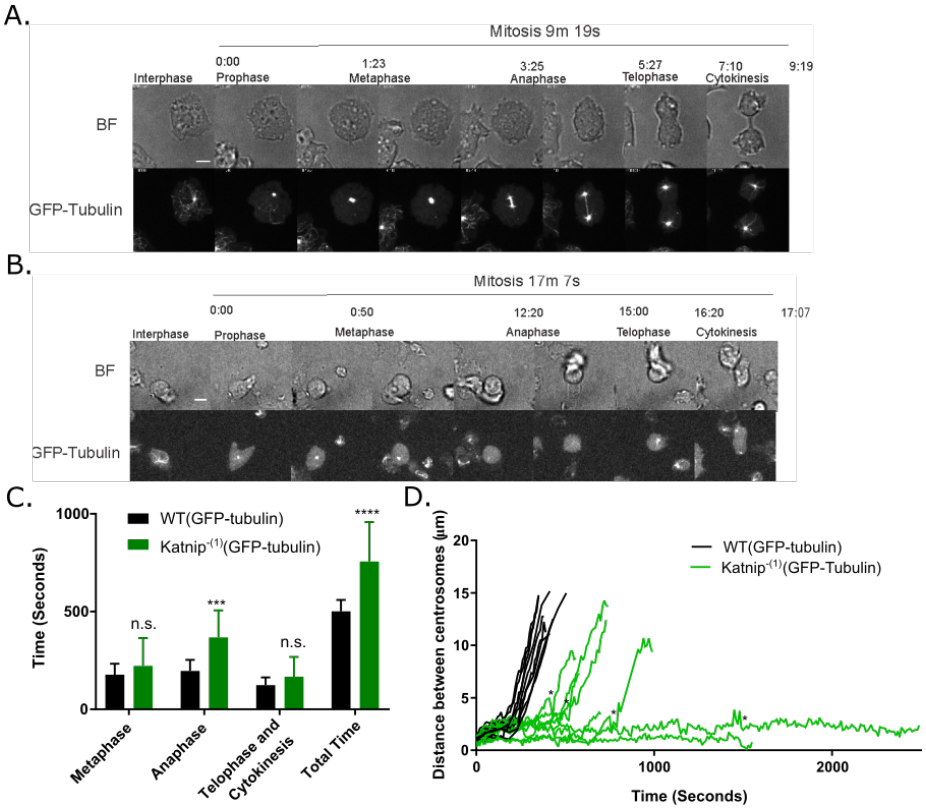

Figure 4.14: **Katnip^{-} cells expressing GFP-tubulin have an elongated anaphase**

A. Example WT cell expressing GFP-tubulin going through mitosis in both brightfeild (top montage) and FITC channel (bottom montage). Imaged on spinning disk confocal at x64 with 0.5μm z-slices, images max-projected. B. Example katnip$^{-(1)}$ (GFP-tubulin) cell going through mitosis in both brightfeild (top montage) and FITC channel (bottom montage). Imaged on spinning disk confocal at x64 with 0.5μm z-slices, images max-projected. B. Quantification of time in mitosis stages from WT(GFP-tubulin) and katnip$^{-(1)}$ (GFP-tubulin) cells, image examples above. Analysed by eye, examples in (A) and (B). Metaphase P value = 0.307, anaphase P value= 0.0006, telophase and cytokinesis P value = 0.162, total time in mitosis P value = 0.0002. WT(GFP-tubulin) N = 16, katnip$^{-(1)}$ (GFP-tubulin) N = 6 cells. C. Distance between centrosomes over time in anaphase. Black stars indicate points

of distance reduction. WT(GFP-tubulin) N = 16 cells, katnip$^{-(1)}$ (GFP-tubulin) N = 6 cells.

4.6 Discussion: Katnip binds to the centrosome and to interphase microtubules under certain conditions

GFP-katnip localises to the centrosome in *Dictyostelium discoideum* cells, which has not been previously observed, but its localisation at the basal body has been observed in mammalian cells, which has a very similar structure. Loss of katnip results in trafficking defect and a sensitivity to GFP-tubulin which results in loss of microtubule organisation. Katnip therefore plays a role in not just regulating cilia microtubules, as published before, but also interphase microtubules. This interphase role is a completely new function of the protein has a wider implications on the cell, including the trafficking defect outlined in Results I.

4.6.1 Katnip localises to centrosomes and transiently to microtubules

Like GFP-katnip overexpression in mammalian cells, both GFP-ddkatnipΔN and GFP-dlkatnip localise to the centrosome in *Dictyostelium discoideum* . Even though these cell types are highly divergent and their centrosomes have different structure (section 1.3.5), katnip still localises to the same place.

In addition to its centrosomal localisation, I found GFP-dlkatnip can also bind along microtubules upon oxidative damage. This may be a transient association, acting as a response to ROS stress. DUF4457 is the only protein domain identified in katnip and therefore, might be a novel microtubule binding domain. Oxidative damage via photodamage is well established *in vitro* and recently *in vivo* cells (Aumeier et al., 2016) to induce microtubule damage, although likely causes other cell effects due to its lack of specificity. As katnip was only seen

to bind to microtubules after oxidative damage, it may bind to ROS generated areas of microtubule damage.

4.6.2 Loss of katnip doesn't affect microtubule stability or dynamics in *Dictyostelium discoideum*

Microtubule quantity and stability was measured through Nocodazole sensitivity as well as differential centrifugation. No difference in polymerisation was observed between WT and katnip$^-$ cell lines indicating this is not the cause of any microtubule defects or the trafficking defect in katnip$^-$. These experiments also suggest that the de/polymerisation dynamics of katnip$^-$ cells were the same, suggesting that the katnip may not function in microtubule dynamics.

4.6.3 Loss of katnip results in a sensitivity to GFP-tubulin

GFP-tubulin sensitivity and organisation defects

GFP-tubulin has long been used as a marker of microtubules in multiple types of cells. The GFP molecule is 27kDa making it over half the size of tubulin (55kDa). Tubulin dimers are incorporated in a highly organised lattice into the microtubules which is close to its depolymerisation conditions to allow quick disintergration upon signalling (section 1.3.1). To our knowledge, deleterious effects of GFP-α-tubulin overexpression has not been reported in mammalian cells however, Kimble et al. (2000) identified that GFP-tubulin was disfavoured when intergrating tubulin dimers into microtubules in *Dictyostelium discoideum* cells. A similar phenotype has also been identified in *S. cerevisiae*, where GFP-tubulin overexpression caused increased microtubule sensitivity to cold (Carminiti and Stearns, 1997) and *S.pombe*, where GFP-tubulin overexpression results in lethality (Da-Qias et al., 1998). Both of these organisms lack Katnip, which may explain there sensitivity to GFP-tubulin in these experiments. This chapter reports more data on GFP-tubulin's affect on microtubules and adds to growing evidence that it may not always be a suitable marker of microtubules due to

this damaging effect.

It was hypothesised that due to the large GFP attached to tubulin, this could affect its incorporation in to microtubules, potentially disrupting the fine regular structure of the microtubule lattice resulting in defects (section 1.3.3). The reduced amount of fixed microtubules and preferential incorporation of untagged tubulin over GFP-tubulin into microtubules, might be due to the reduced structural integrity of GFP-tubulin microtubules, and therefore, increased breakages. The specific defect in anaphase in katnip$^-$ cells expressing GFP-tubulin, when microtubule are under their greatest mechanical stress, also supports a role for katnip in maintaining microtubule integrity.

Tangle phenotype may be dependent on the time since mitosis, increase over time as a result of accumulated microtubule damage. In order to investigate this, several microtubule stabilising drugs were tested on *Dictyostelium discoideum* cells. Unfortunately, taxol and taxol derivatives where not effective due to lack of taxol binding sites in Dictyostelium α-tubulin (section 1.3.5). Other drugs (epithilone B and vinblastine) proved highly variable and mostly had very little effect on *Dictyostelium discoideum* microtubules, probably due to their highly efficient drug efflux pumps. Therefore the effect of increasing microtubule age could not be tested. Another way to increase microtubule lifetimes would be to prevent mitosis, therefore microtubules would be never depolymerised as *Dictyostelium discoideum* don't undergo microtubule catastrophe. Unfortunately, no protocol currently exists for effective synchronisation or delaying mitosis in *Dictyostelium discoideum* despite much investigation.

GFP-tubulin sensitivity in mitosis and anaphase defects

Although katnip binds along the mitotic spindle (figure 4.2), it is non-essential for mitosis as katnip$^-$ cells exhibit no mitosis defects (figure 4.13).

Interestingly, katnip$^-$ (GFP-tubulin) cells with mitosis defects managed to successfully fulfil the spindle assembly checkpoint (SAC), suggesting that their spindle and DNA capture up to this point is successful (as also indicated by

normal metaphase duration). Therefore loss of katnip only affects anaphase, possibly due to this being the stage where microtubule damage is accumulated.

Dimitrov et al. (2008) observed increased labelling of GTP-tubulin in microtubules during anaphase, now thought to be labelling areas of microtubule damage. From this, I hypothesised that the large force exerted on spindle microtubules during anaphase is capable of producing alot of microtubule damage during this stage. Therefore, the sensitivity of katnip$^-$ cells expressing GFP-tubulin to anaphase defect might be due to katnip$^-$'s role in tolerating microtubule damage. Without katnip, microtubules may of not been able to withstand the large amounts of microtubule damage, causing a partial collapse of the spindle. This would be more pronounced in GFP-tubulin expression cells as they have higher levels of microtubule defects.

It may be that this reduced ability to successfully complete anaphase in katnip$^-$ cells is the driving force behind the selection of cells with severe microtubule tangles. This may also cause a genetic variation in these cells as the mitotic defects may leads to increased genetic recombinations and chromosome numbers. This may be also be present in katnip$^-$ cells (without GFP-tubulin), although to a lesser level, and account for the variability in bacterial plaque sizes (figure 3.6) and the variation in the severity of some phenotypes seen between katnip$^{-(1)}$ and katnip$^{-(2)}$ (figure 3.9).

Although the mitosis time in katnip$^-$ cells is significantly longer, the 6 minutes increase is unlikely to account for the almost tripled doubling times. It is likely that the mitosis defect, which may also result in increased cell death due to failed mitosis, together with the reduced nutrient utilisation resulting from trafficking defect causes the increased doubling time.

The main finding from this chapter is that katnip$^-$ has a role in interphase microtubule organisation, and its function is not just limited to cilia. This is further investigated and discussed in Chapter 5.

Softened up some of the stronger conclusions and moved them to the discussion so where they fit in the to extrapolating data and hypothesis of Katnip's potentially function in microtubule damage.

Chapter 5

Results III
The conserved role of Katnip on interphase microtubules in mammalian cells

5.1 Introduction : Katnip binds to and regulates interphase microtubules in *Dictyostelium discoideum*

After identifing that katnip was able to bind to interphase microtubules as well as being responsible for maintaining correct interphase microtubule organisation, possibly through microtubule damage response and/or repair, the next aim was to identify if this function was conserved.

Katnip was originally identified as a gene important in cilia maintenance in mammalian cells (Sanders et al., 2015), and therefore had been overexpressed in mammalian cells before, but it's role in non-ciliary microtubules was unexplored.

Ciliated cells were initially chosen to perform over-expression experiments with to try and recapitulate phenotypes reported in Sanders et al. (2015), but instead focusing on interphase microtubules. Neuronal cells were later investigated due to their sensitivity to microtubule damage, as they have very stable and long lived microtubules (Aumeier et al., 2016; LeDizet and Piperno, 1987). They also have increased sensitivity to autophagy defects resulting in neurodegenerative disease phenotypes. I also had an interest in neuronal cells due to a recent paper reporting a link between loss of katnip and increased neurofibrillary tangles (NFTs, Andres-Benito et al. (2018), section 1.2.2). Katnip was found to be deferentially methylated and had lower expression in brain samples from Alzheimer's patients with NFTs compared to those with no NFTs. Mammalian GFP-katnip has a technical advantages to the *Dictyostelium discoideum* GFP-katnip constructs, used in earlier chapters, as the entire protein length was cloned and therefore may give a more accurate read-out of the native protein localisation and function. Therefore, GFP-katnip was expressed in a range of mammalian cells to see if it localised in a similar manner to *Dictyostelium discoideum* cells.

5.2 GFP-katnip overexpression causes highly acetylated microtubule growth in cell lines capable of producing cilia

Firstly, the results observed in Sanders et al. (2015) were recapitulated by overexpressing GFP-katnip in hTERT RPE-1 cells. Sanders et al. (2015) alluded to the enrichment of GFP-katnip on interphase microtubules in hTERT RPE-1 cells with cilia but didn't present any data, although did show its enrichment on cilia microtubules. They also presented data that GFP-katnip overexpres-

sion caused hyperactylation of microtubules, although this was not observed in *Dictyostelium discoideum* , where a loss of katnip produced no decrease in microtubule stability (section 4.4), although this may be due to a lack of microtubule acetylation in *Dictyostelium discoideum* (section 1.3.5).

hTERT RPE-1 cells are a human retina pigment epithelial cell line which endogenously form cilia when they become confluent and form a mono-layer. In order to observe GFP-katnip in interphase cells, cells were kept underconfluent and therefore had no cilia.

Consistent with GFP-katnip overexpression in *Dictyostelium discoideum* , GFP-katnip localised to the centrosome, but also to a specific subset of centrosomal derived, highly acetylated microtubules (figure 5.1 A.). These microtubules appeared thicker, highly acetylated and, in some severe cases, long, tangled microtubules extensions where observed. These centrosome-derived microtubules were only observed in transfected cells and therefore GFP-katnip overexpression might induce their growth. GFP-katnip decorates these highly acetylated microtubules at low levels along with its usual centrosomal and cytoplasmic expression. These hyper acetylated microtubules are likely a overexpression artefact but do indicate a conditional ability to localise to microtubules and induce these unusual cilia-like microtubules. This confirms that GFP-katnip can localise to the centrosome in hTERT RPE-1 and can also affect interphase microtubule organisation from this position. In order to investigate this further, these cells could be fixed and stain with cilia protein markers, such as Arl13B which was used in Sanders et al. (2015).

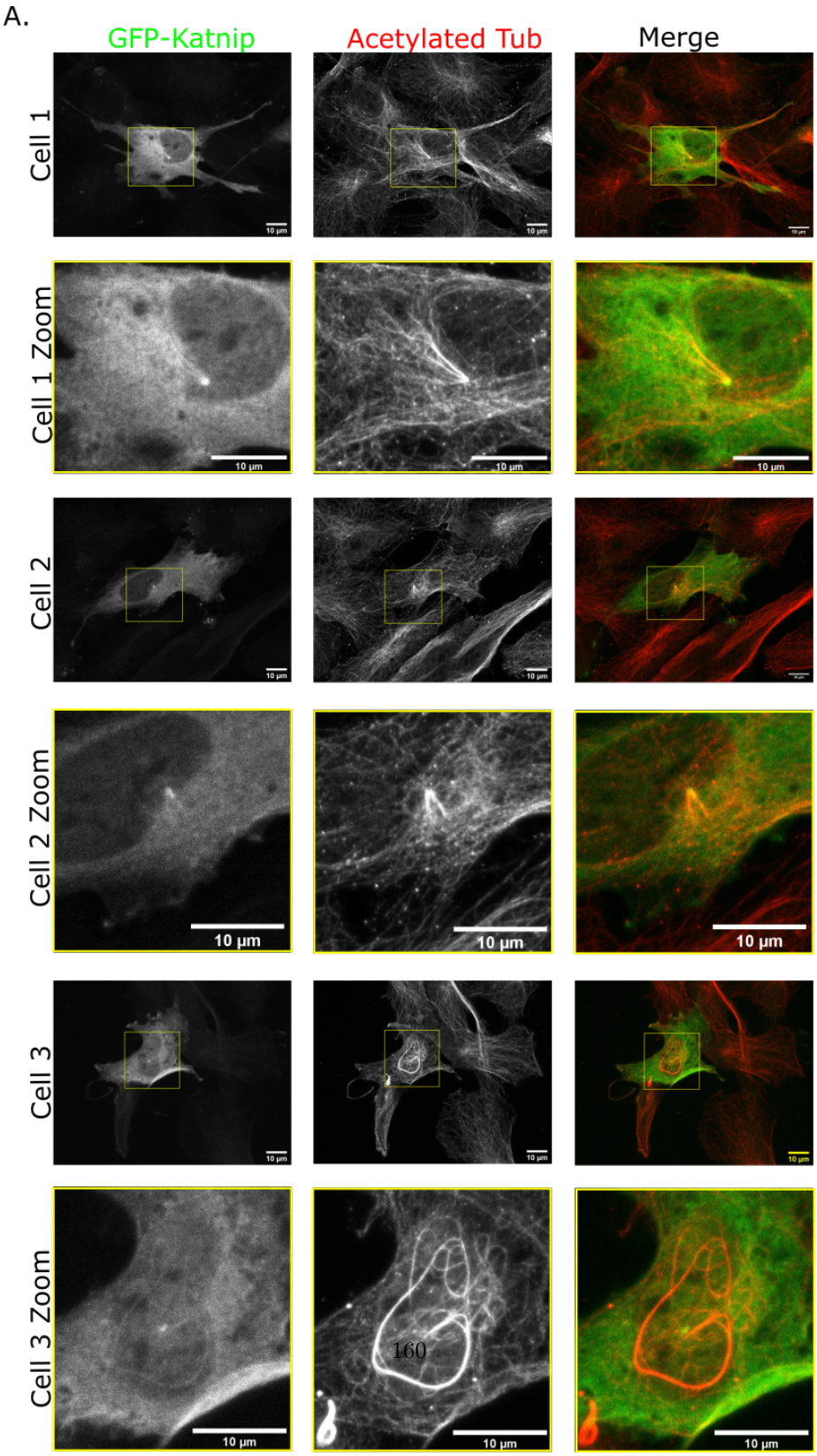

Figure 5.1: **The overexpression of GFP-katnip in hTERT RPE-1 cells co-localises with the centrosome and highly acetylated microtubules**

Examples of methanol fixed hTERT RPE-1 cells over-expressing GFP-katnip (green) and stained for acetylated tubulin (red). Imaged on airyscan at x100 with 0.2 μm z-slices. Images were airy processed and z-stacked.

5.3 GFP-katnip has different localisation dependant on concentration in neuronal cells

5.3.1 GFP-katnip can localise to the centrosome and microtubules in a concentration dependent manner in NSC-34 cells

After confirming localisation of GFP-katnip to the centrosome and microtubules in ciliated cells, neuronal cells were investigated. Neuronal microtubules share many properties with the microtubules of the cilia, being highly stable, highly acetylated and, having long lifetimes. I therefore expressed GFP-katnip in mammalian neuronal cells. NSC-34 are a hybrid mouse/human motor neurone-like cell line used heavily in ALS studies due to their similarity to primary neurones without the complexity of culturing. They were chosen due to ease of transfection and culturing as well as availability.

In order to confirm centrosomal localisation, NSC-34 cells transfected with GFP-katnip were fixed and stained with the centrosomal marker γ-tubulin (section 5.2), as well as tubulin to stain the entire microtubule array.

When GFP-katnip was overexpressed in NSC-34 cells, two distinct localisation were observed. In low expressing cells, GFP-katnip co-localised perfectly with γ-tubulin staining (figure 5.2 A., C.), confirming its centrosomal localisation and replicating the localisation in *Dictyostelium discoideum* and hTERT RPE-1 cells. This gives greater confidence to the localisation of the truncated GFP-katnip plasmids observed in *Dictyostelium discoideum* and indicates that this centrosome localisation isn't cilia cell type specific in mammals.

Highly expressing cells overlapped with tubulin staining as well as centroso-

mal staining (figure 5.2 B., D.). Highly overexpressed GFP-katnip localises to all microtubules in NSC-34 and doesn't appear to affect their organisation, unlike in RPE1 cells. This suggests that the unusual cilia-like microtubule bundles seen in GFP-katnip overexpressing RPE1 cells are specific to this cell types. A possible hypothesis is the microtubule growths observed in RPE1 are a nascent cilia type structure induced by GFP-katnip and are therefore only found in cells capable of growing cilia.

Therefore, katnip localises to the centrosome in NSC-34 cells, a localisation conserved with both *Dictyostelium discoideum* and hTERT RPE-1 cells, and to the microtubules but only when highly expressed.

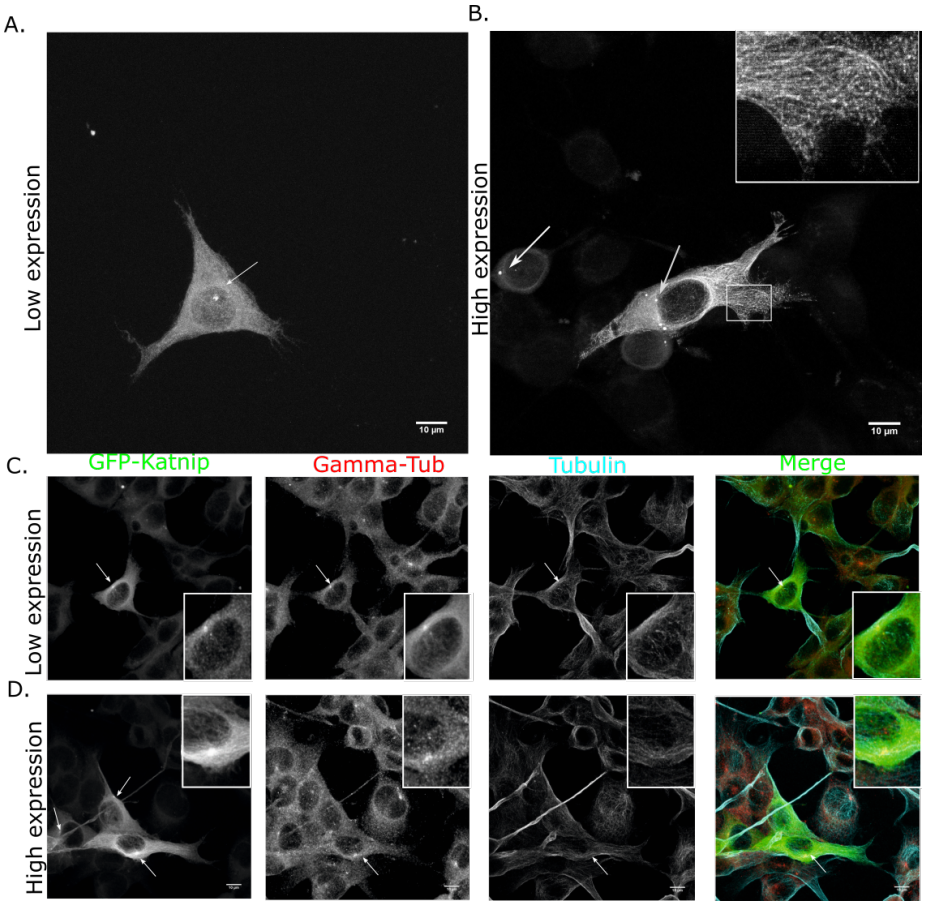

Figure 5.2: **GFP-katnip co-localises with the centrosome in NSC-34 cells**

Methanol fixed NSC-34 cells over-expressing low (A.) and high (B.) levels of GFP-katnip. Imaged on airyscan at x100 with 0.2 μm z-slices, airy processed and max projected. C. Methanol fixed NSC-34 cells overexpressing low levels of GFP-Katnip (green) stained for gamma-tubulin (red) and tubulin (cyan). Imaged on airyscan at x100 with 0.2 μm z-slices, airy processed and max projected. D. Methanol fixed NSC-34 cells overexpressing high levels of GFP-Katnip (green) stained for gamma-tubulin (red) and tubulin (cyan). Imaged on airyscan at x100 with 0.2 μm z-slices, airy processed and max projected.

GFP tagging katnip might alter its localisation and therefore antibodies were sourced in order to observe the endogenous localisation of katnip in these cells. No validated antibodies were available so, in order to assess specificity to katnip, untransfected and GPF-katnip transfected HeLa cells were lysed and western blotted using the 2 anti-katnip antibodies from the Human Protein Atlas project. HeLa cells were used as much higher numbers of cells expressing GFP-katnip could be achieved compared to NSC-34 and hTERT RPE-1 cells. One antibody provided no positive bands (PA5-70906, not shown) whereas the other antibody only stained the GFP-katnip band (HPA035089, figure 5.3) and wasn't able to detect endogenous katnip. As only GFP-katnip could be detected, this suggests that the antibody can only recognise large amounts of the proteins and katnip might be natively expressed at very low levels. Another possibility is that the antibody is only able to bind natively folded epitopes and not the linearlised protein as tested in western blotting. Alternatively, katnip may only expressed in certain tissues, not including neurones, although RNA has been detected in every tissue hlalbeit at low levels except the eyes (TheHumanProteinAltas). Due to the lack of binding to endogenous katnip, the antibody could not be used to observe the endogenous localisation of the protein in the cells. In order to overcome this, an antibody against DUF4457 repeat 2 from human katnip is currently being generated.

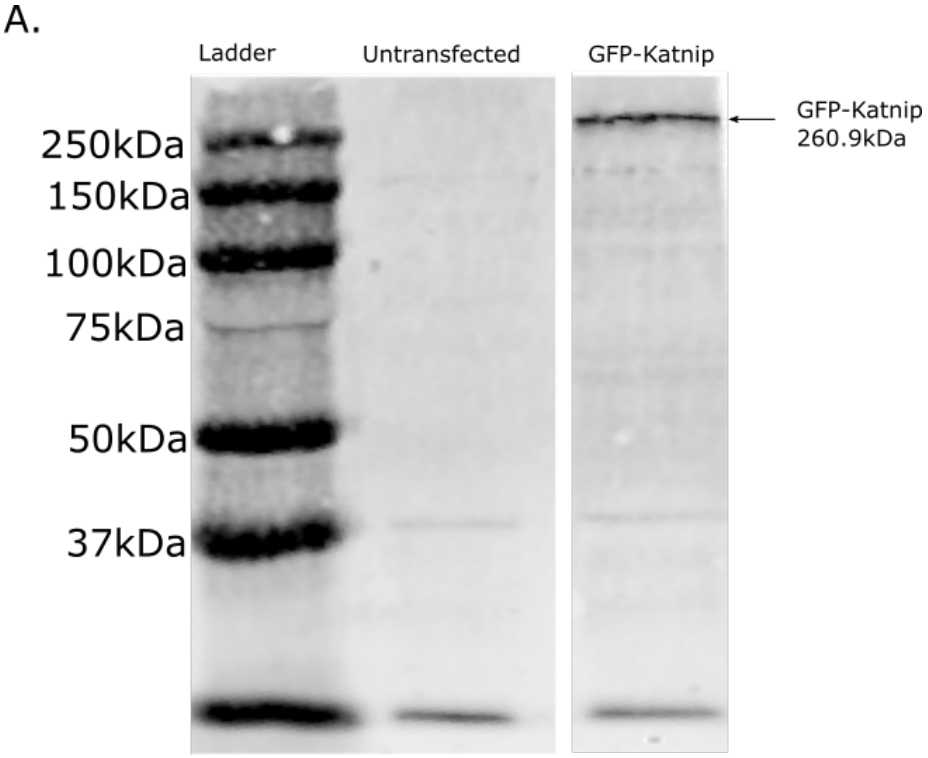

Figure 5.3: **Current available katnip antibodies only detect over-expressed GFP-katnip in NSC-34 cells**

Western blot of cell lysate from untransfected and GFP-katnip transfected HeLa cells stained with anti-katnip antibody HPA035089.

5.3.2 GFP-katnip overexpression does not affect global acetylation in NSC-34 cells

Sanders et al. (2015) previous showed that highly overexpressed GFP-katnip hTERT RPE-1 cells was caused an increase in microtubule acetylation, assayed by imaging and increased resistance to Nocodazole. Based on this, they hypothesised that katnip may have some function in increasing microtubule stability. A similar phenotype was seen in GFP-katnip hTERT RPE-1 imaged in figure 5.1, although increase in acetylation seemed to be due to cilia-like microtubules

rather than a global increase in acetylation, which was hypothesised in Sanders et al. (2015). In order to investigate this in neuronal cells, cells expressing GFP-katnip were stained for tubulin and acetylated tubulin.

In contrast to hTERT RPE-1 cells, NSC-34 cells had no detectable increase in acetylated tubulin at any levels of GFP-katnip overexpression (figure 5.4). However, similar to many neuronal cell types, all cells had very high levels of acetylated tubulin already (figure 5.4). In these cells, levels of microtubule acetylation may already be saturated. GFP-katnip is seen to localise to acetylated microtubules but also to the microtubule network as a whole, most of which is highly acetylated (figure 5.4 C.). The increase in microtubule acetylation reported in Sanders et al. (2015) may be due to the heavy and specific acetylation of cilia-like growths, rather than an increase of acetylation of the entire microtubule network.

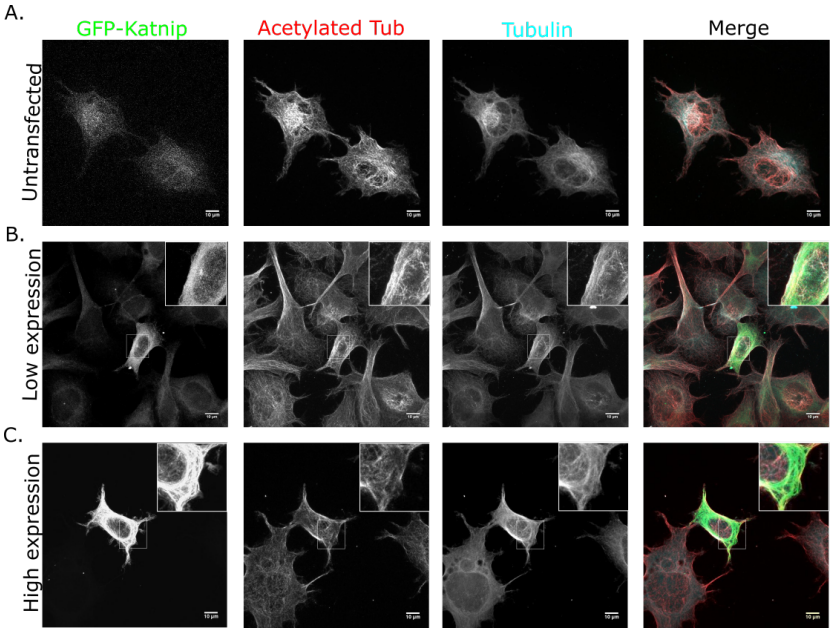

Figure 5.4: **GFP-katnip overexpression doesn't affect global acetylation levels in NSC-34 cells**

Untransfected (A.), low (B.) and highly (C.) expressing GFP-katnip NSC-34 cells fixed and stained with anti-acetylated tubulin (red) and anti-tubulin antibodies (green).Images on airyscan at x100 with 0.2μm z-slices and images airy processed and max-projected.

Images are max projections of entire cells. Imaged on airyscan and airy processed.

5.3.3 GFP-katnip has different localisations dependent on concentration in SH-SY5Y cells

The next aim was to identify a suitable neuronal cell lines for generating katnip knockout cell lines via CRISPR. SH-SY5Y cells are a human neuronal cell line originally cultured from a neuroblastoma sample and widely used in the field of neurodegenerative disease and neuronal development research (Scott et al., 1986). They were chosen due to their ease of producing CRISPR knockout, which is currently ongoing in the lab hlalso due to our interest in seeing if the autophagy defect is conserved in neuronal cells and therefore may be a

risk factor for neurodegenerative disease development. NSC-34 are not suitable for generating CRISPR KO as they are a mouse/human hybrid cell line. In order to identify if SH-SY5Y cells shared the same centrosomal localisation as observed in NSC-34, hTERT RPE-1 and *Dictyostelium discoideum* cells, SH-SY5Y cells were transfected with GFP-katnip and stained for anti-tubulin and anti-acetylated tubulin.

In SHSY cells, expression of GFP-katnip showed 3 distinct localisations; centrosomal (figure 5.5 A.), microtubule (figure 5.5 B.) and punctate on microtubules (figure 5.5 C.). Centrosomal and microtubule localisation were the same as observed in all other cell lines, but the punctate localisation was only observed in SH-SY5Y. Interestingly, a similar punctate localisation of GFP-katnip along microtubules was observed in very highly expressing hTERT RPE-1 in Sanders et al. (2015) but could only be recapitulated in our SH-SY5Y cells and not in RPE1s. This may be due to the increased transfection efficiency of GFP-katnip in SH-SY5Y compared to both RPE1 and NSC-34 cells in my hands, as punctate localisation was only seen in extremely highly expressing SY-SY5Y cells.

Again, unlike RPE1 cells but reflecting NSC-34 phenotypes, acetylated tubulin staining appeared unaffected by any levels of GFP-katnip expression (figure 5.5, punctate example is due to bleed through) once again suggesting that GFP-katnip transfection doesn't affect global acetylation of microtubules.

To confirm that these different localisations were based on the amount of GFP-katnip expressed, the GFP fluorescence intensity of cells with each localisation was quantified (figure 5.5 A.). This confirmed that centrosomal localisation was only found in low expressing cells with microtubule/punctate localisation only found in very highly expressing cells. For comparison, images were taken using the same microscope settings, however this meant that the settings required to image the low expressing cells meant that the very bright puncta were saturated and therefore couldn't be quantified.

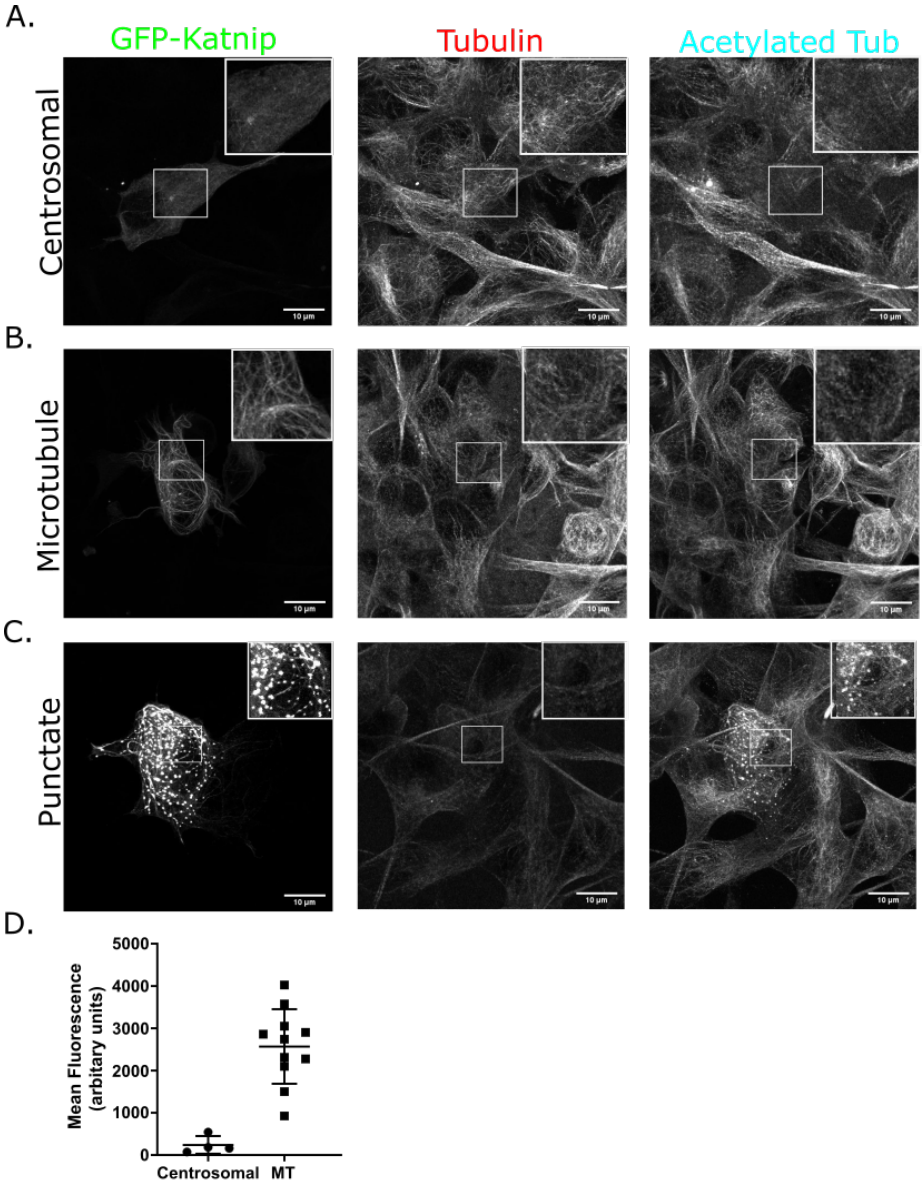

Figure 5.5: **GFP-katnip has 3 distinct localisations in SH-SY5Y neuronal cells**

Examples of neuronal SH-SY5Y cells transiently expressing GFP-katnip with either centrosomal (A.), microtubule (B.) and punctate (C.) GFP-katnip localisation. All images are

taken with the same imaging settings. In (C), GFP-katnip channel has bleed through to the acetylated tubulin channel. Imaged on airyscan microscope at x100 with 0.2 z-slices, images airy processed and max-projected. D. Fluorescence quantification from cells with centrosomal or microtubule (MT) localisation in SH-SY5Y cells. Example cells in figure 5.5). Whole cell areas was manually selected and measured using ImageJ measure function.

5.3.4 GFP-katnip exhibits phase-phase separation dynamics

Both forming bright puncta and having multiple concentration dependent localisation are hallmarks of phase separation dynamics. This behaviour is found when proteins separate from the cytoplasm and form distinct puncta, as they are unable to mix with surrounding but able to fuse with other puncta made of the same protein, like oil and water. In order to elucidate whether GFP-katnip might exhibit this behaviour, overexpressing SHSY cells were imaged live (figure 5.6 A., B.).

In live images, GFP-katnip did not move along microtubules, suggesting it was bound to microtubules, rather than bound to them as cargo being trafficked. Fusion events were seen between GFP-katnip puncta, showing that they do have the ability to fuse with each other. Puncta formation at high concentrations may be important for katnip's function upon microtubule localisation under normal conditions.

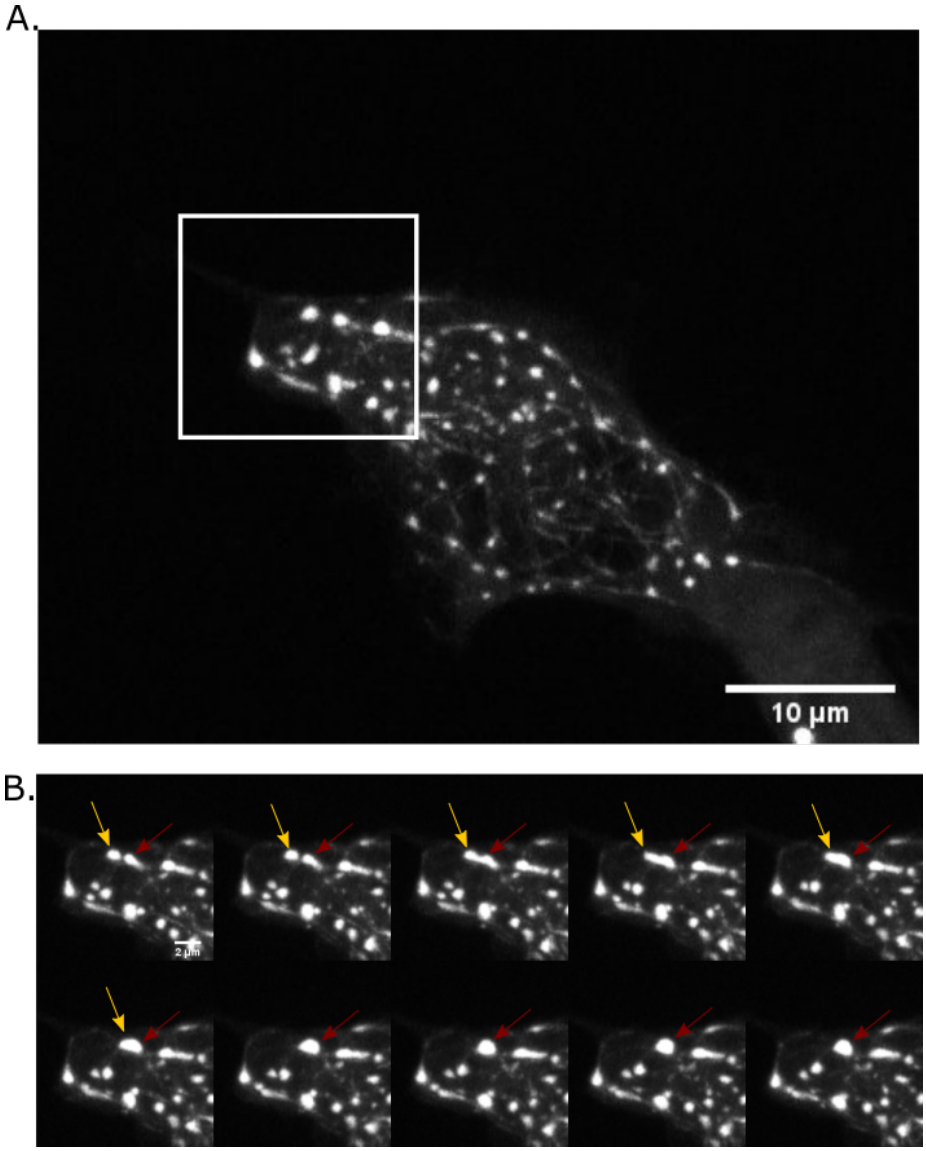

Figure 5.6: **Dynamics of GFP-katnip observed live in SH-SY5Y cells**

A. Image of live SH-SY5Y cell expressed high levels of GFP-katnip. White box indicates area shown in (B). B. Fusion of 2 GFP-katnip puncta in a SH-SY5Y cell imaged live. Each frame represents 5 seconds. Imaged on spinning disk confocal microscope at x64 with 0.5μm z-slices, images max-projected.

5.4 Discussion: Katnip binds to and affects interphase microtubules

5.4.1 Katnip can bind to centrosomes and microtubules

This chapter presents data that katnip localises to the centrosome in RPE1 and 2 neuronal cell lines. This localisation is conserved across evolution, as it is also found in *Dictyostelium discoideum* cells (shown in Results II).

Katnip also has some capacity to bind to microtubules although this appears to be condition and concentration dependent. Similar to the recruitment of GFP-dlkatnip to microtubules upon oxidative damage in *Dictyostelium discoideum* , GFP-katnip only localised to microtubules in highly expressing mammalian cells. In NSC-34 and SH-SY5Y cells, binding all over the microtubule network and in hTERT RPE-1, to a subset of highly acetylated microtubules. In SH-SY5Y cells, highly expressing GFP-katnip cells formed puncta very similar to relocalised GFP-dlkatnip in *Dictyostelium discoideum* after oxidative damage (figure 4.3).

5.4.2 GFP-katnip exhibits phase separation behaviour

GFP-katnip was observed to form puncta, which were able to fuse with other GFP-katnip puncta, and had a multiple concentration-dependent localisation. These are all hallmarks of phase separation behaviour, along with puncta size increase with increased protein concentration, but not their brightness. I hypothesise that this behaviour may be underlying puncta forming in *Dictyostelium discoideum* cells upon oxidative damage and therefore, is conserved between species.

Without the crystal structure of katnip, it is difficult to confirm the chemical cause of its phase separation dynamics, but one hypothesis is the multivalent interaction between its DUF4457 domains. Multivalent interactions between the same protein domains, causes them to associate and decreases their solubility, resulting in puncta which cannot mix with surrounding soluble milieu. This

allows proteins their phase-separation behaviour and therefore, many proteins capable of this behaviour have multiple repeats of the same domains to increase interactions (Alberti et al., 2019). This behaviour has been shown to occur in multiple microtubule regulators, including Tau (King and Petry, 2020; Rale et al., 2018; Ukmar-Godec et al., 2020). This also allows its concentration dependent behaviour as a threshold of protein concentration must be reached until enough multivalent interactions occur for solubility to decrease.

This behaviour is utilised by proteins endogenously by having multiple protein localisations, and therefore functions, based on local concentration. Therefore, regulating protein levels, either at the transcriptional level or recruitment, can allow control of the protein's functions. In katnip's scenario, its strong relocalisation to microtubules upon stress, possibly directly to microtubule damage, causes a large increase in the local concentration as proteins moves from the dilute cytoplasm specific onto microtubules. This may allow for phase separation as seen in the highly overexpressing GFP-katnip cells but at a much smaller levels. This may function to other recruit proteins, such as katanin, which may be specific for only this punctate formation. As these experiments relied on the overexpression of GFP-katnip to very high levels, these are unlikely to replicate the exact phenotypes in native cells, but are a interesting read out of the possible different dynamics that katnip has.

5.4.3 GFP-katnip overexpression may cause nascent cilia

GFP-katnip microtubule binding is only seen on a subset of microtubules in hTERT RPE-1 cells, whereas in NSC-34 and SH-SY5Y cells, it is seen covering microtubule network when expressed high enough. This indicates that GFP-katnip's localisation to microtubules is cell-type dependent. The microtubule protrusions observed in RPE1 cells may be some sort of preliminary cilia from the centrosome resulting from the overexpression of GFP-katnip. Ciliary microtubules are highly stable and acetylated, similar to those found throughout neuronal cells and therefore, it may be that GFP-katnip specifically localises to

highly acetylated microtubules.

These bundles were only seen in hTERT RPE-1 cells and therefore may be specific to cells capable of creating cilia. The tangles observed in some of the ciliated like microtubules are reminiscent of the tangles observed in katnip$^-$ *Dictyostelium discoideum* cells (figure 4.5). If these microtubules bundles are nascent cilia, this suggests a role for katnip in cilia growth, a possible explanation for the loss of microtubule numbers in katnip$^-$ patients with Joubert's syndrome.

5.4.4 Global microtubules acetylation in GFP-katnip expressing cells is unaffected

Global acetylation level of microtubules appear the same between untransfected and GFP-katnip transfected cells in NSC-34 and SH-SY5Y cells. This is consistent with katnip$^-$ *Dictyostelium discoideum* data where no difference in microtubule stability was identified between WT and katnip$^-$ cells (figure 4.10). Co-localisation of GFP-katnip to acetylated microtubules is seen in all cell lines to some degree, binding only to highly acetylated microtubules in hTERT RPE-1 and to all microtubules in neuronal cells which are all acetylated. Therefore GFP-katnip might bind specifically to highly acetylated microtubules but not direct cause microtubule to be acetylated. Equally as likely, GFP-katnip might have a preference for stabilised microtubules, rather than acetylation. As only fixed cells were investigated, this dynamic cannot be assessed from this data alone.

Due to low numbers of transfected cells, it was not possible to quantify tubulin acetylation between transfected and untransfected cells via western, but would provide quantifiable data of whether GFP-katnip affects acetylation. If transfection levels could be manipulated further to control expression levels and therefore the different phenotypes of the cells, this could also be investigated.

5.4.5 GFP-katnip over-expression may affect microtubule function

Another possibility for the differences between cell lines in localisation may be down to transfection efficiency. All cell lines had a very low transfection efficiency of GFP-katnip, with many only achieving 1-2% of cells expressing GFP-katnip (compared to approximately 60% transfection efficiency with eGFP only control). hTERT RPE-1 cells were especially difficult to transfect and therefore levels of GFP-katnip expression may not have reached high enough levels to observe global microtubule localisation or puncta formation. In Sanders et al. (2015), they observed a punctate phenotype on microtubules in RPE1 expressing SF-TAP-katnip, suggesting that this phenotype can be achieved in these cells. It is possible that the tagging of katnip with GFP increases its toxicity.

Issues with transfecting cells may be due to toxicity of the plasmid, possibly due to an effect on microtubules. The western also indicates there is relatively low endogenous expression and therefore cells may not be able to cope with high levels.

Due to the extreme phenotypes seen in over expressing cells (microtubule coating, puncta formation, centrosomal derived microtubule tangles, possible inappropriate cilia growth) and the difficulties with transfecting cells, katnip levels might be tightly regulated endogenously to keep expression at low levels, to prevent these potentially toxic phenotypes.

Interestingly, the katnip interacting protein, katanin is also expressed at very low levels in the cells and is tightly regulated due to the severe phenotypes associated with its too high expression (disintergration of the microtubule network via severing).

GFP-katnip coats microtubules, potentially interfering with their function and forms puncta which are potentially aggregates, a common cell response to too much toxic protein expression (Jucker and Walker, 2013). Another possibly is that the overexpression of katnip could sequester its protein interactors from

their essential function, including katanin. This could be elucidated by staining for Katanin in overexpressing GFP-katnip cells.

5.4.6 Ongoing work on DUF4457 and Katanin

Currently, an antibody against DUF4457-HisTag is being developed for use against endogenous katnip. This will allow for the identification of the endogneous localisation of the protein, recapitulating protein interactions in SH-SY5Y cell lines, and assessing expression levels in CRISPR cells, which which are also being developed currently.

The part of the katnip protein which encodes its microtubule localisation is still unknown. In order to investigate this further, truncations of the protein tagged with GFP are currently being cloned. I hypothese that the DUF4457 domains function as low affinity (and potentially conditional) microtubule binding domains. Observation of different GFP tagged DUF4457 repeats will allow us to identify the exact portions of the protein required for localisation. Once the katnip$^-$ SH-SY5Y cells are generated, these plasmids could be retransfected to identify what elements of the proteins are required to rescue mutant phenotypes. Before this can be addressed, quantifiable defects in katnip$^-$ SH-SY5Y cells need to be identified.

The relationship between katnip and katanin remains elusive, but information regarding their physical interaction could be mapped through identifying the portion of Katnip which is required for katanin binding through use of the truncated GFP-tagged katnip plasmids and co-IPs with the generated GST-DUF4457-HisTag antibody. Following on from this, specific residues could be mutated in GFP-katnip plasmids to identify katanin binding regions.

In summary, GFP-Katnip shares the same localisation to the centrosomes and microtubules across 3 different mammalian cell lines, which is also conserved to the centrosomal and (oxidative damage dependant) microtubule localisation observed in *Dictyostelium discoideum* cells.

Chapter 6

Discussion

6.1 Katnip may function as a novel microtubule regulator

This PhD has been focused on the role of the uncharacterised protein katnip, and identifying defects in katnip$^-$ mutants. Although previous studies identified a role for katnip in cilia microtubule organisation, here I identify a role on interphase microtubules and in non-ciliated cells. Below are the major findings of my work and questions which still remain.

6.1.1 Katnip is required for efficient microtubule-based trafficking

Whilst disruption of katnip$^-$ was previously understood to cause an autophagy defect, the extent and cause of this was unknown. I have characterised this autophagy defect in katnip$^-$ cells and shown that autophagy flux is reduced by around 40% due to elongated formation and degradation of autophagosomes. This defect also extended to phagosome degradation, which was also reduced by 40%, and macropinocytosis, which is disrupted. As all 3 of these trafficking pathways rely on the trafficking of lysosomes for vesicle degradation, I hypothe-

sised that katnip$^-$ mutants had a general lysosomal trafficking defect. I assessed lysosomal function, which showed no defect in total cathepsin D levels or proteolytic activity, suggesting the defect is not caused by defects in these two area. From these data, I suggest that the degradation defect was due to either disrupted trafficking or disrupted fusion, or both. Having identified the microtubule function of katnip and its effect on microtubule organisation, I hypothesise that loss of katnip causes reduced trafficking along microtubules and therefore reduced delivery of vesicles to lysosomes for their degradation. I further this by showing that the speed of autophagosome movement was significantly lower in katnip$^-$ cells compared to wild type cells.

In this PhD, autophagy, phagocytosis and macropinocytosis were investigated for dependence on katnip function, as they all require microtubule trafficking for lysosomal delivery. However, loss of correct microtubule trafficking has many more implications than just these pathways.

In addition to their function as final destination for vesicles, lysosomes move along microtubules in order to adapt their localisation in response to extracellular nutrient levels. Lysosomal positioning is defective in many diseases, due to MAP mutations including; KIF5A kinesin mutations in hereditary spastic paraplegia (Reid et al., 2002) and Rab7, a lysosomal microtubule adaptor, in Charcot-Marie-Tooth disease (Verhoeven et al., 2003). Irregular lysosomal positioning is also observed commonly in cancer due to changes in the tumour microenvironment and paracrine signalling, and affects cellular response to extracellular signalling and nutrient sensing via mTORC1 on the lysosomal surface (Korolchuk et al., 2011). As loss of katnip is hypothesised to result in defective transport along microtubules; it is likely the lysosomal positioning is defective in mutants.

Due to the rapid and essential nature of autophagy and phagocytosis in cellular growth, defects are quickly developed, severe and easy to assay. But over time, it is likely that phenotypes associated with the transport of other cargoes along microtubules would develop in katnip$^-$ cells. Other microtubule cargoes include mRNA (Jambor et al., 2014), and even other microtubules to

allow new seeding, essential in the growth of many neuronal cells (Sánchez-Huertas et al., 2016).

6.1.2 Katnip is a centrosomal protein which can associate with microtubules under certain conditions

Centrosomal binding

GFP tagged katnip expressed in 3 mammalian cells lines and both a truncated *Dictyostelium discoideum* and full length *Dictyostelium lacteum* katnip proteins in *Dictyostelium discoideum* localised to the centrosome. High cytosolic expression was observed in all cells with the relocalisation of GFP-katnip to microtubules under certain conditions. This confirms katnip as a centrosomal protein, which has a conserved localisation between species, even though these species have very different centrosomal structures (section 1.3.5). This is in agreement with the localisation of GFP-katnip to the basal body of cilia as the basal body shares the same structure as centrosomes (Sanders et al., 2015).

The centrosome is the origin of all microtubules and therefore regulates the number of microtubules (via gamma-TuRC complex) and also their organisation and orientation. Loss of katnip does not appear to cause a defect in microtubule nucleation in non-cilia cells, as the same amount of microtubules were observed in katnip$^-$ *Dictyostelium discoideum* cells, as well as same amount of tubulin was polymerised into microtubules (figure 4.10, figure 4.8). However, the unusual microtubule growths observed in GFP-katnip RPE1 cells suggest it may function as a microtubule nucleator. Loss of microtubule numbers in cilia was reported in katnip$^-$ cells in Sanders et al. (2015) and therefore, katnip may have a function in the nucleation of cilia microtubules.

Microtubule binding

Katnip's ability to bind microtubules has previously been hypothesised as multiple tubulin subunits which were reported to complex to katnip (Sanders et al., 2015). However, katnip may also bind to other MAP proteins on the surface of

microtubules for its function. Katnip is known to be an interacting partner to the microtubule severing enzyme katanin (through a yeast 2-hydrid screen) as well with multiple IFT proteins and NUDC, a mitotic microtubule protein, all of which localise to microtubules. Here, I found that GFP-katnip was observed to relocalise to microtubules upon oxidative damage and very high expression. This indicates that katnip can bind to microtubules, but only under certain conditions. I also identified that in very highly expressing cells, GFP-katnip formed puncta which exhibited phase separation behaviour. GFP-katnip has different localisations based on its concentration, and its capacity to phase separate might regulate bindings to microtubule and/or other proteins. Whilst katnip is diffuse in the cytoplasm, its local concentration must rapidly increase upon relocalisation to microtubule patches, as seen in figure 4.4 and figure 1.3.3. Therefore, it is more likely to phase separate, and this dynamic may be integral to regulating its function between its cytoplasm (where it is assumed to be inert) and microtubule bound localisation.

Katnip has no sequence homology to other proteins, but does contain 3 highly conserved repeats of a single unique domain, DUF4457. As DUF4457 is the only identifiable feature of katnip, it is likely that it contains the function of the protein, and therefore I hypothesise that it is a low affinity microtubule binding domain. Having multiple repeats of a low affinity microtubule binding domain is commonly seen in other transient microtubule binding proteins, including the CLASP proteins and multimeric katanin. This repetition is thought to both increase the binding to microtubules and allow it to bind to multiple protofilaments and/or microtubules at one time.

Similarity folding software predicts the structure of DUF4457 as most similar to the motor domains of dynein (heavy and intermediate chain, figure 6.1). Based on this structure alone, GO terms prediction was identified as a centrosomal cellular component, which is in alignment to work presented in this thesis.

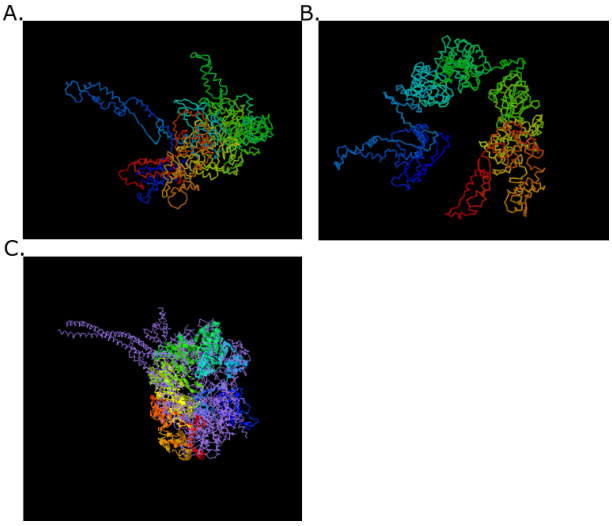

Figure 6.1: **Comparison between the estimated structural folding of DUF4457 and dynein protein**

Estimated structural model of katnip generated by iTasser software. Top two estimated structural analogs are both dyenin proteins. (Dynein motor domain: 2vkgA on RCSB and dynein heavy chain motor domain: 3qmzA on RCSB).

A microtubule binding protein called CLASP2a has recently been shown to facilitate microtubule repair upon damage *in vitro* (Aher et al., 2020). CLASP2a also relocalises to microtubules and bind to areas of microtubule damage. As katnip shares similar behaviour to CLASP2a, it may have a similar function in microtubule repair. CLASP2a may have redundancy with katnip, and may account of the lack of katnip in Drosophila, where a CLASP2a orthologue has previously been shown to be necessary for incorporation of new tubulin subunits into anaphase microtubules (Maiato et al., 2005). Microtubule damage has not been investigated in yeast, which also lacks katnip but, due to the simplicity of the microtubule network in the organism, katnip may not be essential and may have be lost over time like many of the other microtubule regulators.

In RPE1 cells, GFP-katnip localised on unique cilia like protrusions from

the centrosome, which were highly acetylated upon its overexpression. In neuronal cells (SH-SY5Y and NSC-34) where nearly all of the microtubules are acetylated already, GFP-katnip was seen to localise to all microtubules when highly expressed. In all 3 cell lines, GFP-katnip was observed to co-localise with acetylated microtubules, and therefore I hypothesis that katnip binds to acetylated microtubules when highly expressed. Whether this is due to binding generally to stable microtubules or binding specifically to acetylation on tubulin is unknown. This is also suggested in Sanders et al. (2015), as GFP-katnip is seen to localise to the entire length of the cilia.

6.1.3 Loss of katnip affects microtubule organisation

Microtubules have different organisations within cells, dependent on required function.

As katnip$^-$ cells have microtubule disorganisation in both interphase microtubule organisation and cilia, it indicates that katnip is a general regulator of microtubule organisation and is not specific for just one organisation. Other specialised microtubule organisations include during mitosis, neuronal organisation and growth, polarised cells organisation and chemotaxis. Mutants in *Dictyostelium discoideum* exhibited a chemotaxis defect whereby the cells had reduced directionality. This may be due to the loss of receptor trafficking which is regulated by microtubules. Loss of effective chemotaxis has many implications, including disrupted movement of immune cells to sites of injury and infection. This, partnered with the reduced phagocytosis and potential xenophagy defects (the specific autophagy of intracellular bacteria) in katnip$^-$ cells, means that mutants may exhibit complications with infection and inflammation.

Dictyostelium discoideum have robust mitoses and are able to withstand many mitotic defects, including multi-nucleated cells, increased anaphase time (as reported here) and quad mitosis. Mammalian cells are highly sensitive to mitosis defects due to regulation to prevent cancer through p53 and the spindle assembly checkpoint (SAC). Mitosis defects which may not produce phenotypes

in *Dictyostelium discoideum* cells might have severe implications in mammalian cells. As patients survive with katnip mutations, the defects are not severe enough to prevent life (although there may be redundancy with other proteins with similar functions), but cells may be more susceptible to abnormal mitoses. Mitotic defects are associated with the development of cancer due to chromosomal aberrations and, therefore katnip mutations may be linked to an increased susceptibility to development of cancers.

6.1.4 The role of katnip in microtubule damage

After identifying katnip as a centrosomal protein which can transiently bind to microtubules to affect organisation, questions concerning its exact function still remain. Several data suggest loss of katnip causes a sensitivity to microtubule damage, which in turn produces a trafficking defect and loss of microtubule organisation.

I also present data that GFP-katnip may recognise and bind to microtubule damage, and therefore may have future uses as a microtubule damage reporter.

Microtubule damage has been previously reported to result in trafficking disruption through affecting kinesin walking (Ray et al., 1993; Yildiz et al., 2004). Microtubule motors move along single protofilament tracks but when they reach holes in the lattice, they stall or even completely disassociate. In katnip$^-$ cells, this may occur more often, leading to slower trafficking (in the case of motor stalling) and reduced trafficking (in the case of dissociation), as suggested by the reduction of autophagosome movement (figure 4.7).

Loss of katnip$^-$ may affects microtubules in cells in a more universal, but subtle way, and that tangles are an especially severe phenotype. How microtubule damage affects microtubules at a structural levels is currently unknown. Increased microtubule breakages are reported but due to the field's young age, very few papers have looked at the structural affects of microtubule damage and the molecular details of how damage is recognised, and repaired are almost completely unknown. Microtubule damage cannot be observed at the levels of

light microscopy, and therefore these seemingly unaffected cells without tangles may have high levels of unobservable microtubule damage.

The way in which microtubule damage disrupts organisation is unknown, although has been reported before (Xu et al., 2017; Topalidou et al., 2012; Cueva et al., 2012). The increased repair of microtubules after damage might lead to defective microtubule organisation and tangles. It has been previously reported that microtubule repair can act as points of rescue, and therefore repaired microtubules have longer lifetimes and increased resistance to catastrophe (Aumeier et al., 2016). This, ultimately, increases the age of the microtubule network within the cells, and increased age may result in microtubule organisation defects. Microtubules which have been artificially aged by Taxol treatment commonly exhibit microtubule organisation defects and tangles, and therefore the increase in microtubule lifetime and hyper stability may lead to microtubule tangles (Qiang, 2006). The exact molecular mechanisms by which increased microtubule repair and tangle formation are linked are unknown; a possible explanation is that the incorrect repair of microtubules causes them to be connected and bundle together.

GTP-tubulin is initially integrated into microtubules during repair before being converted back into GDP-tubulin over time. Therefore, GTP-tubulin antibody staining highlights areas of recently repaired microtubule damage (Dimitrov et al., 2008). Unfortunately, efforts to stain GTP-tubulin in *Dictyostelium discoideum* were problematic due to the semi-adherent nature of *Dictyostelium discoideum* causing cells to disassociate during pre-fixation antibody staining. Other issues where discovered in SH-SY5Y cells, as GTP-tubulin appears to be non-specific and was seen decorating nearly all microtubules. Therefore microtubule damage could not be quantified directly in cells in this way, although efforts to optimise this antibody are still underway.

Another avenue to image microtubule damage directly was by purifying microtubules from WT and katnip^{-} cells and imaging them for damage via EM. A protocol to extract complete microtubules from cells was created and optimised successfully and optimisation of fixation and EM treatment is ongoing.

Without suitable confirmed reporters of *in vivo* microtubule damage, the way in which microtubule damage affects the microtubules cannot be fully understood.

In light of the lack of microtubule damage reporters, previous research on katnip was investigated for more links to microtubule damage.

Sanders et al. (2015) reported that katnip bound to all subunits of katanin (KATNA1, KATNB1, KATNAL1, KATNBL2), making it one of very few katanin interacting proteins. Katanin has a defined role in microtubule damage, having been reported to require microtubule lattice defects for severing *in vitro* and *in vivo* (Davis et al., 2002; Díaz-Valencia et al., 2011). From this data, katanin was hypothesised to have a role in removing microtubule defects, and katnip could therefore act as a platform for this, binding to areas of microtubule damage and then recruiting katanin for severing. If this was the case, microtubule severing would be expected at points of katnip microtubule binding. Although this was not seen in imaging, the thick coating of overexpressed GFP-katnip may have prevented this interaction so cannot be confirmed nor denied. GFP knockins of katnip would allow for the tracking of native proteins, allowing this to be investigated.

Other links between microtubule damage and katnip include; GFP-katnip colocalisation to acetylated microtubules and high acetylation microtubule damage patches (section 1.3.3, Portran et al. (2017)). Both the loss of katnip and overexpression of GFP-katnip produce similar microtubules tangles phenotypes which increase microtubule overlaps and crossovers, both of which have been shown to be a hotspot of microtubule repair (Aumeier et al., 2016).

6.1.5 Potential implications of katnip$^-$ defects on disease pathology

Phenotypes associated with disease in neuronal and ciliated tissues have been shown in patients lacking katnip. Both these tissues are sensitive to microtubule damage, due to their long lived microtubule, and therefore, phenotypes

may appear in these tissues first due to increased reliance on microtubule damage tolerating proteins (Sanders et al., 2015; Fujita et al., 2019; Cauley et al., 2019). All of these provide more links between katnip and microtubule damage, supporting the hypothesis that katnip functions to tolerate microtubule damage.

Katnip and Joubert's syndrome

Loss of katnip in humans results in the development of Joubert's ciliopathy. Cilia are exposed to more microtubule damaging events and therefore may be more sensitive to the loss of katnip. This is potentially a cause of the ciliopathies in patients and may be the reason that this is one of the first tissues to present a defect. Interestingly, Joubert's patients with katnip mutations are more likely to also carry a mutation in kif7, a microtubule plus end motor (Niceta et al., 2020). These patients exhibit more phenotypes which aren't always associated with Joubert's syndrome, including ocular coloboma, pituitary malformation and growth hormone deficiency. Most of these can be attributed to the loss of cilia signalling, but it is interesting how the loss of another microtubule associated protein can exacerbate Joubert's patients phenotypes and links microtubules to Joubert's syndrome.

Katnip and neurodegeneration

Reduction in autophagy is closely linked to the development of many neurodegenerative diseases in humans (Menzies et al., 2015). In order to assess this, GFP tagged mutant Huntington protein was expressed in *Dictyostelium discoideum* katnip$^-$ cells but no aggregates where observed, indicating that katnip$^-$ still have sufficient levels of autophagy to clear the mutant proteins preventing aggregates. *Dictyostelium discoideum* is highly adapted to remove polyQ proteins and therefore is more efficient than human neuronal cells at removing aggregates. Therefore, katnip$^-$ patients may be at risk for neurodegenerative disease. In addition to complete katnip loss, mutations which partially reduce katnip function may also be risk factors for the development of neurodegenerative diseases.

Evidence of this is a recent research paper which linked loss of katnip to NFT formation (Andres-Benito et al., 2018). Whether loss of katnip expression is a pre-requisite to the development of NFTs in some cases, or as a result of NFTs formation, is unknown. This provides more evidence to the hypothesis that loss of katnip^{-} also causes an autophagy defect in humans and may results in disease. Interestingly, NFTs are the product of mislocalised hyperphosphorylated Tau, a well characterised microtubule stabiliser which also forms liquid-liquid phase separation for its function (Ukmar-Godec et al., 2020).

Whether mammalian katnip^{-} cells have defective autophagy, and whether it is severe enough to cause build up of toxic proteins is unknown, but ongoing work creating a katnip^{-} SH-SY5Y cell line will allow for this to be investigated in the future.

6.1.6 Summary

This PhD presents novel work on the functions of katnip, in both *Dictyostelium discoideum* and human cells. Previously, katnip's only identified role was as a regulator of cilia microtubule organisation. This work further the knowledge surrounding katnip's involvement in autophagy, identifying it as having a degradation defect in autophagosome, phagosomes and disrupted macropinocytosis. I also present a new role of katnip as a conserved centrosomal protein, which can localise to microtubules under certain conditions.

Data in this PhD presents katnip as a strong candidate to be involved in microtubule damage. Further work needs to be performed to confirm this, although there are many links identified in this thesis and in previous research. Whether katnip's role in microtubule damage is protection, repair or removal is still unknown and this should be the focus for future work.

Due to this data, I hypothesis that loss of katnip may have wider implications in patients outside of identified cilia defects, including increased susceptibility to developing neurodegenerative disease (due to reduced autophagy) and increased bacterial burden (due to reduced chemotaxis and phagocytosis).

The main aim of this project was to further expand upon the involvement of katnip in autophagy and identify other defects of these mutants. These were achieved and expanded upon by identifying possible disease implications that these defects may have in katnip$^-$ mutant patients and identifying links to microtubule damage

Although some investigation was performed on how the katnip effects microtubules, the exact function of katnip remains unknown. Focus and increased interested in the microtubule damage field will hopefully makes new resources available to eludicate the exact function of katnip in microtubule damage.

Chapter 7

Bibliography

Bibliography

B. A. Abdulrahman, D. Abdelaziz, S. Thapa, L. Lu, S. Jain, S. Gilch, S. Proniuk, A. Zukiwski, and H. M. Schatzl. The celecoxib derivatives AR-12 and AR-14 induce autophagy and clear prion-infected cells from prions. *Scientific Reports*, 7(1):17565, dec 2017. ISSN 2045-2322. doi: 10.1038/s41598-017-17770-8. URL `http://www.nature.com/articles/s41598-017-17770-8`.

S. J. A. Ae, P. R. Fisher, S. J. Annesley, and Á. P. R. Fisher. Dictyostelium discoideum-a model for many reasons. *Mol Cell Biochem*, 329:73–91, 2009. doi: 10.1007/s11010-009-0111-8.

F. A. Agarraberes, S. R. Terlecky, and J. F. Dice. An intralysosomal hsp70 is required for a selective pathway of lysosomal protein degradation. *Journal of Cell Biology*, 137(4):825–834, may 1997. ISSN 00219525. doi: 10.1083/jcb.137.4.825.

A. Aher, D. Rai, L. Schaedel, J. Gaillard, K. John, L. Blanchoin, M. Thery, and A. Akhmanova. CLASP mediates microtubule repair by promoting tubulin incorporation into damaged lattices. *bioRxiv*, 2019. doi: 10.1101/809251. URL `http://dx.doi.org/10.1101/809251`.

A. Aher, D. Rai, L. Schaedel, J. Gaillard, K. John, Q. Liu, M. Altelaar, L. Blanchoin, M. Thery, and A. Akhmanova. CLASP Mediates Microtubule Repair by Restricting Lattice Damage and Regulating Tubulin Incorporation. *Cur-*

rent Biology, 30(11):2175–2183.e6, jun 2020. ISSN 18790445. doi: 10.1016/j.cub.2020.03.070. URL https://pubmed.ncbi.nlm.nih.gov/32359430/.

J. S. Akella, D. Wloga, J. Kim, N. G. Starostina, S. Lyons-Abbott, N. S. Morrissette, S. T. Dougan, E. T. Kipreos, and J. Gaertig. MEC-17 is an α-tubulin acetyltransferase. *Nature*, 467(7312):218–222, sep 2010. ISSN 00280836. doi: 10.1038/nature09324. URL https://www.nature.com/articles/nature09324.

J. Al-Bassam, H. Kim, G. Brouhard, A. van Oijen, S. C. Harrison, and F. Chang. CLASP promotes microtubule rescue by recruiting tubulin dimers to the microtubule. *Developmental Cell*, 19(2):245–258, aug 2010. ISSN 15345807. doi: 10.1016/j.devcel.2010.07.016.

S. Alberti, A. Gladfelter, and T. Mittag. Considerations and Challenges in Studying Liquid-Liquid Phase Separation and Biomolecular Condensates, jan 2019. ISSN 10974172. URL https://pubmed.ncbi.nlm.nih.gov/30682370/.

L. A. Amos and D. Schlieper. Microtubules and maps. *Advances in Protein Chemistry*, 71(04):257–298, 2005. ISSN 00653233. doi: 10.1016/S0065-3233(04)71007-4.

A. L. Anding and E. H. Baehrecke. Developmental Cell Review Cleaning House: Selective Autophagy of Organelles. 2017. doi: 10.1016/j.devcel.2017.02.016. URL http://dx.doi.org/10.1016/j.devcel.2017.02.016.

P. Andres-Benito, R. Delgado-Morales, and I. Ferrer. Altered Regulation of KIAA0566, and Katanin Signaling Expression in the Locus Coeruleus With Neurofibrillary Tangle Pathology. *Frontiers in Cellular Neuroscience*, 12, 2018. ISSN 1662-5102. doi: ARTN13110.3389/fncel.2018.00131.

A. Aplin, T. Jasionowski, D. L. Tuttle, S. E. Lenk, and W. A. Dunn. Cytoskeletal elements are required for the formation and maturation of autophagic vacuoles. *Journal of Cellular Physiology*, 152(3):458–466, sep 1992. ISSN

0021-9541. doi: 10.1002/jcp.1041520304. URL http://doi.wiley.com/10.1002/jcp.1041520304.

C. Aumeier, L. Schaedel, J. Gaillard, K. John, L. Blanchoin, and M. Thery. Self-repair promotes microtubule rescue. *Nature Cell Biology*, 18(10):1054–1064, 2016. ISSN 1465-7392. doi: 10.1038/ncb3406.

E. L. Axe, S. A. Walker, M. Manifava, P. Chandra, H. L. Roderick, A. Habermann, G. Griffiths, and N. T. Ktistakis. Autophagosome formation from membrane compartments enriched in phosphatidylinositol 3-phosphate and dynamically connected to the endoplasmic reticulum. *Journal of Cell Biology*, 182(4):685–701, aug 2008. ISSN 00219525. doi: 10.1083/jcb.200803137. URL www.jcb.org/cgi/doi/10.1083/jcb.200803137.

D. C. Bassham, M. Laporte, F. Marty, Y. Moriyasu, Y. Ohsumi, L. J. Olsen, and K. Yoshimoto. Autophagy in development and stress responses of plants, 2006. ISSN 15548635. URL https://www.tandfonline.com/doi/abs/10.4161/auto.2092.

S. Bechstedt and G. J. Brouhard. Doublecortin Recognizes the 13-Protofilament Microtubule Cooperatively and Tracks Microtubule Ends. *Developmental Cell*, 23(1):181–192, jul 2012. ISSN 15345807. doi: 10.1016/j.devcel.2012.05.006.

S. M. Block. Kinesin Motor Mechanics: Binding, Stepping, Tracking, Gating, and Limping. *Biophys J*, 92(9):2986–2895, 2007. doi: 10.1529/biophysj.106.100677. URL http://www.biophysics.org/discussions.

D. A. Brito, J. Strauss, V. Magidson, I. Tikhonenko, A. Khodjakov, and M. P. Koonce. Pushing forces drive the comet-like motility of microtubule arrays in Dictyostelium. *Molecular Biology of the Cell*, 16(7):3334–3340, jul 2005. ISSN 10591524. doi: 10.1091/mbc.E05-01-0057.

C. M. Buckley and J. S. King. Drinking problems: mechanisms of

macropinosome formation and maturation. *FEBS Journal*, 284(22):3778–3790, 2017. ISSN 17424658. doi: 10.1111/febs.14115.

C. M. Buckley, V. L. Heath, A. Guého, C. Bosmani, P. Knobloch, P. Sikakana, N. Personnic, S. K. Dove, R. H. Michell, R. Meier, H. Hilbi, T. Soldati, R. H. Insall, and J. S. King. Pikfyve/fab1 is required for efficient V-ATPase and hydrolase delivery to phagosomes, phagosomal killing, and restriction of legionella infection. *PLoS Pathogens*, 15(2), feb 2019. ISSN 15537374. doi: 10.1371/journal.ppat.1007551. URL `https://pubmed.ncbi.nlm.nih.gov/30730983/`.

J. Calvo-Garrido and R. Escalante. Autophagy dysfunction and ubiquitin-positive protein aggregates in Dictyostelium cells lacking Vmp1. *Autophagy*, 6(1):100–109, jan 2010. ISSN 15548635. doi: 10.4161/auto.6.1.10697. URL `https://www.tandfonline.com/doi/abs/10.4161/auto.6.1.10697`.

M. Caplow and J. Shanks. Evidence that a single monolayer tubulin-GTP cap is both necessary and sufficient to stabilize microtubules. *Molecular Biology of the Cell*, 7(4):663–675, oct 1996. ISSN 10591524. doi: 10.1091/mbc.7.4.663. URL `https://www.molbiolcell.org/doi/abs/10.1091/mbc.7.4.663`.

E. Cardenal-Muñoz, S. Arafah, A. T. López-Jiménez, S. Kicka, A. Falaise, F. Bach, O. Schaad, J. S. King, M. Hagedorn, and T. Soldati. Mycobacterium marinum antagonistically induces an autophagic response while repressing the autophagic flux in a TORC1- and ESX-1-dependent manner. *PLoS pathogens*, 13(4):e1006344, apr 2017. ISSN 1553-7374. doi: 10.1371/journal.ppat.1006344. URL `http://www.ncbi.nlm.nih.gov/pubmed/28414774http://www.pubmedcentral.nih.gov/articlerender.fcgi?artid=PMC5407849`.

E. S. Cauley, A. Hamed, I. N. Mohamed, M. Elseed, S. Martinez, A. Yahia, F. Abozar, R. Abubakr, M. Koko, L. Elsayed, X. Piao, M. A. Salih, and M. C. Manzini. Overlap of polymicrogyria, hydrocephalus, and Joubert syndrome in a family with novel truncating mutations in ADGRG1/GPR56 and KIAA0556. *neurogenetics*, 20(2):91–98, may 2019. ISSN 1364-6745. doi:

10.1007/s10048-019-00577-2. URL http://link.springer.com/10.1007/s10048-019-00577-2.

S. Chaaban and G. J. Brouhard. A microtubule bestiary: Structural diversity in tubulin polymers, 2017. ISSN 19394586.

D. Chretien, E. Metoz, E. Verde, E. Karsenti, and R. H. Wade. Lattice Defects in Microtubules: Protofilament Numbers Vary Within Individual Microtubules. *Journal of Cell Biology*, 117(5):1031–1040, 1992.

M. Clarke, J. Kohler, Q. Arana, L. TOngyao, J. Heuser, and G. Gerisch. Dynamics of the vacuolar H+-ATPase in the contractile vacuole complex and the endosomal pathway of Dictyostelium cells — Journal of Cell Science, 2002. URL https://jcs.biologists.org/content/115/14/2893.short.

C. Coombes, A. Yamamoto, M. McClellan, T. A. Reid, M. Plooster, G. W. G. Luxton, J. Alper, J. Howard, and M. K. Gardner. Mechanism of microtubule lumen entry for the α-tubulin acetyltransferase enzyme αTAT1. *Proceedings of the National Academy of Sciences of the United States of America*, 113(46):E7176–E7184, nov 2016. ISSN 1091-6490. doi: 10.1073/pnas.1605397113. URL http://www.ncbi.nlm.nih.gov/pubmed/27803321http://www.pubmedcentral.nih.gov/articlerender.fcgi?artid=PMC5135325.

G. A. Cox, C. L. Mahaffey, A. Nystuen, V. A. Letts, and W. N. Frankel. The mouse fidgetin gene defines a new role for AAA family proteins in mammalian development. *Nature Genetics*, 26(2):198–202, oct 2000. ISSN 10614036. doi: 10.1038/79923. URL https://pubmed.ncbi.nlm.nih.gov/11017077/.

J. G. Cueva, J. Hsin, K. C. Huang, and M. B. Goodman. Posttranslational acetylation of α-tubulin constrains protofilament number in native microtubules. *Current Biology*, 22(12):1066–1074, jun 2012. ISSN 09609822. doi: 10.1016/j.cub.2012.05.012.

D. Da-Qias, C. Yuji, H. Tokuko, and H. Yasushi. Oscillatory nuclear movement in fission yeast meiotic prophase is driven by astral microtubules, as revealed

by continuous observation of chromosomes and microtubules in living cells. Technical report, Kansai Advanced Research Center, Communications Research Laboratory, 588-2 Iwaoka, Iwaoka-cho, Nishi-ku, Kobe 651-24, Japan, 1998.

T. David-Pfeuty, C. Simon, and D. Pantaloni. Effect of antimitotic drugs on tubulin GTPase activity and self-assembly., 1979. URL `https://www.jbc.org/content/254/22/11696.short`.

A. J. Davidson, J. S. King, and R. H. Insall. The use of streptavidin conjugates as immunoblot loading controls and mitochondrial markers for use with Dictyostelium discoideum. *BioTechniques*, 55(1), jul 2013. ISSN 1940-9818. doi: 10.2144/000114054. URL `https://www.future-science.com/doi/10.2144/000114054`.

L. J. Davis, D. J. Odde, S. M. Block, and S. P. Gross. The importance of lattice defects in katanin-mediated microtubule severing in vitro. *Biophysical Journal*, 82(6):2916–2927, 2002. ISSN 00063495. doi: 10.1016/S0006-3495(02)75632-4.

K. J. De Vos, A. J. Grierson, S. Ackerley, and C. C. Miller. Role of Axonal Transport in Neurodegenerative Diseases. *Annual Review of Neuroscience*, 31(1):151–173, jul 2008. ISSN 0147-006X. doi: 10.1146/annurev.neuro.31.061307.090711. URL `http://www.annualreviews.org/doi/10.1146/annurev.neuro.31.061307.090711`.

A. Desai and T. J. Mitchison. MICROTUBULE POLYMERIZATION DYNAMICS. *Annual Review of Cell and Developmental Biology*, 13(1):83–117, nov 1997. ISSN 1081-0706. doi: 10.1146/annurev.cellbio.13.1.83. URL `http://www.annualreviews.org/doi/10.1146/annurev.cellbio.13.1.83`.

S. Devkota, H. Jeong, Y. Kim, M. Ali, J. I. Roh, D. Hwang, and H. W. Lee. Functional characterization of EI24-induced autophagy in the degradation of RING-domain E3 ligases. *Autophagy*, 12(11):2038–2053, nov 2016.

ISSN 15548635. doi: 10.1080/15548627.2016.1217371. URL https://www.tandfonline.com/doi/full/10.1080/15548627.2016.1217371.

J. D. Díaz-Valencia, M. M. Morelli, M. Bailey, D. Zhang, D. J. Sharp, and J. L. Ross. Drosophila katanin-60 depolymerizes and severs at microtubule defects. *Biophysical Journal*, 100(10):2440–2449, 2011. ISSN 15420086. doi: 10.1016/j.bpj.2011.03.062.

A. Dimitrov, M. Quesnoit, S. Moutel, I. Cantaloube, C. Poüs, and F. Perez. Detection of GTP-tubulin conformation in vivo reveals a role for GTP remnants in microtubule rescues. *Science (New York, N.Y.)*, 322(5906): 1353–6, nov 2008. ISSN 1095-9203. doi: 10.1126/science.1165401. URL http://www.ncbi.nlm.nih.gov/pubmed/18927356.

K. H. Downing and E. Nogales. Tubulin and microtubule structure. *Current Opinion in Cell Biology*, 10(1):16–22, feb 1998. ISSN 09550674. doi: 10.1016/S0955-0674(98)80082-3.

D. R. Drummond, S. Kain, A. Newcombe, C. Hoey, M. Katsuki, and R. A. Cross. Purification of tubulin from the fission yeast schizosaccharomyces pombe. *Methods in Molecular Biology*, 777:29–55, 2011. ISSN 10643745. doi: 10.1007/978-1-61779-252-6_3.

Q. Du, Y. Kawabe, C. Schilde, Z. H. Chen, and P. Schaap. The Evolution of Aggregative Multicellularity and Cell-Cell Communication in the Dictyostelia, nov 2015. ISSN 10898638.

E. E. Dymek, P. A. Lefebvre, and E. F. Smith. PF15p is the Chlamydomonas homologue of the katanin p80 subunit and is required for assembly of flagellar central microtubules. *Eukaryotic Cell*, 3(4):870–879, aug 2004. ISSN 15359778. doi: 10.1128/EC.3.4.870-879.2004. URL https://ec.asm.org/content/3/4/870https://ec.asm.org/content/3/4/870.abstract.

A. Edelstein, N. Amodaj, K. Hoover, R. Vale, and N. Stuurman. Computer control of microscopes using μManager. *Current protocols in molecular biology*,

Chapter 14:Unit14.20, oct 2010. ISSN 1934-3647. doi: 10.1002/0471142727.mb1420s92. URL http://www.ncbi.nlm.nih.gov/pubmed/20890901http://www.pubmedcentral.nih.gov/articlerender.fcgi?artid=PMC3065365.

A. D. Edelstein, M. A. Tsuchida, N. Amodaj, H. Pinkard, R. D. Vale, and N. Stuurman. Advanced methods of microscope control using μManager software. *Journal of biological methods*, 1(2):10, nov 2014. ISSN 2326-9901. doi: 10.14440/jbm.2014.36. URL http://www.jbmethods.org/jbm/article/view/36http://www.ncbi.nlm.nih.gov/pubmed/25606571http://www.pubmedcentral.nih.gov/articlerender.fcgi?artid=PMC4297649.

L. Eichinger, J. A. Pachebat, G. Glöckner, M.-A. Rajandream, R. Sucgang, M. Berriman, J. Song, R. Olsen, K. Szafranski, Q. Xu, B. Tunggal, S. Kummerfeld, M. Madera, B. A. Konfortov, F. Rivero, A. T. Bankier, R. Lehmann, N. Hamlin, R. Davies, P. Gaudet, P. Fey, K. Pilcher, G. Chen, D. Saunders, E. Sodergren, P. Davis, A. Kerhornou, X. Nie, N. Hall, C. Anjard, L. Hemphill, N. Bason, P. Farbrother, B. Desany, E. Just, T. Morio, R. Rost, C. Churcher, J. Cooper, S. Haydock, N. Van Driessche, A. Cronin, I. Goodhead, D. Muzny, T. Mourier, A. Pain, M. Lu, D. Harper, R. Lindsay, H. Hauser, K. James, M. Quiles, M. Madan Babu, T. Saito, C. Buchrieser, A. Wardroper, M. Felder, M. Thangavelu, D. Johnson, A. Knights, H. Loulseged, K. Mungall, K. Oliver, C. Price, M. A. Quail, H. Urushihara, J. Hernandez, E. Rabbinowitsch, D. Steffen, M. Sanders, J. Ma, W. F. Loomis, M. Platzer, R. R. Kay, J. Williams, P. H. Dear, A. A. Noegel, B. Barrell, and A. Kuspa. The genome of the social amoeba Dictyostelium discoideum. Technical Report 7038, 2005. URL https://www.ncbi.nlm.nih.gov/pmc/articles/PMC1352341/pdf/nihms4715.pdf.

R. A. Entwistle, R. D. Winefield, T. B. Foland, G. H. Lushington, and R. H. Himes. The paclitaxel site in tubulin probed by site-directed mutagenesis of Saccharomyces cerevisiae β-tubulin. *FEBS Letters*, 582(16): 2467–2470, jul 2008. ISSN 00145793. doi: 10.1016/j.febslet.2008.06.

013. URL /pmc/articles/PMC2577837/?report=abstracthttps://www.ncbi.nlm.nih.gov/pmc/articles/PMC2577837/.

A. Errico, A. Ballabio, and E. I. Rugarli. Spastin, the protein mutated in autosomal dominant hereditary spastic paraplegia, is involved in microtubule dynamics. *Hum Mol Genet*, 11(2):153–163, 2002. ISSN 0964-6906 (Print) 0964-6906 (Linking). URL http://www.ncbi.nlm.nih.gov/pubmed/11809724.

U. Euteneuer, R. Gräf, E. Kube-Granderath, and M. Schliwa. Dictyostelium gamma-tubulin: molecular characterization and ultrastructural localization — Journal of Cell Science, 1998. URL https://jcs.biologists.org/content/111/3/405.short.

K. J. Evans, E. R. Gomes, S. M. Reisenweber, G. G. Gundersen, and B. P. Lauring. Linking axonal degeneration to microtubule remodeling by Spastin-mediated microtubule severing. *Journal of Cell Biology*, 168(4):599–606, feb 2005. ISSN 00219525. doi: 10.1083/jcb.200409058.

J.-C. Farré and S. Subramani. Mechanistic insights into selective autophagy pathways: lessons from yeast. *Nature Publishing Group*, 2016. doi: 10.1038/nrm.2016.74. URL www.nature.com/nrm.

T. Frickey and A. N. Lupas. Phylogenetic analysis of AAA proteins. In *Journal of Structural Biology*, volume 146, pages 2–10. Academic Press, apr 2004. doi: 10.1016/j.jsb.2003.11.020.

A. Fujita, T. Higashijima, H. Shirozu, H. Masuda, M. SOnoda, J. Tohyama, M. Kato, M. Nakashima, Y. Tsurusaki, S. Mitsuhashi, T. Mizuguchi, A. Takata, S. Miyatake, N. Miyake, M. Fukuda, S. Kameyama, H. Saitsu, and N. Matsumoto. Pathogenic variants of DYNC2H1, KIAA0556, and PTPN11 associated with hypothalamic hamartoma. *Neurology*, 2019.

C. P. Garnham and A. Roll-Mecak. The chemical complexity of cellular microtubules: Tubulin post-translational modification enzymes and their roles in tuning microtubule functions, jul 2012. ISSN 19493584. URL https:

//www.onlinelibrary.wiley.com/doi/full/10.1002/cm.21027https://www.onlinelibrary.wiley.com/doi/abs/10.1002/cm.21027https://onlinelibrary.wiley.com/doi/10.1002/cm.21027.

I. R. Gibbons and A. J. Rowe. Dynein: A protein with adenosine triphosphatase activity from cilia. *Science*, 149(3682):424–426, jul 1965. ISSN 00368075. doi: 10.1126/science.149.3682.424. URL https://science.sciencemag.org/content/149/3682/424https://science.sciencemag.org/content/149/3682/424.abstract.

P. Gönczy and G. N. Hatzopoulos. Centriole assembly at a glance, feb 2019. ISSN 14779137.

D. Gotthardt, H. J. Warnatz, O. Henschel, F. Brückert, M. Schleicher, and T. Soldati. High-resolution dissection of phagosome maturation reveals distinct membrane trafficking phases. *Molecular Biology of the Cell*, 13(10): 3508–3520, oct 2002. ISSN 10591524. doi: 10.1091/mbc.E02-04-0206. URL https://www.molbiolcell.org/doi/abs/10.1091/mbc.e02-04-0206.

M. W. Gramlich, L. Conway, W. H. Liang, J. A. Labastide, S. J. King, J. Xu, and J. L. Ross. Single molecule investigation of kinesin-1 motility using engineered microtubule defects. *Scientific Reports*, 7, mar 2017. ISSN 20452322. doi: 10.1038/srep44290.

K. Gull. Protist tubulins: new arrivals, evolutionary relationships and insights to cytoskeletal function. Technical report, 2001.

F. Guo, X. Liu, H. Cai, and W. Le. Autophagy in neurodegenerative diseases: pathogenesis and therapy, jan 2018. ISSN 17503639.

M. G. Gutierrez, S. S. Master, S. B. Singh, G. A. Taylor, M. I. Colombo, and V. Deretic. Autophagy is a defense mechanism inhibiting BCG and Mycobacterium tuberculosis survival in infected macrophages. *Cell*, 119(6): 753–766, dec 2004. ISSN 00928674. doi: 10.1016/j.cell.2004.11.038.

M. Hagedorn, E. M. Neuhaus, and T. Soldati. Optimized fixation and immunofluorescence staining methods for Dictyostelium cells. *Methods in molecular biology (Clifton, N.J.)*, 346:327–338, 2006. ISSN 10643745. doi: 10.1385/1-59745-144-4:327. URL https://pubmed.ncbi.nlm.nih.gov/16957300/.

H. T. Haigler, J. A. McKanna, and S. Cohen. Rapid stimulation of pinocytosis in human carcinoma cells A-431 by epidermal growth factor. *Journal of Cell Biology*, 83(1):82–90, oct 1979. ISSN 00219525. doi: 10.1083/jcb.83.1.82.

R. E. Harrison, C. Bucci, O. V. Vieira, T. A. Schroer, and S. Grinstein. Phagosomes Fuse with Late Endosomes and/or Lysosomes by Extension of Membrane Protrusions along Microtubules: Role of Rab7 and RILP. *Molecular and Cellular Biology*, 23(18):6494–6506, sep 2003. ISSN 0270-7306. doi: 10.1128/mcb.23.18.6494-6506.2003. URL https://mcb.asm.org/content/23/18/6494https://mcb.asm.org/content/23/18/6494.abstract.

T. Hawkins, M. Mirigian, M. Selcuk Yasar, and J. L. Ross. Mechanics of microtubules. *Journal of Biomechanics*, 43(1):23–30, jan 2010. ISSN 00219290. doi: 10.1016/j.jbiomech.2009.09.005.

J. Hazan, N. Fonknechten, D. Mavel, C. Paternotte, D. Samson, F. Artiguenave, C. S. Davoine, C. Cruaud, A. Dürr, P. Wincker, P. Brottier, L. Cattolico, V. Barbe, J. M. Burgunder, J. F. Prud'homme, A. Brice, B. Fontaine, R. Heilig, and J. Weissenbach. Spastin, a new AAA protein, is altered in the most frequent form of autosomal dominant spastic paraplegia. *Nature Genetics*, 23(3):296–303, 1999. ISSN 10614036. doi: 10.1038/15472. URL https://www.nature.com/articles/ng1199{_}296.

N. Hirokawa. Kinesin and dynein superfamily proteins and the mechanism of organelle transport, jan 1998. ISSN 00368075. URL https://science.sciencemag.org/content/279/5350/519https://science.sciencemag.org/content/279/5350/519.abstract.

M. A. Hoyt, L. Totis, and B. T. Roberts. S. cerevisiae Genes Required for Cell

Cycle Arrest in Response to Loss of Microtubule Function. Technical report, 1991.

C. Hubbert, A. Guardiola, R. Shao, Y. Kawaguchi, A. Ito, A. Nixon, M. Yoshida, X. F. Wang, and T. P. Yao. HDAC6 is a microtubule-associated deacetylase. *Nature*, 417(6887):455–458, may 2002. ISSN 00280836. doi: 10.1038/417455a. URL `https://www.nature.com/articles/417455a`.

T. J. Itoh and H. Hotani. Microtubule-Stabilizing Activity of Microtubule-Associated Proteins (MAPs) Is Due to Increase in Frequency of Rescue in Dynamic Instability: Shortening Length Decreases with Binding of MAPs onto Microtubules. *Cell Structure and Function*, 19(5):279–290, 1994. ISSN 1347-3700. doi: 10.1247/csf.19.279. URL `http://joi.jlc.jst.go.jp/JST.Journalarchive/csf1975/19.279?from=CrossRef`.

H. Jambor, S. Mueller, S. L. Bullock, and A. Ephrussi. A stem-loop structure directs oskar mRNA to microtubule minus ends. *RNA*, 20(4):429–439, 2014. ISSN 14699001. doi: 10.1261/rna.041566.113.

I. Jordens, M. Fernandez-Borja, M. Marsman, S. Dusseljee, L. Janssen, J. Calafat, H. Janssen, R. Wubbolts, and J. Neefjes. The Rab7 effector protein RILP controls lysosomal transport by inducing the recruitment of dynein-dynactin motors. *Current Biology*, 11(21):1680–1685, oct 2001. ISSN 09609822. doi: 10.1016/S0960-9822(01)00531-0.

R. J. K. Jr and R. C. Williams. Microtubule-associated protein 2 alters the dynamic properties of microtubule assembly and disassembly., 1993. URL `https://www.jbc.org/content/268/13/9847.short`.

M. Jucker and L. C. Walker. Self-propagation of pathogenic protein aggregates in neurodegenerative diseases, sep 2013. ISSN 00280836. URL `https://www.nature.com/articles/nature12481`.

N. Kalebic, S. Sorrentino, E. Perlas, G. Bolasco, C. Martinez, and P. A. Heppenstall. αTAT1 is the major α-tubulin acetyltransferase in

mice. *Nature Communications*, 4(1):1962, oct 2013. ISSN 2041-1723. doi: 10.1038/ncomms2962. URL http://www.ncbi.nlm.nih.gov/pubmed/23748901http://www.nature.com/articles/ncomms2962.

R. Kang, H. J. Zeh, M. T. Lotze, and D. Tang. The Beclin 1 network regulates autophagy and apoptosis, apr 2011. ISSN 13509047. URL https://www.nature.com/articles/cdd2010191.

L. C. Kapitein and C. C. Hoogenraad. Building the Neuronal Microtubule Cytoskeleton, aug 2015. ISSN 10974199.

M. Katoh, G. Chen, E. Roberge, G. Shaulsky, and A. Kuspa. Developmental commitment in Dictyostelium discoideum. *Eukaryotic Cell*, 6(11):2038–2045, nov 2007. ISSN 15359778. doi: 10.1128/EC.00223-07. URL https://ec.asm.org/content/6/11/2038https://ec.asm.org/content/6/11/2038.abstract.

K. Kawaguchi. Energetics of kinesin-1 stepping mechanism. *FEBS Letters*, 582 (27):3719–3722, nov 2008. ISSN 0014-5793. doi: 10.1016/j.febslet.2008.10.019.

M. C. Kerr and R. D. Teasdale. Defining macropinocytosis, apr 2009. ISSN 13989219. URL https://onlinelibrary.wiley.com/doi/full/10.1111/j.1600-0854.2009.00878.xhttps://onlinelibrary.wiley.com/doi/abs/10.1111/j.1600-0854.2009.00878.xhttps://onlinelibrary.wiley.com/doi/10.1111/j.1600-0854.2009.00878.x.

N. V. Khobrekar, S. Quintremil, T. J. Dantas, and R. B. Vallee. The Dynein Adaptor RILP Controls Neuronal Autophagosome Biogenesis, Transport, and Clearance. *Developmental Cell*, 53(2):141–153.e4, apr 2020. ISSN 18781551. doi: 10.1016/j.devcel.2020.03.011.

R. Kikuno, T. Nagase, M. Nakayama, H. Koga, N. Okazaki, D. Nakajima, and O. Ohara. HUGE: a database for human KIAA proteins, a 2004 update integrating HUGEppi and ROUGE. *Nucleic acids research*, 1(32):D502–D504,

2004. doi: 10.1093/nar/gkh035. URL http://www.kazusa.or.jp/huge/ppihttp://www.kazusa.or.jp/rouge.

M. Kimble, C. Kuzmiak, K. N. McGovern, and E. L. de Hostos. Microtubule organization and the effects of GFP-tubulin expression in Dictyostelium discoideum. *Cell Motility and the Cytoskeleton*, 47(1):48–62, 2000. ISSN 0886-1544. doi: Doi10.1002/1097-0169(200009)47:1⟨48::Aid-Cm5⟩3.0.Co;2-Q.

J. S. King, D. M. Veltman, and R. H. Insall. The induction of autophagy by mechanical stress. *Autophagy*, 7(12):1490–1499, dec 2011. ISSN 15548635. doi: 10.4161/auto.7.12.17924. URL http://www.tandfonline.com/doi/abs/10.4161/auto.7.12.17924.

M. R. King and S. Petry. Phase separation of TPX2 enhances and spatially coordinates microtubule nucleation. *Nature Communications*, 11(1):1–13, dec 2020. ISSN 20411723. doi: 10.1038/s41467-019-14087-0. URL https://doi.org/10.1038/s41467-019-14087-0.

S. M. King. Integrated control of axonemal dynein AAA+ motors, aug 2012. ISSN 10478477.

T. Kirisako, Y. Ichimura, H. Okada, Y. Kabeya, N. Mizushima, T. Yoshimori, M. Ohsumi, T. Takao, T. Noda, and Y. Ohsumi. The reversible modification regulates the membrane-binding state of Apg8/Aut7 essential for autophagy and the cytoplasm to vacuole targeting pathway. *Journal of Cell Biology*, 151 (2):263–275, oct 2000. ISSN 00219525. doi: 10.1083/jcb.151.2.263.

D. Kitagawa, I. Vakonakis, N. Olieric, M. Hilbert, D. Keller, V. Olieric, M. Bortfeld, M. C. Erat, I. Flückiger, P. Gönczy, and M. O. Steinmetz. Structural basis of the 9-fold symmetry of centrioles. *Cell*, 144(3):364–375, feb 2011. ISSN 00928674. doi: 10.1016/j.cell.2011.01.008.

T. Kitanishi, H. Shibaoka, and Y. Fukui. Disruption of Microtubules and Retardation of Development of Dictyostelium with Ethyl N-Phenylcarbamate and Thiabendazole. Technical report, 1984.

D. J. Klionsky, J. M. Cregg, W. A. Dunn, and S. D. Emr. A Unified Nomenclature for Yeast Autophagy-Related Genes. Technical report, 2003.

D. R. Klopfenstein, E. A. Holleran, and R. D. Vale. Kinesin motors and microtubule-based organelle transport in Dictyostelium discoideum, 2002. ISSN 01424319. URL https://link.springer.com/article/10.1023/A:1024403006680.

K. V. Koch, Y. Reinders, T. H. Ho, A. Sickmann, and R. Gräf. Identification and isolation of Dictyostelium microtubule-associated protein interactors by tandem affinity purification. *European Journal of Cell Biology*, 85(9-10):1079–1090, sep 2006. ISSN 01719335. doi: 10.1016/j.ejcb.2006.05.008.

R. Köchl, X. W. Hu, E. Y. Chan, and S. A. Tooze. Microtubules facilitate autophagosome formation and fusion of autophagosomes with endosomes. *Traffic*, 7(2):129–145, feb 2006. ISSN 13989219. doi: 10.1111/j.1600-0854.2005.00368.x. URL http://www.ncbi.nlm.nih.gov/pubmed/16420522.

J. M. Kollman, A. Merdes, L. Mourey, and D. A. Agard. Microtubule nucleation by γ-tubulin complexes, nov 2011. ISSN 14710072.

M. Kollmar and G. Glöckner. Identification and phylogenetic analysis of Dictyostelium discoideum kinesin proteins, nov 2003. ISSN 14712164. URL https://link.springer.com/articles/10.1186/1471-2164-4-47https://link.springer.com/article/10.1186/1471-2164-4-47.

M. P. Koonce. Dictyostelium, a model organism for microtubule based transport. *Protist*, 151:17–25, 2000.

M. P. Koonce. 13 Plus 1: A 30-Year Perspective on Microtubule-Based Motility in Dictyostelium. *Cells*, 9(3):528, feb 2020. ISSN 2073-4409. doi: 10.3390/cells9030528. URL https://www.mdpi.com/2073-4409/9/3/528.

M. P. Koonce and A. Khodjakov. Dynamic microtubules in Dictyostelium. *J Muscle Res Cell Motil*, 23(7-8):613–619, 2002. ISSN 0142-4319 (Print) 0142-4319 (Linking). URL http://www.ncbi.nlm.nih.gov/pubmed/12952060.

M. P. Koonce and D. A. Knecht. Cytoplasmic dynein heavy chain is an essential gene product in Dictyostelium. *Cell Motility and the Cytoskeleton*, 39(1):63–72, jan 1998. ISSN 1097-0169. doi: 10.1002/(SICI)1097-0169(1998)39:1⟨63::AID-CM6⟩3.0.CO;2-H. URL https://onlinelibrary.wiley.com/doi/full/10.1002/{%}28SICI{%}291097-0169{%}281998{%}2939{%}3A1{%}3C63{%}3A{%}3AAID-CM6{%}3E3.0.CO{%}3B2-Hhttps://onlinelibrary.wiley.com/doi/abs/10.1002/{%}28SICI{%}291097-0169{%}281998{%}2939{%}3A1{%}3C63{%}3A{%}3AAID-CM6{%}3E3.0.CO{%}3B2-Hhttps://onlinelibrar.

V. I. Korolchuk, S. Saiki, M. Lichtenberg, F. H. Siddiqi, E. A. Roberts, S. Imarisio, L. Jahreiss, S. Sarkar, M. Futter, F. M. Menzies, C. J. O'Kane, V. Deretic, and D. C. Rubinsztein. Lysosomal positioning coordinates cellular nutrient responses. *Nature Cell Biology*, 13(4):453–462, apr 2011. ISSN 14657392. doi: 10.1038/ncb2204.

A. Kosta, C. Roisin-Bouffay, M. F. Luciani, G. P. Otto, R. H. Kessin, and P. Golstein. Autophagy gene disruption reveals a non-vacuolar cell death pathway in Dictyostelium. *Journal of Biological Chemistry*, 279(46): 48404–48409, nov 2004. ISSN 00219258. doi: 10.1074/jbc.M408924200. URL http://www.jbc.org/content/279/46/48404.fullhttp://www.jbc.org/content/279/46/48404http://www.jbc.org/content/279/46/48404.abstract/content/279/46/48404.short.

F. M. K.P. McNally, O.A. Bazirgan. Two domains of p80 katanin regulate microtubule severing and spindle pole targeting by p60 katanin — Journal of Cell Science, 2000. URL https://jcs.biologists.org/content/113/9/1623.short.

B. Lacroix, J. van Dijk, N. D. Gold, J. Guizetti, G. Aldrian-Herrada, K. Rogowski, D. W. Gerlich, and C. Janke. Tubulin polyglutamylation stimulates spastin-mediated microtubule severing. *J Cell Biol*, 189(6):945–954, 2010. ISSN 1540-8140 (Electronic) 0021-

9525 (Linking). doi: 10.1083/jcb.201001024. URL internal-pdf://5.136.53.177/Lacroix-2010-Tubulinpolyglutamyl.pdfhttp://www.ncbi.nlm.nih.gov/pubmed/20530212http://jcb.rupress.org/content/jcb/189/6/945.full.pdf.

G. Laevsky and D. A. Knecht. Under-agarose folate chemotaxis of Dictyostelium discoideum amoebae in permissive and mechanically inhibited conditions. *BioTechniques*, 31(5):1140–1149, 2001. ISSN 07366205. doi: 10.2144/01315rr03. URL https://pubmed.ncbi.nlm.nih.gov/11730020/.

H. Lataste, V. Senilh, M. Wright, D. Guénard, and P. Potier. Relationships between the structures of taxol and baccatine III derivatives and their in vitro action on the disassembly of mammalian brain and Physarum amoebal microtubules. *Proceedings of the National Academy of Sciences of the United States of America*, 81(13 I):4090–4094, 1984. ISSN 00278424. doi: 10.1073/pnas.81.13.4090. URL /pmc/articles/PMC345374/?report=abstracthttps://www.ncbi.nlm.nih.gov/pmc/articles/PMC345374/.

E. J. Lawrence and M. Zanic. Rescuing microtubules from the brink of catastrophe: CLASPs lead the way, 2019. ISSN 18790410.

M. LeDizet and G. Piperno. Identification of an acetylation site of Chlamydomonas alpha-tubulin. *Proceedings of the National Academy of Sciences of the United States of America*, 84(16):5720–5724, aug 1987. ISSN 00278424. doi: 10.1073/pnas.84.16.5720. URL https://www.pnas.org/content/84/16/5720https://www.pnas.org/content/84/16/5720.abstract.

J. E. Lee, J. L. Silhavy, M. S. Zaki, J. Schroth, S. L. Bielas, S. E. Marsh, J. Olvera, F. Brancati, M. Iannicelli, K. Ikegami, A. M. Schlossman, B. Merriman, T. Attié-Bitach, C. V. Logan, I. A. Glass, A. Cluckey, C. M. Louie, J. H. Lee, H. R. Raynes, I. Rapin, I. P. Castroviejo, M. Setou, C. Barbot, E. Boltshauser, S. F. Nelson, F. Hildebrandt, C. A. Johnson, D. A. Doherty, E. M. Valente, and J. G. Gleeson. CEP41 is mutated in Joubert syndrome

and is required for tubulin glutamylation at the cilium. *Nature Genetics*, 44 (2):193–199, feb 2012. ISSN 10614036. doi: 10.1038/ng.1078.

B. Levine and G. Kroemer. Autophagy in the pathogenesis of disease. *Cell*, 132(1):27–42, jan 2008. ISSN 0092-8674. doi: 10.1016/j.cell.2007.12.018. URL http://www.ncbi.nlm.nih.gov/pubmed/18191218http://www.pubmedcentral.nih.gov/articlerender.fcgi?artid=PMC2696814.

S. W. L'Hernaul and J. L. Rosenbaum. Chlamydomonas α-Tubulin Is Posttranslationally Modified by Acetylation on the ϵ-Amino Group of a Lysine. *Biochemistry*, 24(2):473–478, jan 1985. ISSN 15204995. doi: 10.1021/bi00323a034. URL https://pubs.acs.org/doi/pdf/10.1021/bi00323a034.

W. W. Li, J. Li, and J. K. Bao. Microautophagy: Lesser-known self-eating, apr 2012. ISSN 1420682X. URL https://pubmed.ncbi.nlm.nih.gov/22080117/.

W. H. Liang, Q. Li, K. M. Rifat Faysal, S. J. King, A. Gopinathan, and J. Xu. Microtubule Defects Influence Kinesin-Based Transport in Vitro. *Biophysical Journal*, 110(10):2229–2240, may 2016. ISSN 15420086. doi: 10.1016/j.bpj.2016.04.029.

J. P. Lim and P. A. Gleeson. Macropinocytosis: an endocytic pathway for internalising large gulps. *Immunol Cell Biol*, 89(8):836–843, 2011. ISSN 1440-1711 (Electronic) 0818-9641 (Linking). doi: 10.1038/icb.2011.20. URL internal-pdf://121.40.145.196/Lim-2011-Macropinocytosis{_}an.pdfhttp://www.ncbi.nlm.nih.gov/pubmed/21423264http://www.nature.com/icb/journal/v89/n8/pdf/icb201120a.pdf.

S. J. Lord, K. B. Velle, R. Dyche Mullins, and L. K. Fritz-Laylin. SuperPlots: Communicating reproducibility and variability in cell biology, jun 2020. ISSN 15408140. URL https://doi.org/10.1083/jcb.202001064.

M. F. Luciani, C. Giusti, B. Harms, Y. Oshima, H. Kikuchi, Y. Kubohara, and P. Golstein. Atg1 allows second-signaled autophagic cell death in Dictyostelium. *Autophagy*, 7(5):501–508, 2011. ISSN 15548635. doi: 10.4161/auto.7.5.14957. URL https://www.tandfonline.com/doi/abs/10.4161/auto.7.5.14957.

J. J. Lum, D. E. Bauer, M. Kong, M. H. Harris, C. Li, T. Lindsten, and C. B. Thompson. Growth factor regulation of autophagy and cell survival in the absence of apoptosis. *Cell*, 120(2):237–248, jan 2005. ISSN 00928674. doi: 10.1016/j.cell.2004.11.046.

S. Maday and E. L. Holzbaur. Autophagosome biogenesis in primary neurons follows an ordered and spatially regulated pathway. *Developmental Cell*, 30 (1):71–85, jul 2014. ISSN 18781551. doi: 10.1016/j.devcel.2014.06.001.

M. M. Magiera and C. Janke. Post-translational modifications of tubulin. *Curr Biol*, 24(9):R351–4, 2014. ISSN 1879-0445 (Electronic) 0960-9822 (Linking). doi: 10.1016/j.cub.2014.03.032. URL http://www.ncbi.nlm.nih.gov/pubmed/24801181.

H. Maiato, A. Khodjakov, and C. L. Rieder. Drosophila CLASP is required for the incorporation of microtubule subunits into fluxing kinetochore fibres. *Nature Cell Biology*, 7(1):42–47, jan 2005. ISSN 14657392. doi: 10.1038/ncb1207. URL https://www.nature.com/articles/ncb1207.

M. C. Maiuri, E. Zalckvar, A. Kimchi, and G. Kroemer. Self-eating and self-killing: Crosstalk between autophagy and apoptosis, sep 2007. ISSN 14710072. URL https://www.nature.com/articles/nrm2239https://www.nature.com/articles/nrm2239/.

L. Malinovska, S. Palm, K. Gibson, J. M. Verbavatz, and S. Alberti. Dictyostelium discoideum has a highly Q/N-rich proteome and shows an unusual resilience to protein aggregation. *Proceedings of the National Academy of Sciences of the United States of America*, 112(20):E2620–E2629, may 2015. ISSN

10916490. doi: 10.1073/pnas.1504459112. URL www.pnas.org/cgi/doi/10.1073/pnas.1504459112.

C. X. Mao, X. Wen, S. Jin, and Y. Q. Zhang. Increased acetylation of microtubules rescues human tau-induced microtubule defects and neuromuscular junction abnormalities in Drosophila. *Dis Model Mech*, 10(10):1245–1252, 2017. ISSN 1754-8411 (Electronic) 1754-8403 (Linking). doi: 10.1242/dmm.028316. URL https://www.ncbi.nlm.nih.gov/pubmed/28819043.

M. Mari, J. Griffith, E. Rieter, L. Krishnappa, D. J. Klionsky, and F. Reggiori. An Atg9-containing compartment that functions in the early steps of autophagosome biogenesis. *Journal of Cell Biology*, 190(6):1005–1022, sep 2010. ISSN 00219525. doi: 10.1083/jcb.200912089. URL /pmc/articles/PMC3101592/?report=abstracthttps://www.ncbi.nlm.nih.gov/pmc/articles/PMC3101592/.

R. T. Marquez and L. Xu. Bcl-2:Beclin 1 complex: multiple, mechanisms regulating autophagy/apoptosis toggle switch. *American journal of cancer research*, 2(2):214–21, feb 2012. ISSN 2156-6976. URL http://www.ncbi.nlm.nih.gov/pubmed/22485198http://www.pubmedcentral.nih.gov/articlerender.fcgi?artid=PMC3304572.

R. Mathew, S. Kongara, B. Beaudoin, C. M. Karp, K. Bray, K. Degenhardt, G. Chen, S. Jin, and E. White. Autophagy suppresses tumor progression by limiting chromosomal instability. *Genes and Development*, 21(11):1367–1381, jun 2007. ISSN 08909369. doi: 10.1101/gad.1545107. URL http://genesdev.cshlp.org/content/21/11/1367.fullhttp://genesdev.cshlp.org/content/21/11/1367http://genesdev.cshlp.org/content/21/11/1367.abstract.

K. Matsunaga, E. Morita, T. Saitoh, S. Akira, N. T. Ktistakis, T. Izumi, T. Noda, and T. Yoshimori. Autophagy requires endoplasmic reticulum targeting of the PI3-kinase complex via Atg14L. *Journal of Cell Biology*, 190(4):511–521, aug 2010. ISSN 00219525. doi: 10.1083/jcb.200911141.

G. McCaffrey and R. Vale. Identification of a kinesin-like microtubule-based motor protein in Dictyostelium discoideum. *The EMBO Journal*, 8(11):3229–3234, nov 1989. ISSN 02614189. doi: 10.1002/j.1460-2075.1989.tb08482.x. URL http://doi.wiley.com/10.1002/j.1460-2075.1989.tb08482.x.

J. R. McIntosh and M. P. Koonce. Mitosis. *Science*, 246(4930): 622–628, nov 1989. ISSN 00368075. doi: 10.1126/science.2683078. URL https://science.sciencemag.org/content/246/4930/622https://science.sciencemag.org/content/246/4930/622.abstract.

F. J. McNally and R. D. Vale. Identification of katanin, an ATPase that severs and disassembles stable microtubules. *Cell*, 75(3):419–429, nov 1993. ISSN 00928674. doi: 10.1016/0092-8674(93)90377-3.

F. M. Menzies, A. Fleming, and D. C. Rubinsztein. Compromised autophagy and neurodegenerative diseases. *Nature Reviews Neuroscience*, 16(6):345–357, jun 2015. ISSN 1471-003X. doi: 10.1038/nrn3961. URL http://www.ncbi.nlm.nih.gov/pubmed/25991442http://www.nature.com/articles/nrn3961.

A. Mesquita, J. Calvo-Garrido, S. Carilla-Latorre, and R. Escalante. Monitoring Autophagy in Dictyostelium. In *Methods in molecular biology (Clifton, N.J.)*, volume 983, pages 461–470. Methods Mol Biol, 2013. doi: 10.1007/978-1-62703-302-2_26.

A. Mesquita, E. Cardenal-Muñoz, E. Dominguez, S. Muñoz-Braceras, B. Nuñez-Corcuera, B. A. Phillips, L. C. Tábara, Q. Xiong, R. Coria, L. Eichinger, P. Golstein, J. S. King, T. Soldati, O. Vincent, and R. Escalante. Autophagy in Dictyostelium: Mechanisms, regulation and disease in a simple biomedical model. *Autophagy*, 13(1):24–40, 2017. ISSN 15548635. doi: 10.1080/15548627.2016.1226737.

S. Millecamps and J. P. Julien. Axonal transport deficits and neurodegenerative diseases, mar 2013. ISSN 1471003X. URL www.nature.com/reviews/neuro.

T. Mitchison and M. Kirschner. Dynamic instability of microtubule growth. *Nature*, 312(5991):237–242, nov 1984. ISSN 0028-0836. doi: 10.1038/312237a0. URL http://www.ncbi.nlm.nih.gov/pubmed/6504138http://www.nature.com/articles/312237a0.

N. Mizushima. Autophagy: Process and function, nov 2007. ISSN 08909369. URL http://genesdev.cshlp.org/content/21/22/2861.fullhttp://genesdev.cshlp.org/content/21/22/2861http://genesdev.cshlp.org/content/21/22/2861.abstract.

P. B. Moens. Spindle and kinetochore morphology of Dictyostelium Discoideum. *Journal of Cell Biology*, 68(1):113–122, jan 1976. ISSN 15408140. doi: 10.1083/jcb.68.1.113. URL https://rupress.org/jcb/article-pdf/68/1/113/451338/113.pdf.

N. Mohan, E. M. Sorokina, I. V. Verdeny, A. S. Alvarez, and M. Lakadamyali. Detyrosinated microtubules spatially constrain lysosomes facilitating lysosome–autophagosome fusion. *The Journal of Cell Biology*, 218(2):632–643, feb 2019. ISSN 0021-9525. doi: 10.1083/JCB.201807124. URL http://jcb.rupress.org/content/218/2/632/tab-figures-data.

A. Musacchio and E. D. Salmon. The spindle-assembly checkpoint in space and time, may 2007. ISSN 14710072. URL www.nature.com/reviews/molcellbio.

S. Nagata, J. Suzuki, K. Segawa, and T. Fujii. Exposure of phosphatidylserine on the cell surface, jun 2016. ISSN 14765403. URL https://www.nature.com/articles/cdd20167.

S. Nakamura and T. Yoshimori. New insights into autophagosome-lysosome fusion, apr 2017. ISSN 14779137.

A. C. Nascimbeni, P. Codogno, and E. Morel. Phosphatidylinositol[U+2010]3[U+2010]phosphate in the regulation of autophagy membrane dynamics. *The FEBS Journal*, 284(9):1267–1278, may 2017. ISSN

1742-4658. doi: 10.1111/FEBS.13987@10.1111/(ISSN)1742-4658.112. URL https://febs.onlinelibrary.wiley.com/doi/full/10.1111/febs.13987{%}4010.1111/{%}28ISSN{%}291742-4658.112https://febs.onlinelibrary.wiley.com/doi/abs/10.1111/febs.13987{%}4010.1111/{%}28ISSN{%}291742-4658.112https://febs.onlinelibrary.wiley.com/doi/10.1111/febs.1398.

M. Niceta, M. L. Dentici, A. Ciolfi, R. Marini, S. Barresi, F. R. Lepri, A. Novelli, E. Bertini, M. Cappa, M. C. Digilio, B. Dallapiccola, and M. Tartaglia. Co-occurrence of mutations in KIF7 and KIAA0556 in Joubert syndrome with ocular coloboma, pituitary malformation and growth hormone deficiency: A case report and literature review. *BMC Pediatrics*, 20(1):1–9, mar 2020. ISSN 14712431. doi: 10.1186/s12887-020-2019-0. URL https://link.springer.com/articles/10.1186/s12887-020-2019-0https://link.springer.com/article/10.1186/s12887-020-2019-0.

E. Nogales, M. Whittaker, R. A. Milligan, and K. H. Downing. High-resolution model of the microtubule. *Cell*, 96(1):79–88, jan 1999. ISSN 00928674. doi: 10.1016/S0092-8674(00)80961-7.

P. M. Novikoff, A. B. Novikoff, N. Quintana, and J. J. Hauw. Golgi apparatus, gerl, and lysosomes of neurons in rat dorsal root ganglia, studied by thick section and thin section cytochemistry. *Journal of Cell Biology*, 50(3):859–886, sep 1971. ISSN 15408140. doi: 10.1083/jcb.50.3.859.

B. R. Oakley, V. Paolillo, and Y. Zheng. γ-tubulin complexes in microtubule nucleation and beyond. *Molecular Biology of the Cell*, 26(17):2957–2962, sep 2015. ISSN 19394586. doi: 10.1091/mbc.E14-11-1514.

C. E. Oakley and B. R. Oakley. Identification of γ-tubulin, a new member of the tubulin superfamily encoded by mipA gene of Aspergillus nidulans. *Nature*, 338(6217):662–664, 1989. ISSN 00280836. doi: 10.1038/338662a0. URL https://www.nature.com/articles/338662a0.

O. Ohara, T. Nagase, K.-I. Ishikawa, D. Nakajima, M. Ohira, N. Seki, and N. Nomura. Construction and Characterization of Human Brain cDNA Libraries Suitable for Analysis of cDNA Clones Encoding Relatively Large Proteins. Technical report, 1997. URL https://academic.oup.com/dnaresearch/article-abstract/4/1/53/372236.

F. Omura and Y. Fukui. Nt0TON SNI Dictyostelium MTOC: Structure and Linkage to the Nucleus. Technical report, 1985.

G. P. Otto, M. Y. Wu, N. Kazgan, O. R. Anderson, and R. H. Kessin. Macroautophagy is required for multicellular development of the social amoeba Dictyostelium discoideum. *Journal of Biological Chemistry*, 278(20):17636–17645, may 2003. ISSN 00219258. doi: 10.1074/jbc.M212467200.

G. P. Otto, M. Y. Wu, M. Clarke, H. Lu, O. Roger Anderson, H. Hilbi, H. A. Shuman, and R. H. Kessin. Macroautophagy is dispensable for intracellular replication of Legionella pneumophila in Dictyostelium discoideum, jan 2004. ISSN 0950382X. URL https://onlinelibrary.wiley.com/doi/full/10.1046/j.1365-2958.2003.03826.xhttps://onlinelibrary.wiley.com/doi/abs/10.1046/j.1365-2958.2003.03826.xhttps://onlinelibrary.wiley.com/doi/10.1046/j.1365-2958.2003.03826.x.

S. Paglin, T. Hollister, T. Delohery, N. Hackett, M. McMahill, E. Sphicas, D. Domingo, and J. Yahalom. A novel response of cancer cells to radiation involves autophagy and formation of acidic vesicles. *Cancer Research*, 61(2):439–444, jan 2001. ISSN 00085472. URL http://cancerres.aacrjournals.org/cgi/content/full/61/2/439https://europepmc.org/article/med/11212227.

M. Pan, X. Xu, Y. Chen, and T. Jin. Identification of a Chemoattractant G-Protein-Coupled Receptor for Folic Acid that Controls Both Chemotaxis and Phagocytosis. *Developmental cell*, 36(4):428–39, feb 2016. ISSN 1878-1551. doi: 10.1016/j.devcel.2016.01.

012. URL http://www.ncbi.nlm.nih.gov/pubmed/26906738http://www.pubmedcentral.nih.gov/articlerender.fcgi?artid=PMC4768320.

I. Y. Park, P. Chowdhury, D. N. Tripathi, R. T. Powell, R. Dere, E. A. Terzo, W. K. Rathmell, and C. L. Walker. Methylated α-tubulin antibodies recognize a new microtubule modification on mitotic microtubules. *mAbs*, 8(8): 1590–1597, nov 2016. ISSN 1942-0862. doi: 10.1080/19420862.2016.1228505. URL https://www.tandfonline.com/doi/full/10.1080/19420862.2016.1228505.

V. R. Pollock N, Koonce MP, de Hostos EL. In vitro microtubule[U+2010]based organelle transport in wild[U+2010]type Dictyostelium and cells overexpressing a truncated dynein heavy chain. *Cytoskeleton*, 40(3):304–314, 1998. URL https://onlinelibrary.wiley.com/doi/epdf/10.1002/{%}28SICI{%}291097-0169{%}281998{%}2940{%}3A3{%}3C304{%}3A{%}3AAID-CM8{%}3E3.0.CO{%}3B2-C.

H. Ponstingl, E. Krauhs, M. Little, and T. Kempf. Complete amino acid sequence of alpha-tubulin from porcine brain. *Proceedings of the National Academy of Sciences of the United States of America*, 78(5): 2757–2761, may 1981. ISSN 00278424. doi: 10.1073/pnas.78.5.2757. URL https://www.pnas.org/content/78/5/2757https://www.pnas.org/content/78/5/2757.abstract.

D. Portran, L. Schaedel, Z. J. Xu, M. Thery, and M. V. Nachury. Tubulin acetylation protects long-lived microtubules against mechanical ageing. *Nature Cell Biology*, 19(4):391–+, 2017. ISSN 1465-7392. doi: 10.1038/ncb3481.

S. Putzler, I. Meyer, and R. Gräf. CP91 is a component of the Dictyostelium centrosome involved in centrosome biogenesis. *European Journal of Cell Biology*, 95(3-5):124–135, mar 2016. ISSN 16181298. doi: 10.1016/j.ejcb.2016.03.001.

L. Qiang. Tau Protects Microtubules in the Axon from Severing by Katanin. *Journal of Neuroscience*, 26(12):3120–3129, 2006. ISSN 0270-6474. doi: 10.1523/jneurosci.5392-05.2006.

M. S. R. Graf, C. Daunderer. Dictyostelium DdCP224 is a microtubule-associated protein and a permanent centrosomal resident involved in centrosome duplication — Journal of Cell Science, 2000. URL https://jcs.biologists.org/content/113/10/1747.short.

A. Rai, D. Pathak, S. Thakur, S. Singh, A. K. Dubey, and R. Mallik. Dynein Clusters into Lipid Microdomains on Phagosomes to Drive Rapid Transport toward Lysosomes. *Cell*, 164(4):722–734, feb 2016. ISSN 10974172. doi: 10.1016/j.cell.2015.12.054.

M. J. Rale, R. S. Kadzik, and S. Petry. Phase Transitioning the Centrosome into a Microtubule Nucleator, jan 2018. ISSN 15204995. URL /pmc/articles/PMC6193265/?report=abstracthttps://www.ncbi.nlm.nih.gov/pmc/articles/PMC6193265/.

S. Ray, E. Meyhöfer, R. A. Milligan, and J. Howard. Kinesin follows the microtubule's protofilament axis. *Journal of Cell Biology*, 121(5):1083–1093, jun 1993. ISSN 00219525. doi: 10.1083/jcb.121.5.1083.

E. Reid, M. Kloos, A. Ashley-Koch, L. Hughes, S. Bevan, I. K. Svenson, F. L. Graham, P. C. Gaskell, A. Dearlove, M. A. Pericak-Vance, D. C. Rubinsztein, and D. A. Marchuk. A kinesin heavy chain (KIF5A) mutation in hereditary spastic paraplegia (SPG10). *American Journal of Human Genetics*, 71 (5):1189–1194, nov 2002. ISSN 00029297. doi: 10.1086/344210. URL http://www.cell.com/article/S0002929707604121/fulltexthttp://www.cell.com/article/S0002929707604121/abstracthttps://www.cell.com/ajhg/abstract/S0002-9297(07)60412-1.

G. C. Rogers, S. L. Rogers, and D. J. Sharp. Spindle microtubules in flux. *Journal of Cell Science*, 118(6):1105–1116, mar 2005. ISSN 00219533. doi: 10.1242/jcs.02284. URL https://jcs.biologists.org/content/118/6/1105https://jcs.biologists.org/content/118/6/1105.abstract.

A. Roll-Mecak and R. D. Vale. Structural basis of microtubule severing by

the hereditary spastic paraplegia protein spastin. *Nature*, 451(7176):363–367, jan 2008. ISSN 14764687. doi: 10.1038/nature06482. URL https://www.nature.com/articles/nature06482.

M. Romani, A. Micalizzi, and E. M. Valente. Joubert syndrome: Congenital cerebellar ataxia with the molar tooth, sep 2013. ISSN 14744422. URL http://dx.doi.org/10.1016/.

U. P. Roos, M. De Brabander, and J. De Mey. Indirect immunofluorescence of microtubules in Dictyostelium discoideum. A study with polyclonal and monoclonal antibodies to tubulins. *Experimental Cell Research*, 151(1):183–193, mar 1984. ISSN 00144827. doi: 10.1016/0014-4827(84)90367-7.

U.-P. Roos, M. De Brabander, and R. Nuydens. Movements of intracellular particles in undifferentiated amebae ofDictyostelium discoideum. *Cell Motility and the Cytoskeleton*, 7(3):258–271, jan 1987. ISSN 0886-1544. doi: 10.1002/cm.970070308. URL http://doi.wiley.com/10.1002/cm.970070308.

S. Roosing, R. O. Rosti, B. Rosti, E. de Vrieze, J. L. Silhavy, E. van Wijk, E. Wakeling, and J. G. Gleeson. Identification of a homozygous nonsense mutation in KIAA0556 in a consanguineous family displaying Joubert syndrome. *Human Genetics*, 135(8):919–921, aug 2016. ISSN 14321203. doi: 10.1007/s00439-016-1689-z. URL https://link.springer.com/article/10.1007/s00439-016-1689-z.

C. Rosales and E. Uribe-Querol. Phagocytosis: A Fundamental Process in Immunity. 2017. doi: 10.1155/2017/9042851. URL https://doi.org/10.1155/2017/9042851.

A. Rupper and J. Cardelli. Regulation of phagocytosis and endo-phagosomal trafficking pathways in Dictyostelium discoideum, mar 2001. ISSN 03044165.

M. Samereier, O. Baumann, I. Meyer, and R. Gräf. Analysis of Dictyostelium TACC reveals differential interactions with CP224 and unusual dynamics of

Dictyostelium microtubules. *Cellular and Molecular Life Sciences*, 68(2):275–287, jan 2011. ISSN 1420682X. doi: 10.1007/s00018-010-0453-0. URL https://pubmed.ncbi.nlm.nih.gov/20658257/.

C. Sánchez-Huertas, F. Freixo, R. Viais, C. Lacasa, E. Soriano, and J. Lüders. Non-centrosomal nucleation mediated by augmin organizes microtubules in post-mitotic neurons and controls axonal microtubule polarity. *Nature Communications*, 7(1):1–14, jul 2016. ISSN 20411723. doi: 10.1038/ncomms12187.

N. Sanchez-Soriano, M. Travis, F. Dajas-Bailador, C. Gonçalves-Pimentel, A. J. Whitmarsh, and A. Prokop. Mouse ACF7 and Drosophila Short stop modulate filopodia formation and microtubule organisation during neuronal growth. *Journal of Cell Science*, 122(14):2534–2542, jul 2009. ISSN 00219533. doi: 10.1242/jcs.046268.

A. A. W. M. Sanders, E. de Vrieze, A. M. Alazami, F. Alzahrani, E. B. Malarkey, N. Sorusch, L. Tebbe, S. Kuhns, T. J. P. van Dam, A. Alhashem, B. Tabarki, Q. Lu, N. J. Lambacher, J. E. Kennedy, R. V. Bowie, L. Hetterschijt, S. van Beersum, J. van Reeuwijk, K. Boldt, H. Kremer, R. A. Kesterson, D. Monies, M. Abouelhoda, R. Roepman, M. H. Huynen, M. Ueffing, R. B. Russell, U. Wolfrum, B. K. Yoder, E. van Wijk, F. S. Alkuraya, and O. E. Blacque. KIAA0556 is a novel ciliary basal body component mutated in Joubert syndrome. *Genome Biology*, 16 (1):293, dec 2015. ISSN 1474-760X. doi: 10.1186/s13059-015-0858-z. URL http://www.ncbi.nlm.nih.gov/pubmed/26714646http://www.pubmedcentral.nih.gov/articlerender.fcgi?artid=PMC4699358http://genomebiology.com/2015/16/1/293.

A. Sanger, Y. Y. Yip, T. S. Randall, S. Pernigo, R. A. Steiner, and M. P. Dodding. SKIP controls lysosome positioning using a composite kinesin-1 heavy and light chain-binding domain. *Journal of Cell Science*, 130(9):1637–1651, may 2017. ISSN 14779137. doi: 10.1242/jcs.198267. URL https://pubmed.ncbi.nlm.nih.gov/28302907/.

P. Satir. Studies on cilia. 3. Further studies on the cilium tip and a "sliding filament" model of ciliary motility. *The Journal of cell biology*, 39(1):77–94, oct 1968. ISSN 00219525. doi: 10.1083/jcb.39.1.77. URL https://rupress.org/jcb/article-pdf/39/1/77/445766/77.pdf.

N. Sattler, R. Monroy, and T. Soldati. Quantitative Analysis of Phagocytosis and Phagosome Maturation. pages 383–402. Humana Press, Totowa, NJ, 2013. doi: 10.1007/978-1-62703-302-2_21. URL http://link.springer.com/10.1007/978-1-62703-302-2{_}21.

L. Schaedel, K. John, J. Gaillard, M. V. Nachury, L. Blanchoin, and M. Thery. Microtubules self-repair in response to mechanical stress. *Nature Materials*, 14(11):1156–+, 2015. ISSN 1476-1122. doi: 10.1038/NMAT4396.

L. Schaedel, S. Triclin, D. Chrétien, A. Abrieu, C. Aumeier, J. Gaillard, L. Blanchoin, M. Théry, and K. John. Lattice defects induce microtubule self-renewal. *Nature Physics*, 15(8), 2019. ISSN 17452481. doi: 10.1038/s41567-019-0542-4.

A. H. Schapira. Mitochondrial disease, jul 2006. ISSN 01406736.

I. G. Scott, K. E. Åkerman, J. E. Heikkilä, K. Kaila, and L. C. Andersson. Development of a neural phenotype in differentiating ganglion cell[U+2010]derived human neuroblastoma cells. *Journal of Cellular Physiology*, 128(2):285–292, 1986. ISSN 10974652. doi: 10.1002/jcp.1041280221. URL https://pubmed.ncbi.nlm.nih.gov/3090056/.

R. Sekine, T. Kawata, and T. Muramoto. CRISPR/Cas9 mediated targeting of multiple genes in Dictyostelium. *Scientific reports*, 8(1): 8471, may 2018. ISSN 2045-2322. doi: 10.1038/s41598-018-26756-z. URL http://www.ncbi.nlm.nih.gov/pubmed/29855514http://www.pubmedcentral.nih.gov/articlerender.fcgi?artid=PMC5981456.

N. Sharma, J. Bryant, D. Wloga, R. Donaldson, R. C. Davis, M. Jerka-Dziadosz, and J. Gaertig. Katanin regulates dynamics of microtubules and biogenesis

of motile cilia. *Journal of Cell Biology*, 178(6):1065–1079, sep 2007. ISSN 00219525. doi: 10.1083/jcb.200704021. URL http://www.jcb.org/cgi/.

D. J. Sharp and J. L. Ross. Microtubule-severing enzymes at the cutting edge. *J Cell Sci*, 125(Pt 11):2561–2569, 2012. ISSN 1477-9137 (Electronic) 0021-9533 (Linking). doi: 10.1242/jcs.101139. URL internal-pdf://196.137.253.79/Sharp-2012-Microtubule-severing.pdfhttp://www.ncbi.nlm.nih.gov/pubmed/22595526http://jcs.biologists.org/content/joces/125/11/2561.full.pdf.

P. Shi, A. L. Ström, J. Gal, and H. Zhu. Effects of ALS-related SOD1 mutants on dynein- and KIF5-mediated retrograde and anterograde axonal transport. *Biochimica et Biophysica Acta - Molecular Basis of Disease*, 1802(9):707–716, sep 2010. ISSN 09254439. doi: 10.1016/j.bbadis.2010.05.008.

F. Solomon. Binding Sites for Calcium on Tubulin. *Biochemistry*, 16(3):358–363, feb 1977. ISSN 15204995. doi: 10.1021/bi00622a003. URL https://pubs.acs.org/doi/pdf/10.1021/bi00622a003.

J. M. Solowska, M. D'Rozario, D. C. Jean, M. W. Davidson, D. R. Marenda, and P. W. Baas. Pathogenic mutation of spastin has gain-of-function effects on microtubule dynamics. *Journal of Neuroscience*, 34(5):1856–1867, jan 2014. ISSN 15292401. doi: 10.1523/JNEUROSCI.3309-13.2014. URL https://www.jneurosci.org/content/34/5/1856https://www.jneurosci.org/content/34/5/1856.abstract.

C. D. Sorbara, N. E. Wagner, A. Ladwig, I. Nikić, D. Merkler, T. Kleele, P. Marinković, R. Naumann, L. Godinho, F. M. Bareyre, D. Bishop, T. Misgeld, and M. Kerschensteiner. Pervasive axonal transport deficits in multiple sclerosis models. *Neuron*, 84(6):1183–1190, dec 2014. ISSN 10974199. doi: 10.1016/j.neuron.2014.11.006.

J. E. Strassmann, Y. Zhu, and D. C. Queller. Altruism and social cheating in the social amoeba Dictyostelium discoideum. *Nature*, 408(6815):965–967, dec

2000. ISSN 00280836. doi: 10.1038/35050087. URL https://www.nature.com/articles/35050087.

H. Sudo and P. W. Baas. Acetylation of Microtubules Influences Their Sensitivity to Severing by Katanin in Neurons and Fibroblasts. *Journal of Neuroscience*, 30(21):7215–7226, 2010. ISSN 0270-6474. doi: 10.1523/jneurosci.0048-10.2010.

K. Sugawara, N. N. Suzuki, Y. Fujioka, N. Mizushima, Y. Ohsumi, and F. Inagaki. The crystal structure of microtubule-associated protein light chain 3, a mammalian homologue of Saccharomyces cerevisiae Atg8. *Genes to Cells*, 9 (7):611–618, jul 2004. ISSN 13569597. doi: 10.1111/j.1356-9597.2004.00750.x. URL https://onlinelibrary.wiley.com/doi/full/10.1111/j.1356-9597.2004.00750.xhttps://onlinelibrary.wiley.com/doi/abs/10.1111/j.1356-9597.2004.00750.xhttps://onlinelibrary.wiley.com/doi/10.1111/j.1356-9597.2004.00750.x.

J. A. Swanson and C. Watts. Macropinocytosis, nov 1995. ISSN 09628924.

A. Szyk, A. M. Deaconescu, J. Spector, B. Goodman, M. L. Valenstein, N. E. Ziolkowska, V. Kormendi, N. Grigorieff, and A. Roll-Mecak. Molecular basis for age-dependent microtubule acetylation by tubulin acetyltransferase. *Cell*, 157(6):1405–1415, jun 2014. ISSN 10974172. doi: 10.1016/j.cell.2014.03.061.

TheHumanProteinAltas. Tissue expression of KIAA0556 - Summary - The Human Protein Atlas. URL https://www.proteinatlas.org/ENSG00000047578-KIAA0556/tissue.

C. Thom and K. B. Raper. The Aspergillus Nidulans Group. *Mycologia*, 31(6):653–669, nov 1939. ISSN 0027-5514. doi: 10.1080/00275514.1939.12017382. URL https://www.tandfonline.com/doi/abs/10.1080/00275514.1939.12017382.

Y. Tian, Z. Li, W. Hu, H. Ren, E. Tian, Y. Zhao, Q. Lu, X. Huang, P. Yang, X. Li, X. Wang, A. L. Kovács, L. Yu, and H. Zhang. C. elegans Screen

Identifies Autophagy Genes Specific to Multicellular Organisms. *Cell*, 141(6): 1042–1055, jun 2010. ISSN 00928674. doi: 10.1016/j.cell.2010.04.034.

I. Tikhonenko, K. Irizarry, A. Khodjakov, and M. P. Koonce. Organization of microtubule assemblies in Dictyostelium syncytia depends on the microtubule crosslinker, Ase1. *Cell Mol Life Sci*, 73(4):859–868, 2016. ISSN 1420-9071 (Electronic) 1420-682X (Linking). doi: 10.1007/s00018-015-2026-8. URL `internal-pdf://134.30.245.49/Tikhonenko-2016-Organizationofmicr.pdfhttp://www.ncbi.nlm.nih.gov/pubmed/26298292http://download.springer.com/static/pdf/409/art{%}253A10.1007{%}252Fs00018-015-2026-8.pdf?originUrl=http{%}3A{%}2F{%}2Flink.springer.com{%}2Farticle{%}2F10`.

S. A. Tooze and T. Yoshimori. The origin of the autophagosomal membrane, 2010. ISSN 14657392.

I. Topalidou, C. Keller, N. Kalebic, K. C. Nguyen, H. Somhegyi, K. A. Politi, P. Heppenstall, D. H. Hall, and M. Chalfie. Genetically separable functions of the MEC-17 tubulin acetyltransferase affect microtubule organization. *Current Biology*, 22(12):1057–1065, jun 2012. ISSN 09609822. doi: 10.1016/j.cub.2012.03.066.

P. Torija, J. J. Vicente, T. B. Rodrigues, A. Robles, S. Cerdán, L. Sastre, R. M. Calvo, and R. Escalante. Functional genomics in Dictyostelium: MidA, a new conserved protein, is required for mitochondrial function and development. *Journal of Cell Science*, 119(6):1154–1164, mar 2006. ISSN 00219533. doi: 10.1242/jcs.02819. URL `https://jcs.biologists.org/content/119/6/1154https://jcs.biologists.org/content/119/6/1154.abstract`.

P. T. Tran, R. A. Walker, and E. D. Salmon. A metastable intermediate state of microtubule dynamic instability that differs significantly between plus and minus ends. *Journal of Cell Biology*, 138(1):105–117, jul 1997. ISSN 00219525. doi: 10.1083/jcb.138.1.105.

S. Triclin, D. Inoue, J. Gaillard, Z. M. Htet, M. E. Desantis, D. Portran, E. Derivery, C. Aumeier, L. Schaedel, K. John, C. Leterrier, S. L. Reck-Peterson, L. Blanchoin, and M. Théry. Self-repair protects microtubules from their destruction by molecular motors. *BioRxiV*, 2018. doi: 10.1101/499020. URL `http://dx.doi.org/10.1101/499020`.

L. Trivinos-Lagos, T. Ohmachi, C. Albrightson, R. G. Burns, and H. L. Ennis. The highly divergent alpha- and beta-tubulins from Dictyostelium discoideum are encoded by single genes — Journal of Cell Science, 1993. URL `https://jcs.biologists.org/content/105/4/903.short`.

M. Ueda, M. Schliwa, and U. Euteneuer. Unusual centrosome cycle in Dictyostelium: Correlation of dynamic behavior and structural changes. *Molecular Biology of the Cell*, 10(1):151–160, 1999. ISSN 10591524. doi: 10.1091/mbc.10.1.151.

T. Ukmar-Godec, S. Wegmann, and M. Zweckstetter. Biomolecular condensation of the microtubule-associated protein tau, mar 2020. ISSN 10963634.

R. D. Vale. The molecular motor toolbox for intracellular transport, feb 2003. ISSN 00928674.

M. Van Breugel, M. Hirono, A. Andreeva, H. A. Yanagisawa, S. Yamaguchi, Y. Nakazawa, N. Morgner, M. Petrovich, I. O. Ebong, C. V. Robinson, C. M. Johnson, D. Veprintsev, and B. Zuber. Structures of SAS-6 suggest its organization in centrioles. *Science*, 331(6021):1196–1199, mar 2011. ISSN 00368075. doi: 10.1126/science.1199325. URL `https://science.sciencemag.org/content/331/6021/1196https://science.sciencemag.org/content/331/6021/1196.abstract`.

D. M. Veltman, G. Akar, L. Bosgraaf, and P. J. Van Haastert. A new set of small, extrachromosomal expression vectors for Dictyostelium discoideum. *Plasmid*, 61(2):110–118, mar 2009. ISSN 0147-619X. doi: 10.1016/J.PLASMID.2008.11.003. URL `https://www.sciencedirect.com/science/article/pii/S0147619X08001054?via{%}3Dihub`.

K. Verhoeven, P. De Jonghe, K. Coen, N. Verpoorten, M. Auer-Grumbach, J. M. Kwon, D. FitzPatrick, E. Schmedding, E. De Vriendt, A. Jacobs, V. Van Gerwen, K. Wagner, H. P. Hartung, and V. Timmerman. Mutations in the small GTP-ase late endosomal protein RAB7 cause Charcot-Marie-Tooth type 2B neuropathy. *American Journal of Human Genetics*, 72(3):722–727, mar 2003. ISSN 00029297. doi: 10.1086/367847. URL `https://pubmed.ncbi.nlm.nih.gov/12545426/`.

J. H. Vines and J. S. King. The endocytic pathways of Dictyostelium discoideum. *The International Journal of Developmental Biology*, 63(8-9-10): 461–471, dec 2019. ISSN 0214-6282. doi: 10.1387/ijdb.190236jk. URL `http://www.intjdevbiol.com/paper.php?doi=190236jk`.

B. Vitre, F. M. Coquelle, C. Heichette, C. Garnier, D. Chrétien, and I. Arnal. EB1 regulates microtubule dynamics and tubulin sheet closure in vitro. *Nature Cell Biology*, 10(4):415–421, mar 2008. ISSN 14657392. doi: 10.1038/ncb1703. URL `https://www.nature.com/articles/ncb1703`.

C. E. Walczak, T. J. Mitchison, and A. Desai. XKCM1: A Xenopus kinesin-related protein that regulates microtubule dynamics during mitotic spindle assembly. *Cell*, 84(1):37–47, jan 1996. ISSN 00928674. doi: 10.1016/S0092-8674(00)80991-5.

P. Wang, D. Kou, and W. Le. Roles of VMP1 in Autophagy and ER–Membrane Contact: Potential Implications in Neurodegenerative Disorders. *Frontiers in Molecular Neuroscience*, 13:42, mar 2020. ISSN 1662-5099. doi: 10.3389/fnmol.2020.00042. URL `https://www.frontiersin.org/article/10.3389/fnmol.2020.00042/full`.

Y. Wang and D. J. Burke. Checkpoint genes required to delay cell division in response to nocodazole respond to impaired kinetochore function in the yeast Saccharomyces cerevisiae. *Molecular and Cellular Biology*, 15(12):6838–6844, dec 1995. ISSN 0270-7306. doi: 10.1128/mcb.15.12.6838. URL `http://mcb.asm.org/`.

A. Welin, S. Weber, and H. Hilbi. Quantitative Imaging Flow Cytometry of Legionella-Infected Dictyostelium Amoebae Reveals the Impact of Retrograde Trafficking on Pathogen Vacuole Composition GENETICS AND MOLECULAR BIOLOGY crossm Downloaded from. Technical report, 2018. URL http://aem.asm.org/.

C. L. Wellington, R. Singaraja, L. Ellerby, J. Savill, S. Roy, B. Leavitt, E. Cattaneo, A. Hackam, A. Sharp, N. Thornberry, D. W. Nicholson, D. E. Bredesen, and M. R. Hayden. Inhibiting caspase cleavage of huntingtin reduces toxicity and aggregate formation in neuronal and nonneuronal cells. *Journal of Biological Chemistry*, 275(26):19831–19838, jun 2000. ISSN 00219258. doi: 10.1074/jbc.M001475200.

X. Wen and D. J. Klionsky. An overview of macroautophagy in yeast, may 2016. ISSN 10898638. URL /pmc/articles/PMC4846508/?report=abstracthttps://www.ncbi.nlm.nih.gov/pmc/articles/PMC4846508/.

E. White, E. M. Tolbert, and E. R. Katz. Identification of tubulin in Dictyostelium discoideum: characterization of some unique properties. *J Cell Biol*, 97(4):1011–1019, 1983. ISSN 0021-9525 (Print) 0021-9525 (Linking). URL http://www.ncbi.nlm.nih.gov/pubmed/6352709.

G. J. Wilson, M. J. Marakalala, J. C. Hoving, A. Van Laarhoven, R. A. Drummond, B. Kerscher, R. Keeton, E. Van De Vosse, T. H. Ottenhoff, T. S. Plantinga, B. Alisjahbana, D. Govender, G. S. Besra, M. G. Netea, D. M. Reid, J. A. Willment, M. Jacobs, S. Yamasaki, R. Van Crevel, and G. D. Brown. The C-type lectin receptor CLECSF8/CLEC4D is a key component of anti-mycobacterial immunity. *Cell Host and Microbe*, 17(2):252–259, feb 2015. ISSN 19346069. doi: 10.1016/j.chom.2015.01.004.

J. B. Woodruff, O. Wueseke, and A. A. Hyman. Pericentriolar material structure and dynamics. *Philosophical Transactions of the Royal Society B: Biological Sciences*, 369(1650):20130459, sep 2014. ISSN 0962-8436. doi:

10.1098/rstb.2013.0459. URL https://royalsocietypublishing.org/doi/10.1098/rstb.2013.0459.

Z. J. Xu, L. Schaedel, D. Portran, A. Aguilar, J. Gaillard, M. P. Marinkovich, M. Thery, and M. V. Nachury. Microtubules acquire resistance from mechanical breakage through intralumenal acetylation. *Science*, 356(6335):328–332, 2017. ISSN 0036-8075. doi: 10.1126/science.aai8764.

A. Yildiz, M. Tomishige, R. D. Vale, and P. R. Selvin. Kinesin Walks Hand-Over-Hand. *Science*, 303(5658):676–678, jan 2004. ISSN 00368075. doi: 10.1126/science.1093753. URL https://science.sciencemag.org/content/303/5658/676https://science.sciencemag.org/content/303/5658/676.abstract.

E. Zehr, A. Szyk, G. Piszczek, E. Szczesna, X. B. Zuo, and A. Roll-Mecak. Katanin spiral and ring structures shed light on power stroke for microtubule severing. *Nature Structural & Molecular Biology*, 24(9):717–+, 2017. ISSN 1545-9993. doi: 10.1038/nsmb.3448.

D. Zhang, G. C. Rogers, D. W. Buster, and D. J. Sharp. Three microtubule severing enzymes contribute to the "Pacman- flux" machinery that moves chromosomes. *Journal of Cell Biology*, 177(2):231–242, 2007. ISSN 00219525. doi: 10.1083/jcb.200612011.

H. Zhang, A. Griggs, J. C. Rochet, and L. A. Stanciu. In vitro study of α-synuclein protofibrils by Cryo-EM suggests a Cu2+-dependent aggregation pathway. *Biophysical Journal*, 104(12):2706–2713, jun 2013. ISSN 00063495. doi: 10.1016/j.bpj.2013.04.050.

F. Zhou, S. Zou, Y. Chen, Z. Lipatova, D. Sun, X. Zhu, R. Li, Z. Wu, W. You, X. Cong, Y. Zhou, Z. Xie, V. Gyurkovska, Y. Liu, Q. Li, W. Li, J. Cheng, Y. Liang, and N. Segev. A Rab5 GTPase module is important for autophagosome closure. *PLOS Genetics*, 13(9):e1007020, sep 2017. ISSN 1553-7404. doi: 10.1371/journal.pgen.1007020. URL https://dx.plos.org/10.1371/journal.pgen.1007020.

F. Zhou, Z. Wu, M. Zhao, R. Murtazina, J. Cai, A. Zhang, R. Li, D. Sun, W. Li, L. Zhao, Q. Li, J. Zhu, X. Cong, Y. Zhou, Z. Xie, V. Gyurkovska, L. Li, X. Huang, Y. Xue, L. Chen, H. Xu, H. Xu, Y. Liang, and N. Segev. Rab5-dependent autophagosome closure by ESCRT. *Journal of Cell Biology*, 218(6):1908–1927, jun 2019. ISSN 15408140. doi: 10.1083/JCB.201811173. URL `https://doi.org/10.1083/jcb.201811173`.

R. E. Zirkle. Ultraviolet-Microbeam Irradiation of Newt-Cell Cytoplasm: Spindle Destruction, False Anaphase, and Delay of True Anaphase. *Radiation Research*, 41(3):516, mar 1970. ISSN 00337587. doi: 10.2307/3572841.